ENERGY MANAGEMENT SYSTEM FOR OPTIMAL OPERATION OF MICROGRID CONSISTING OF PV, FUEL CELL AND BATTERY

SHIVASHANKAR SUKUMAR

FACULTY OF ENGINEERING
UNIVERSITY OF MALAYA
KUALA LUMPUR

2017

ENERGY MANAGEMENT SYSTEM FOR OPTIMAL OPERATION OF MICROGRID CONSISTING OF PV, FUEL CELL AND BATTERY

SHIVASHANKAR SUKUMAR

THESIS SUBMITTED IN FULFILMENT OF THE REQUIREMENTS FOR THE DEGREE OF DOCTOR OF PHILOSOPHY

FACULTY OF ENGINEERING
UNIVERSITY OF MALAYA
KUALA LUMPUR

2017

UNIVERSITY OF MALAYA

ORIGINAL LITERARY WORK DECLARATION

Name of Candidate: Shivashankar Sukumar

Registration/Matric No: KHA130136

Name of Degree: Doctor of Philosophy

Title of Project Paper/Research Report/Dissertation/Thesis ("this Work"):

ENERGY MANAGEMENT SYSTEM FOR OPTIMAL OPERATION OF MICROGRID CONSISTING OF PV, FUEL CELL AND BATTERY

Field of Study: Power Systems

I do solemnly and sincerely declare that:

(1) I am the sole author/writer of this Work;
(2) This Work is original;
(3) Any use of any work in which copyright exists was done by way of fair dealing and for permitted purposes and any excerpt or extract from, or reference to or reproduction of any copyright work has been disclosed expressly and sufficiently and the title of the Work and its authorship have been acknowledged in this Work;
(4) I do not have any actual knowledge nor do I ought reasonably to know that the making of this work constitutes an infringement of any copyright work;
(5) I hereby assign all and every rights in the copyright to this Work to the University of Malaya ("UM"), who henceforth shall be owner of the copyright in this Work and that any reproduction or use in any form or by any means whatsoever is prohibited without the written consent of UM having been first had and obtained;
(6) I am fully aware that if in the course of making this Work I have infringed any copyright whether intentionally or otherwise, I may be subject to legal action or any other action as may be determined by UM.

Candidate's Signature Date:

Subscribed and solemnly declared before,

Witness's Signature Date:

Name:

Designation:

ABSTRACT

Operating a microgrid with intermittent source such as photovoltaic (PV) introduces uncertainty in its operation. Therefore, it is necessary to manage the energy from this type of distributed energy resources (DERs) to optimize it usage in optimal manner. In this work, an energy management system (EMS) is proposed for a grid connected microgrid where the DERs is able to supply the local load based on directives provided by an EMS and minimize the power oscillations caused by PV plant. The proposed EMS is for grid connected microgrid consisting of solar PV plant, battery energy storage system (BESS) and fuel cell.

In this work, a novel ramp-rate control strategy is proposed where the energy storage is used to control the ramp-rate of PV output power within the desirable level. In addition, a novel 'mix-mode' operating strategy is proposed to reduce the microgrid's daily operating cost. The objective functions in the proposed strategies are solved using linear programming and mixed integer linear programming. Since battery size influences operating cost of microgrid, a sizing method to determine optimal energy capacity of BESS in kWh is also proposed. The BESS sizing problem is solved using grey wolf optimizer (GWO), particle swarm optimization (PSO), artificial bee colony (ABC), gravitational search algorithm (GSA), and genetic algorithm (GA). It was found that GWO presents the optimal solution.

The proposed EMS module integrates the proposed ramp-rate control strategy and mix-mode operating strategy and solved using receding horizon economic dispatch (RHED) approach. Comparison on solving the energy management problem using RHED approach with metaheuristic methods like PSO and evolutionary programming (EP) was also conducted and found that RHED approach provides the optimal solution with less computational run time. The results indicate that the proposed EMS can reduce the operating cost by 10.2% when compared with metaheuristic methods.

ABSTRAK

Mengendalikan microgrid dengan sumber sekala seperti photovoltaic (PV) memperkenalkan ketidakpastian dalam operasinya. Oleh itu, adalah perlu untuk menguruskan tenaga dari jenis sumber tenaga diedarkan (DERs) untuk mengoptimumkan penggunaan dengan cara yang optimum. Dalam kajian ini, sistem pengurusan tenaga (EMS) dicadangkan untuk grid disambungkan dengan microgrid dimana DERs mampu membekalkan beban tempatan berdasarkan arahan yang disediakan oleh EMS dan mengurangkan ayunan kuasa yang disebabkan oleh kilang PV. EMS yang dicadangkan ini adalah untuk grid disambungkan dengan microgrid yang terdiri daripada kilang solar PV, sistem bateri penyimpanan tenaga (BESS) dan sel bahan api.

Dalam kajian ini, satu novel strategi kawalan kadar-ramp dicadangkan di mana penyimpanan tenaga digunakan untuk mengawal kadar-ramp kuasa output PV di dalam tahap yang wajar. Selain itu, strategi operasi novel 'mix-mode' dicadangkan untuk mengurangkan kos operasi harian microgrid. Fungsi objektif dalam strategi yang dicadangkan diselesaikan menggunakan pengaturcaraan linear dan pengaturcaraan linear integer campuran. Disebaktan saiz bateri mempengaruhi kos operasi microgrid, satu kaedah untuk menentukan saiz kapasiti saiz tenaga optimum bagi BESS dalam kWh juga dicadangkan. Masalah saiz BESS diselesaikan dengan menggunakan pengoptimasi kelabu serigala (GWO), pengoptimuman zarah sekumpulan (PSO), lebah tiruan tanah jajahan (ABC), carian graviti algoritma (GSA), dan algoritma genetik (GA). Ianya didapati bahawa GWO membentangkan penyelesaian yang paling optimum.

Modul EMS yang dicadangkan mengintegrasikan strategi kawalan kadar-ramp dan strategi operasi mod-campuran dan diselesaikan dengan menggunakan pendekatan penghantaran ekonomi surut ufuk (RHED). Perbandingan kepada menyelesaikan

masalah pengurusan tenaga menggunakan pendekatan RHED dan kaedah metaheuristic seperti PSO dan program evolusi (EP) juga telah dijalankan dan mendapati bahawa pendekatan RHED menyediakan penyelesaian yang paling optimum dengan jangka masa pengiraan yang sedikit. Keputusan menunjukkan bahawa EMS yang dicadangkan boleh mengurangkan kos operasi sebanyak 10.2% berbanding dengan kaedah metaheuristic.

ACKNOWLEDGEMENTS

First and foremost, I would like to kindly express my sincere thanks and deepest gratitude to my supervisors Prof.Dr.Hazlie Mokhlis and Prof.Dr.Saad Mekhilef whose recommendations and support encouraged me to put my ideas forward here and develop such relevant results. Their advice, enthusiasm and motivation in assisting me to successfully complete this project are wholeheartedly appreciated.

I would like to sincerely than my additional supervisor Dr.Mazaher Karimi for his advice and feedback in completing my PhD work. I would like to thank Dr.Kanendra Naidu for helping me in solving the optimization part in my project. I would also like to thank University of Malaya for providing academic support and encouragement and also the necessary facility in ensuring a conductive atmosphere in order to accomplish my project.

I would like to take this opportunity to extend my gratitude and sincere thanks to my wife, my son and my parents who played an instrumental role in helping me by providing their full support and encouragement. I would also like to extend my gratitude to thank all my friends in the power system group laboratory for all their assistance.

Last but not least, my heartfelt gratitude and appreciation to all of you and others who has contributed towards the successful completion of this project.

TABLE OF CONTENTS

Abstract iii

Abstrak iv

Acknowledgements vi

Table of Contents vii

List of Figures xii

List of Tables xv

List of Symbols and Abbreviations xvi

List of Appendices xix

CHAPTER 1: INTRODUCTION 1

1.1 Overview 1

1.2 Problem Statement 2

1.3 Research Objectives 5

1.4 Scope and Limitation 5

1.5 Research Methodology 6

1.6 Thesis Outline 8

CHAPTER 2: LITERATURE REVIEW 10

2.1 Introduction 10

2.2 Microgrid Concept 10

2.3 Distributed Energy Resources (DERs) 12

2.3.1 Utility Scale Distributed Energy Resource 13

2.3.2 Medium and Small Scale Distributed Energy Resource 13

2.4 Status of non-dispatchable solar photovoltaic DERs and its related issues 14

2.4.1 Solar Photovoltaic Status in the World 14

2.4.2 Solar Photovoltaic Status in Malaysia 15
2.4.3 Technical Impacts of Solar Photovoltaic Plant 16
2.5 Dispatchable Distributed Energy Resources (DERs) 24
2.5.1 Battery Energy Storage System 24
2.5.2 Solid Oxide Fuel Cell (SOFC) System 26
2.6 Smoothing PV output power fluctuation using energy storage technologies 29
2.7 Energy Management System (EMS) for microgrid operation 34
2.7.1 EMS using numerical methods 39
2.7.2 EMS using metaheurictic methods 40
2.8 BESS sizing methods for economic operation of microgrid 43
2.9 Summary 47

CHAPTER 3: METHODOLOGY OF THE PROPOSED ENERGY MANAGEMENT SYSTEM 49

3.1 Introduction 49
3.2 Proposed Microgrid Configuration and Operation 49
3.2.1 Overview 49
3.2.2 Energy Management System (EMS) module 51
3.2.3 Parameters of Solar PV Plant 52
3.2.3.1 Maximum Power Point Tracking (MPPT) 52
3.2.4 Modeling of Battery Energy Storage System (BESS) 54
3.2.5 Modeling of Solid Oxide Fuel Cell (SOFC) system 57
3.2.6 Voltage Source Converter (VSC) 59
3.3 Analysis of moving average and conventional exponential smoothing methods .. 62
3.3.1 n-point Moving Average (MA) method 62
3.3.2 Conventional Exponential Smoothing (CES) method 64
3.4 Proposed Solar PV Ramp-Rate Control Strategy 66

3.5 Illustration of the Proposed Ramp-Rate Control Strategy 70
3.6 Proposed Optimal BESS Sizing Method and Operating Strategy to Reduce Microgrid's Daily Operation Cost 72
3.6.1 Proposed "Mix-Mode" Operating Strategy 73
3.6.1.1 Strategy 1: Continuous Run Mode 73
3.6.1.2 Strategy 2: Power Sharing Mode 75
3.6.1.3 Strategy 3: ON/OFF Mode 76
3.6.2 Development of "Mix-Mode" Operating Strategy 77
3.6.3 Proposed Algorithm to Solve the Mix-Mode Operating Strategy 78
3.6.4 Proposed BESS Sizing Method: Problem Formulation 79
3.6.5 Proposed Algorithm for Solving the BESS Sizing Problem 81
3.6.5.1 Grey Wolf Optimizer (GWO) 84
3.6.5.2 Particle Swarm Optimization (PSO) 85
3.6.5.3 Artificial Bee Colony (ABC) 86
3.6.5.4 Genetic Algorithm (GA) 88
3.6.5.5 Gravitational Search Algorithm (GSA) 88
3.7 Development of Energy Management System (EMS) 90
3.7.1 Receding Horizon Economic Dispatch (RHED) Approach for mix-mode operating strategy 91
3.7.2 Implementation of mix-mode strategy using RHED approach 94
3.8 Summary 96

CHAPTER 4: VALIDATION OF PROPOSED RAMP-RATE CONTROL STRATEGY AND MIX-MODE OPERATING STRATEGY 97

4.1 Introduction 97
4.2 Test system for validation of the proposed ramp-rate control strategy 97
4.3 Solar radiation data 98

4.4 Application of the proposed ramp-rate control strategy 100
4.5 Relation between smoothing parameter 'σ' and ramp-rate 109
4.6 Data used for validation of the proposed mix-mode operating strategy 111
4.7 Validation of the proposed mix-mode operating strategy 113
4.8 Summary 115

CHAPTER 5: VALIDATION OF BESS SIZING METHOD AND EMS USING RECEDING HORIZON ECONOMIC DISPATCH APPROACH 117

5.1 Introduction 117
5.2 Data used for validation of the proposed BESS sizing method 117
5.3 Validation of the proposed BESS sizing method 118
5.4 Analysis of variation in optimal energy capacity of BESS 123
5.5 Analysis of variation of microgrid's operating cost for different initial SOC levels 125
5.5.1 Microgrid operation without BESS 126
5.5.2 Microgrid operation with BESS having initial SOC levels of 100%, 70% and 50% 127
5.6 Recommendation on BESS initial SOC level for effective microgrid operation 133
5.7 Validation of EMS using RHED approach 133
5.8 Energy Management System (EMS) with and without smoothing functionality 140
5.9 Summary 142

CHAPTER 6: CONCLUSION AND FUTURE WORKS 143

6.1 Conclusions 143
6.2 Future Works 145
References 147
list of publications and papers presented 162

Appendix 163

LIST OF FIGURES

Figure 1.1: Flowchart for the research methodology 7

Figure 2.1: Global PV capacity between 2005-2014 (*Renewable Energy Policy Network for 21st Century (REN21), Renewables Global Status Report* 2015) 14

Figure 2.2: Typical output power from PV (Omran, Kazerani, & Salama, 2011a) 17

Figure 2.3: Problem of voltage rise at distribution network 21

Figure 2.4: Voltage flicker induced from PV by movement of clouds 22

Figure 2.5: Functions of a real-time EMS for a microgrid (Katiraei, Iravani et al., 2008) 35

Figure 3.1: Proposed grid-connected microgrid configuration 50

Figure 3.2: IC algorithm in order to estimate V_{ref} for DC bus controller 53

Figure 3.3: Equivalent dynamic model of battery module 54

Figure 3.4: SOFC dynamic model(X. Wang, Huang, & Chen, 2007) 57

Figure 3.5: Grid-connected mode power controller of VSC 60

Figure 3.6: Output power of solar PV plant 62

Figure 3.7: Actual PV power and smoothed power using 41 point MA waveform 64

Figure 3.8: Actual PV output and PV power smoothed using CES method 66

Figure 3.9: Calculating P_{ES} for battery energy storage and working of proposed ramp-rate control strategy 70

Figure 3.10: Illustration for proposed ramp-rate control strategy 71

Figure 3.11: Variation in smoothing parameter for the proposed ramp-rate strategy 71

Figure 3.12: Mix-mode operating strategy 77

Figure 3.13: Flowchart of the proposed sizing method for mix-mode operating strategy 83

Figure 3.14: Receding horizon economic dispatch approach 91

Figure 3.15: Development of mix-mode operating strategy 92

Figure 3.16: Mix-mode operating strategy using RHED approach 94

Figure 4.1: Schematic of grid connected PV-energy storage for proposed ramp-rate strategy 98

Figure 4.2: Forecasted solar irradiation profile by HOMER in sampling location in Peninsular Malaysia on May and the noise applied on it 100

Figure 4.3: Solar output power obtained from 1-min radiation data 101

Figure 4.4: Smoothing PV output power by using MA method 101

Figure 4.5: Smoothing PV output power by using CES method 102

Figure 4.6: Smoothing PV output power by using proposed ramp-rate control strategy 102

Figure 4.7: Actual power and smoothed power profiles for different methods for specific time period 104

Figure 4.8: Battery utilization for MA method 104

Figure 4.9: Battery utilization for CES method 105

Figure 4.10: Battery utilization for proposed ramp-rate strategy 105

Figure 4.11: Control of PV ramp-rate using proposed strategy 106

Figure 4.12: Variation of smoothing parameter 'σ 'for proposed ramp-rate strategy .. 106

Figure 4.13: THD at phase A voltage without and with battery storage for 3 methods 108

Figure 4.14: Variation of smoothing parameter with ramp-rate violation 110

Figure 4.15: Residential customer load profile in Malaysia 111

Figure 4.16: Energy prices in ($/kWh) 112

Figure 4.17: Optimal output of distributed source in microgrid for mix-mode strategy 113

Figure 4.18: BESS SOC level for mix-mode operating strategy 114

Figure 5.1: Optimal value of energy capacity in kWh using trade-off method 119

Figure 5.2: Convergence characteristics of GWO with other optimization techniques 122

Figure 5.3: Optimal value of energy capacity in kWh using trade-off method for initial BESS SOC at 100%, 90% and 80%.....124

Figure 5.4: Optimal operation of microgrid without BESS.....126

Figure 5.5: Optimal output of distributed source in microgrid for when BESS initial SOC at 100% of 2056.80kWh.....128

Figure 5.6: BESS SOC level for mix-mode operating strategy when BESS initial SOC at 100% of 2056.80kWh.....128

Figure 5.7: Optimal output of distributed source in microgrid for when BESS initial SOC at 70% of 2056.80kWh.....130

Figure 5.8: BESS SOC level for mix-mode operating strategy when BESS initial SOC at 70% of 2056.80kWh.....131

Figure 5.9: Optimal output of distributed source in microgrid for when BESS initial SOC at 50% of 2056.80kWh.....131

Figure 5.10: BESS SOC level for mix-mode operating strategy when BESS initial SOC at 50% of 2056.80kWh.....132

Figure 5.11: Microgrid operation using directive energy management system solved using RHED approach.....135

Figure 5.12: BESS SOC profile.....135

Figure 5.13: Variation of *Kp* for BESS plant.....138

Figure 5.14: Variation of *Ti* for BESS plant.....138

Figure 5.15: Variation of *Kp* for fuel cell plant.....139

Figure 5.16: Variation of *Ti* for fuel cell plant.....139

Figure 5.17: Microgrid operation using directive energy management system solved using RHED approach without smoothing function.....141

Figure 5.18: BESS SOC profile without smoothing function.....141

LIST OF TABLES

Table 2.1: Comparison between different mitigating methods to mitigate PV power fluctuation using MA and CES methods 33

Table 2.2: Summary on different EMS using metaheuristic and mathematical methods 42

Table 2.3: Summary on different BESS sizing method 46

Table 3.1: Electrical specification of solar module (HIT-N210A01)("HIT Photovoltaic Module Power 210A," 2010) 52

Table 3.2: Logic behind the IC MPPT algorithm 54

Table 3.3: Technical specification of 12V battery module (RM12-75DC)(RemcoLtd., 2012) 56

Table 3.4: Parameters used for SOFC model (X. Wang et al., 2007) 59

Table 4.1: Comparison on battery storage (BS) operation for the three methods 107

Table 4.2: Average THD level when PV and battery storage is operated 109

Table 4.3: Comparison of daily operating cost 114

Table 5.1: Comparison between optimal value obtained using trade-off method and proposed sizing method 121

Table 5.2: Comparison between operation cost of microgrid obtained using various optimization techniques for 10 trial runs 121

Table 5.3: Comparison between optimal value obtained using trade-off method and proposed sizing method for BESS initial SOC levels 100%, 90% and 80% 125

Table 5.4: Comparison between operating cost with and without BESS case 132

Table 5.5: Comparison between operating cost obtained using RHED approach, PSO and EP 136

Table 5.6: Optimal K_P and T_i ranges found using simplex method for both BESS and fuel cell plants 137

LIST OF SYMBOLS AND ABBREVIATIONS

ABC	:	Artificial Bee Colony
BES	:	Battery Energy Storage
BESS	:	Battery Energy Storage System
CBA	:	Conventional Bat Algorithm
CES	:	Conventional Exponential Smoothing
COE	:	Cost of Electricity
DG	:	Distributed Generator
DNO	:	Distribution Network Operator
DOE	:	Department of Energy
DR	:	Demand Response
DS	:	Distributed Storage
DER	:	Distributed Energy Resource
EI	:	Electronically Interfaced
EIDG	:	Electronically Interfaced Distributed Generation
EMS	:	Energy Management System
EP	:	Evolutionary Programming
EDLC	:	Electric Double Layer Capacitor
ES	:	Energy Storage
FC	:	Fuel Cell
FiT	:	Feed in Tariff
GSA	:	Gravitational Search Algorithm
GA	:	Genetic Algorithm
GWO	:	Grey Wolf Optimizer
IBA	:	Improved Bat Algorithm

IC	:	Incremental Conductance
LP	:	Linear Programming
LVRT	:	Low Voltage Ride Through
MPP	:	Maximum Power Point
MPPT	:	Maximum Power Point Tracking
MA	:	Moving Average
MADS	:	Mesh Adaptive Direct Search
MILP	:	Mixed Integer Linear Programming
MRCGA	:	Matrix Real Coded Genetic Algorithm
NPV	:	Net Present Value
OC	:	Operating Cost
PCC	:	Point of Common Coupling
PEM	:	Proton Exchange membrane
PI	:	Proportional Integral
PLL	:	Phase Locked Loop
P&O	:	Perturb and Observe
PSO	:	Particle Swarm Optimization
PV	:	Photovoltaic
PWM	:	Pulse Width Modulation
RE	:	Renewable Energy
RES	:	Renewable Energy Sources
RHED	:	Receding Horizon Economic Dispatch
SEDA	:	Sustainable Energy Development Authority
SMES	:	Superconducting Magnetic Energy Storage
SOC	:	State of Charge
SOFC	:	Solid Oxide Fuel Cell

TCPD	:	Total Cost Per Day
TLBO	:	Teaching Learning Based Optimization
THD	:	Total Harmonic Distortion
TNB	:	Tenaga National Berhad
TS	:	Tabu Search
UPS	:	Uninterruptible Power Supply
VRB	:	Vanadium Redox Battery
VSC	:	Voltage Sourced Converter

LIST OF APPENDICES

Appendix A: Modelling of grid connected microgrid…….... 163

CHAPTER 1: INTRODUCTION

1.1 Overview

Electricity generated from fossil fuels has a major impact on the environment due to emission of greenhouse gases. It is estimated that 24% of greenhouse gases emission into atmosphere are caused by electricity generation (Varaiya, Wu, & Bialek, 2011). Such emission should be reduced to avoid disastrous effect of global warming. This scenario will become worse with the increase of global electricity demand, where it is projected to rise from 145 billion MW in 2007 to 218 billion MW in 2035 (Hasanuzzaman et al., 2012). To address this demand, more power plants are needed to be developed. However, power plants based on coal, oil or natural gas will further contribute to increase of greenhouse gases emission. Thus, renewable energy sources (RES) such as sunlight, wind, rain, tides and geothermal heat has been explored to generate electricity with the objective of reducing greenhouse gases emission.

In the year 2014, RES has contributed to 22.8% of global electricity production(*Renewable Energy Policy Network for 21st Century (REN21), Renewables Global Status Report* 2015). Grid connected solar photovoltaic (PV) is the fastest growing RES power generation technology. Solar PV has started to play an important role in electricity generation in many countries as the cost of PV panel has reduced. The installation of PV plants around the world is increased by 28% from 138GW in 2013 to 177GW in 2014(*Renewable Energy Policy Network for 21st Century (REN21), Renewables Global Status Report* 2015). China, Japan and the United States accounted for the vast majority of new capacity in the year 2014. However, Germany continued to lead the world in terms of total solar PV capacity. In developing countries, obtaining financial assistance for installing solar PV at affordable rates is a common challenge.

On the other hand, new business models and innovative financing options continues to emerge to facilitate solar PV installation with low capital costs and reduced generation costs (*Renewable Energy Policy Network for 21st Century (REN21), Renewables Global Status Report* 2015).

The growing interest in generating electricity by utilizing RES creates a new type of power system network which includes both renewable and fossil fuel power plants. The main aim of this network is to establish an energy system that is sustainable, particularly with respect to reducing greenhouse gas emissions and improving security and reliability of energy supply to all its consumers with lowest possible operating cost. These RES are mostly connected in the distribution system which can be operated in parallel with other distributed generators (DG) and distributed storage (DS). Parallel operation of DG, DS and load with the main utility grid or in autonomous modes is collectively referred to as microgrid. Remarkable attention was paid to microgrid concept by the IEEE Std P1547.4 on Guide for Design, Operation, and Integration of Distributed Resource Island Systems with Electric Power Systems (Kroposki et al., 2008). This guide was initially drafted to deal with the missing information in IEEE Std 1547-2008 about intentional islanding. The benefits of microgrid are to facilitate the increase in RES depth of penetration and reduce the emission of greenhouse gases, provide ancillary services, deliver continuous power supply to strike a balance between generation and load and utilize waste heat for other applications where co-generation is possible (Cornforth, 2011; Mears, Gotschall, & Kamath, 2003).

1.2 Problem Statement

The microgrid is expected to provide sufficient generation, control and operational strategy to supply at least a small portion of the load. Therefore, it is necessary to integrate energy management system (EMS) into the power networks, where microgrid

is connected. Through the EMS, the power generated from the distributed sources in the microgrid can be managed in a coordinated and effective manner. The main aim of the EMS is to coordinate the distributed sources in the microgrid to supply the required power to the load with lowest operating cost. The EMS should be enabled with functionalities such as load forecasting, fault detection and clearance and peak shaving. When the microgrid consists of intermittent source like PV generator, the EMS should be equipped with PV output smoothing function.

Over the years, many EMS have been proposed such as coordinated EMS, centralized EMS or smart power management system (Koohi-Kamali, Rahim, & Mokhlis, 2014; K. Tan, Peng, So, Chu, & Chen, 2012; K. Tan, So, Chu, & Chen, 2013). Many EMS focused on operating the microgrid with lowest operating cost which is based on a particular operating strategy. Moreover, many researchers do not consider economic operation of microgrid. Besides, for more reliable operation the optimal solution should be calculated on a minute-by-minute basis. Many researchers focused on the application of mathematical methods like linear programming (LP), mixed integer linear programming (MILP), sequential quadratic programming for solving the microgrid's energy management problem(Ci Chen, Sisi Duan, Tong Cai, Bangyin Liu, & Gangwei Hu, 2011; Mohamed & Koivo, 2010, 2012; Tenfen & Finardi, 2015). The comparative study on addressing the economic operation of microgrid between mathematical methods and metaheuristic methods lacks in the literature. Addressing all these above limitations, the present work is based on a hypothesis that, optimizing the daily operation cost of the hybrid system for a single operating strategy may not necessarily incur lower operating cost as majority of the papers have mentioned in the literature. Unlike the papers in the literature, the present work is focused on developing an EMS which incurs the lowest operating cost of the hybrid system by combining two or more operating strategies.

Presence of battery energy storage system (BESS) in the microgrid influences the microgrid's performance particularly microgrid's daily operational cost. Moreover, there are only few articles in the literature which considers sizing of BESS which is an important aspect of economic operation for microgrid (Bahmani-Firouzi & Azizipanah-Abarghooee, 2014; Fossati, Galarza, Martín-Villate, & Fontán, 2015; Sharma, Bhattacharjee, & Bhattacharya, 2016). In addition, the articles in the literature present BESS sizing methods which considers the economic operation of microgrid for one particular strategy only. Therefore in-order to operate the microgrid with lowest operating cost, it is absolutely necessary to accurately evaluate the size of BESS used for microgrid operated under the proposed operating strategy.

Mitigating solar PV fluctuation is a challenge because solar PV penetration with high ramp-rate introduces significant voltage fluctuation in weak radial distribution network. To alleviate the power fluctuations the energy storage technologies such as capacitors, electric double layer capacitor (EDLC), superconducting magnetic energy storage (SMES), and battery storage can be considered as a possible solution (Kakimoto, Satoh, Takayama, & Nakamura, 2009; Tam, Kumar, & Foreman, 1989). Limited literature is available on EMS with solar PV output power ramp-rate limiting function. Application of moving average (MA) and conventional exponential smoothing (CES) methods is predominantly used by researchers to mitigate PV output power fluctuation problem. The main issue involved in these methods is they exhibit "memory effect", where energy storage devices are operated even though there is no significant fluctuation (Alam, Muttaqi, & Sutanto, 2014). In general memory effect is due to illogical distribution of weights associated with PV data points. Since the memory effect forces the energy storage to operate all the time, it decreases its lifespan. Therefore, it is necessary to design a ramp-rate control strategy which limits the PV ramp-rate within desirable level and also eliminate the memory effect.

1.3 Research Objectives

The aim of this research is to proposed a new energy management system (EMS) which is to operate the microgrid with lowest daily operating cost. In-order to achieve it the following objectives are defined:

(i) To model an EMS for a smart microgrid system consisting of PV plant, battery energy storage system (BESS) and fuel cell system.

(ii) To develop a ramp-rate control strategy to mitigate solar PV output fluctuation in the developed microgrid system.

(iii) To propose a new operating strategy referred to as "mix-mode" in the EMS to reduce the microgrid's overall daily operating cost.

(iv) To develop a BESS sizing method for the proposed "mix-mode" operating strategy based on metaheuristic methods.

(v) To propose an optimal power dispatch in EMS for the microgrid sources using receding horizon economic dispatch (RHED) approach.

1.4 Scope and Limitation

The main focus of this research is to present the EMS to operate the microgrid with lowest daily operating cost. This is particularly useful for network planning engineers and future researchers to benchmark their results. In this research an operating strategy namely "mix-mode" is proposed based on three operating strategies. The idea is to operate the microgrid with lowest daily operating cost by delivering the required real power to the load by efficiently managing the distributed energy resources (DERs) in the microgrid. Since the reactive power in the system can be compensated locally, only the active power is considered in this investigation. The EMS is suggested to assist the

system owner to exploit the BESS in the most efficient way. The proposed smoothing parameter in the solar PV ramp-rate control strategy is formulated based on actual solar PV ramp-rate. The proposed smoothing equation is effectively utilized to smooth out significant fluctuations. The smoothing parameter and the proposed smoothing equation can be applied on any range or size of intermittent solar PV plant since it does not involve any complicated computational method. The proposed ramp-rate control method can be used for both planning and real time application. However, for real-time application, the effectiveness of the proposed ramp-rate control approach can be realized only when the PV output power forecasting module is highly accurate. Here the proposed ramp-rate control method will eventually control the PV output power ramp rate within the desirable level. The proposed ramp-rate control method will not produce smoothed output like the MA method. Although significant PV output power fluctuations above the ramp-rate setting can be removed.

1.5 Research Methodology

In order to achieve the mentioned objectives, research methodology shown in Figure 1.1 is carried out. Literature review on different EMS for the grid connected microgrid is carried out. Then the modeling of grid connected distributed sources such as PV, battery, and fuel cell is carried out in PSCAD software. The EMS is proposed with PV output power smoothing functionality. Related to this, MA and CES methods are reviewed. Based on this the smoothing parameters which is based on PV output power ramp-rate is proposed. And based on this the proposed ramp-rate control strategy is formulated. The main aim of the EMS is to reduce the operating cost of the microgrid and related to it a operating strategy to reduce the microgrid's operating cost is proposed and a battery sizing method is also proposed. And finally the entire EMS is solved using receding horizon economic dispatch (RHED) approach and is compated with other

metaheuristic methods. The obtained results is implemented in PSCAD module for the grid conncted microgrid model.

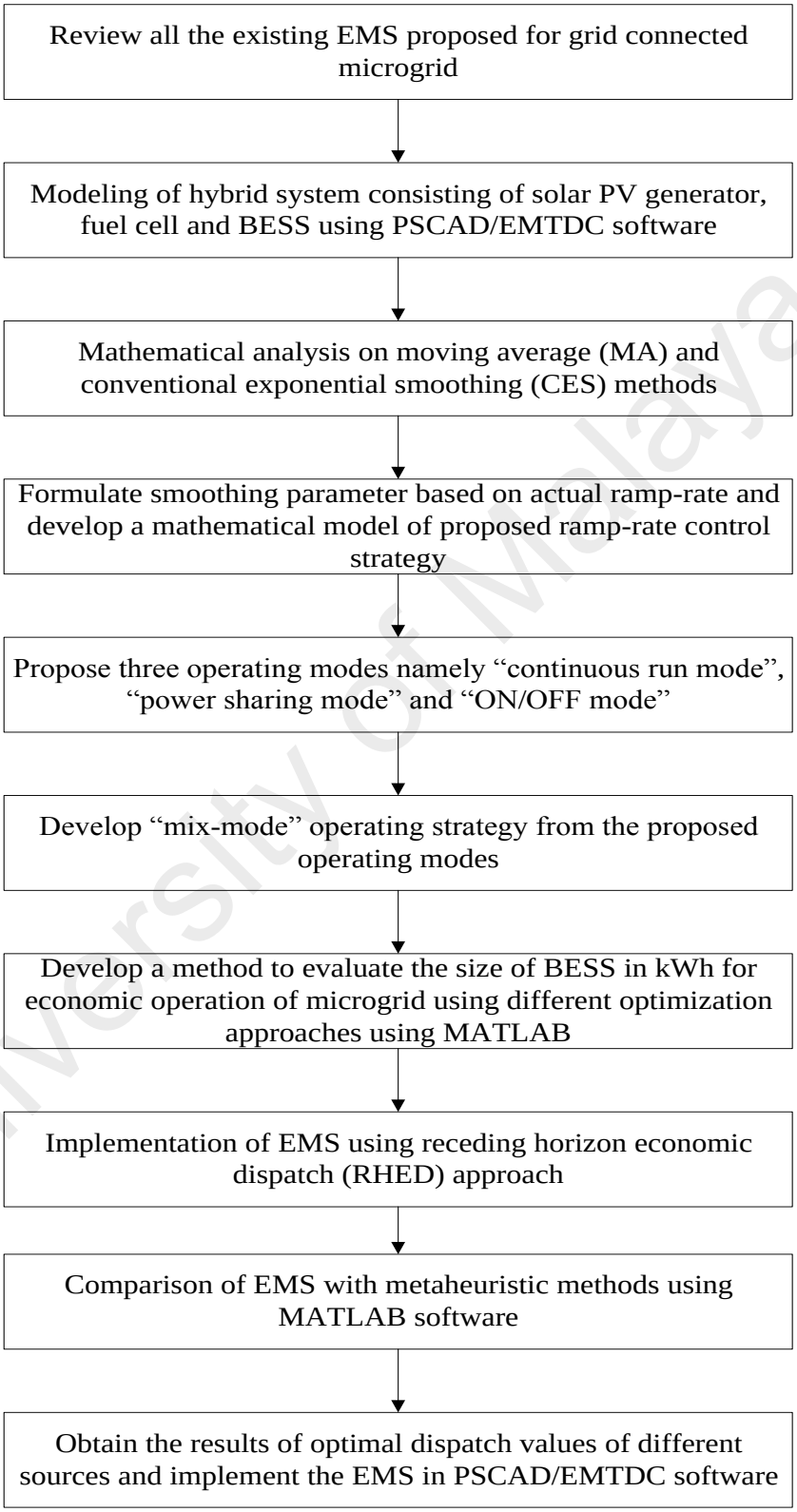

Figure 1.1: Flowchart for the research methodology

1.6 Thesis Outline

In this thesis, Chapter 2 summarizes the literature review associated with this thesis i.e. microgrid and distributed generation (DG) concepts, and technical impact of solar PV plant during grid connection. Various EMS implemented for grid connected microgrid systems are reviewed. In addition to this, sizing method for BESS and different PV output smoothing methods are also reviewed.

Chapter 3 presents the proposed microgrid configuration with its modelling. In this chapter, the methodology of the proposed energy management system, ramp-rate control strategy and the BESS sizing method for economic operation of microgrid is presented.

In chapter 4, simulation results are brought to the readers and technical matters are investigated in depth. The validation of the proposed ramp-rate control strategy is carried out. The results of the proposed ramp-rate control strategy are compared with MA and CES methods. In addition, the validation of "mix-mode" operating strategy and its comparison with other operating strategy is also carried out.

In Chapter 5, the results of proposed BESS sizing method are presented. Further the impact on microgrid's associated cost on BESS with different initial state of charge (SOC) levels is presented. The results of BESS capacity evaluated by different optimization techniques are also presented. A recommendation on choice of BESS initial SOC level during start of the day for microgrid's economic operation is suggested. In addition, the results of the proposed energy management system using RHED approach. Analysis of variation in microgrid's operating cost with and without the smoothing functionality is carried out. For the smoothing function the proposed ramp-rate control strategy is applied. In addition to it, performance comparison of the

proposed strategy using RHED approach with metaheuristic methods like PSO and evolutionary programming (EP) is also presented.

Chapter 6 concludes this thesis and the future research opportunities in this field are presented.

CHAPTER 2: LITERATURE REVIEW

2.1 Introduction

Microgrids are used to meet the increasing electricity demand. Normally, a microgrid consists of distributed energy resource (DER) such as solar, wind turbines, hyrdo, and fuel cells.

This chapter begins with an overview of microgrid and DER concept. Since solar PV generator is utilized in this research, the current condition of solar PV status in the world and the solar PV status in Malaysia is discussed completely. In addition to it the technical impact of solar PV on utility grid is also presented in detail. This chapter also provides a review on various energy management systems (EMS). A review on various sizing methods of BESS and PV output power smoothing methods is also discussed with its relative merits and demerits.

2.2 Microgrid Concept

Microgrid concept assumes a cluster of loads and microsources operating as a single controllable system that provides both power and heat to its local area (Lasseter, 2002). From the view of utility network operator, the microgrid can be considered as a controllable load which is able to support the main supply and keep the system stability during the transients. The microgrid also brings many advantages for the customers i.e. reducing feeder losses, improving voltage profile of the system, continuity of power supply (UPS application), and increasing the efficiency by using the waste heat and correction of voltage sag.

In the utility network microgrids are generally connected at the distribution level. They can supply different types of customers such as residential, commercial and industrial.

This categorization of loads is necessary in order to define the microgrid's expected operating strategy. Microgrid should be capable of operating in:

(i) Grid-connected mode;

(ii) Islanded (autonomous) mode;

(iii) Transition mode between grid-connected and islanded modes;

(iv) Ride-through (through voltage sags) for each DER in either grid-connected.

Ride-through capability is the ability of a power source to deliver usable power for a limited time interval during a power loss. A microgrid (as a power source) should be able to provide low-voltage ride-through (LVRT) capability when the voltage is temporarily drops due to a fault or load change in one, two or all the three phases of the AC grid.

In grid-connected mode, the utility grid can be taken into account as an electric "swing bus" which absorbs and/or supplies any power discrepancy in the microgrid to maintain the balance between the generation and demand. Generation or load shedding within a microgrid is also an option if the net import/export power limit does not meet operational limits or contractual obligations. In autonomous mode of operation, load/generation shedding is often required to stabilize the microgrid voltage and frequency. Also, the operating strategy must ensure that the critical loads of microgrid receive service priority. Load shedding and demand response (DR) are normally run and supervised through energy management system of microgrid (Katiraei, Abbey, Tang, & Gauthier, 2008; Lidula & Rajapakse, 2011).

2.3 Distributed Energy Resources (DERs)

A distributed energy resource (DER) refers to a distributed generation (DG) unit, a distributed storage (DS) unit or any combination of DG and DS units. In terms of prime mover (e.g. sunlight and wind) availability, DG systems are classified to two groups which are "dispatchable" and "non-dispatchable" entities. In the former case, DG guarantees the amount of power requested by the system operator provided that this value is within its power capability. Diesel gen-set plant and fuel cell are two examples brought to this end. However, in the latter case, as much as power (uncertain amount) which is available from the prime mover (such as sun and wind) can be transferred to the AC grid or stored in a storage system. DERs are divided in two groups based on their interfacing units to the AC power grid. The first group is interconnected through the conventional rotary systems such as synchronous generators and the second group is coupled through power electronic converters.

For an electronically interfaced (EI) DG (EIDG) unit, the interfacing converter provides a fast dynamic response for the system. Interfacing converter also is capable of limiting short-circuit current of the unit to less than 200% of rated current and thus extra fault current sent from the EIDG is practically prohibited by the voltage source converter (VSC).

Against to a rotary based DG unit, an EIDG unit does not exhibit any inertia during the microgrid transients and hence has no inherent tendency to keep the frequency of microgrid stable.

Interfacing converter can also minimize the dynamic interactions between the primary source of power and the distribution system (these reactions are normally severe in the case of conventional DG units) (Chowdhury & Crossley, 2009).

2.3.1 Utility Scale Distributed Energy Resource

A utility scale DER refers to a distributed energy power plant with a same capacity which is defined for a conventional fossil fuel power plant. For example, we can point out to a utility sized solar photovoltaic distributed generator system. This type of power plant is constructed from plenty of single solar cells which are mounted on a PV module/panel. Solar modules are usually installed in groups and each set have a separated supportive structure. Solar PV DG systems can be designed in order to track the sun in the sky through single or double axis tracking mechanisms (Bhatnagar & Nema, 2013; Eltawil & Zhao, 2013). In double tracking system the solar radiation input is higher but it is complex and expensive than the first type. In short, the utility scaled DG system term reflects a large commercial or industrial DG based power plant which is able to supply the three-phase loads more than 1MW (IEEE, 2000; Katiraei & Agüero, 2011; Photovoltaics, 2009; Sørensen et al., 2008).

2.3.2 Medium and Small Scale Distributed Energy Resource

Medium scale DER refers to an electricity generation plant which can supply electrical power for both single and three phase loads between 10kW to 1MW.

The small scale DERs where their capacity of generation is less than 10kW and hence they are commonly prone to supply single-phase loads (IEEE, 2000; Katiraei & Agüero, 2011; Photovoltaics, 2009; Sørensen et al., 2008).

2.4 Status of non-dispatchable solar photovoltaic DERs and its related issues

2.4.1 Solar Photovoltaic Status in the World

Solar energy is the fundamental source for all sorts of energy resources on the earth. There are generally two ways to produce electrical power from sunlight i.e. through solar thermal and photovoltaic (PV) systems. In this section and this dissertation, only solar PV system would be discussed.

Solar PV is a rapid developing renewable energy technology. Though the total capacity of solar PV installed in the worldwide is much less than wind power (about 50%), it has grown even faster than wind power throughout the past decade (from 2005-2014) (*Renewable Energy Policy Network for 21st Century (REN21), Renewables Global Status Report* 2015). The global PV capacity for the last 10 years (2005-2014) is shown in Figure 2.1.

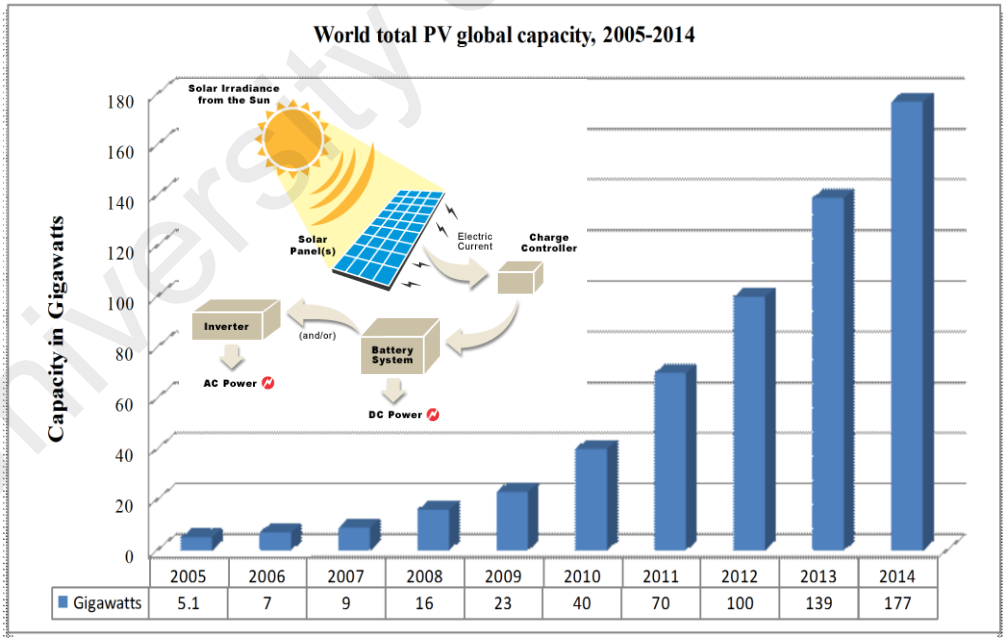

Figure 2.1: Global PV capacity between 2005-2014 (*Renewable Energy Policy Network for 21st Century (REN21), Renewables Global Status Report* 2015)

Due to improvements in semiconductor materials, device design, product quality, and the expansion of production capacity, initial investment for PV modules have been declined significantly, from about $1/W in 2001 to about $0.52/W in 2013. The cost of electricity (CoE) generated by solar PV systems keeps on dropping. It has decreased from $0.9/kWh in 1980 to about 0.2$/kWh today. In the U.S., the department of energy (DoE) goal is to reduce the CoE of PV to $0.06/kWh by 2020 (*International Energy Agency, PVPS Trends in Photovoltaic Applications*, 2014). There are many applications for which a PV system is the most economic long-term solution, particularly in inaccessible areas such as power for remote lighting, remote telecommunications, remote houses, and recreational vehicles (C. Wang, 2006). In general, energy from the solar PV is still more costly than energy from the local utility. Currently, the capital cost of a PV system is also higher than that of a diesel generator.

2.4.2 Solar Photovoltaic Status in Malaysia

By the end of 2011, total capacity of solar PV system installed in Malaysia was about 13.5MW. 2.5MW of this amount was grid-connected PV systems. More than 60% of the grid-connected solar PV plants in Malaysia are domestic installations and the rest is related to educational and commercial applications (PVPS, 2012). Although the financial support from the Malaysia Building Integrated Photovoltaic (MBIPV) project expired in 2010, the installation of grid-connected solar PV systems grew in order to complete the outstanding financially supported projects (PVPS, 2012).

PV policy developed significantly in 2011 in Malaysia. In this case, the government passed to approve the Renewable Energy (RE) Act 2011, the Sustainable Energy Development Authority (SEDA) Act 2011, and the associated implementation of a feed-in tariff (FiT) scheme. The opening share allocated to solar PV was 150MW over three years (50MW for every of years 2012, 2013 and 2014), with 90% assigned for commercial sector developments and 10% for households. House owners are permitted

to install up to 12kW solar PV for each application whereas the commercial entities are permitted up to 5MW for each purpose.

The country's major national electricity utility, Tenaga National Berhad (TNB) is one of the key stakeholders in order to implement the feed-in tariff scheme (TNB adds 1% extra charge on the electricity bill for those consumers who use above 300kWh of electricity monthly) (PVPS, 2012). This is put down into the RE Fund and is governed by SEDA Malaysia and will be utilized to pay FiT. A feature of the Malaysian FiT scheme is the e-FiT online system that provides the users with an online FiT processing system. This system gives this facility to the public to submit their applications through internet within three hours. Three hours start counting once the quota for any commercial sector project is completed (PVPS, 2012).

2.4.3 Technical Impacts of Solar Photovoltaic Plant

The intermittency nature of solar PV plant can affect the operation of main distribution power grid by creating steady-state and/or transient problems. The quantity of electricity produced from PV directly depends on intensity of sun light. Solar PV when connected to the grid have positive impact on the network. At the same time, they also can have a negative impact. The PV penetration relies on solar radiation which fluctuates daily, hourly and over a shorter period of time (minutes and seconds). Figure 2.2 shows a typical output power from PV plant due to changes in solar radiation.

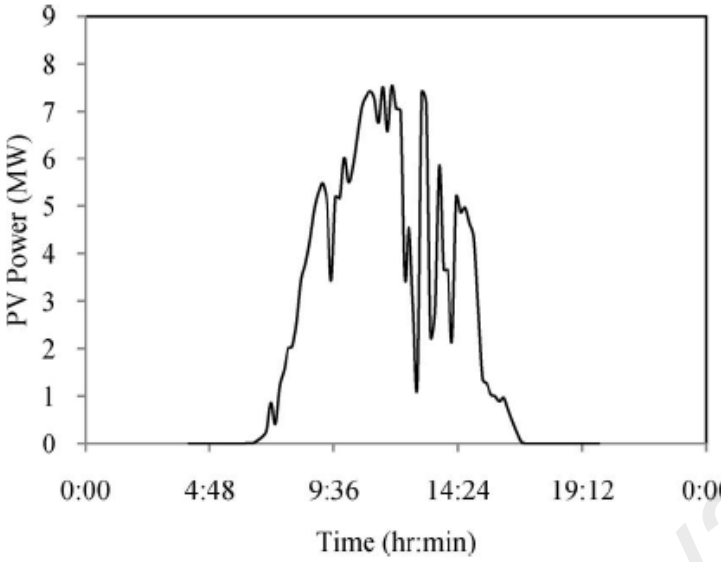

Figure 2.2: Typical output power from PV (Omran, Kazerani, & Salama, 2011a)

Estimating solar radiation is essential to determine the power generated by the PV. Predicting solar radiation using mathematical models based on artificial neural network (ANN) is found to be more accurate compared to the regression model, empirical regression model, empirical coefficient model, angstrom model and models based on fuzzy logic (Yadav & Chandel, 2014). A neural network model for predicting system output is done in (Giraud & Salameh, 1999) for a PV system connected with battery storage. The model can accurately predict the system output and the amount of battery capacity needed to compensate the PV output power fluctuation with the help of weather information and cloud pattern as inputs. Changes in weather conditions, rain fall and movement of clouds affect the output power from PV. The primary reason for output power fluctuation in PVs is due to movement of clouds (Lim & Tang, 2014).

Given below are some of the issues of PV output power fluctuation caused by cloud movement as reported by the researchers,

(i) When PV penetration increases, it is not easy for conventional generators in the system to track the quick change in PV generation (Anderson, 1985).

(ii) When PV output power changes rapidly, the area control error of two or more interconnected area may exceed its prescribed limit (Anderson, 1985).

(iii) Large uncontrolled PV penetration may change dispatch of regulating units in the utility causing a violation in dispatch regulating margins (Anderson, 1985; W. T. Jewell & Unruh, 1990).

(iv) Frequent changes in PV output caused by changes in cloud pattern increases overall operating cost of the system (W. Jewell & Ramakumar, 1987; W. T. Jewell & Unruh, 1990).

Due to these negative impacts, some power utilities had imposed ramp limits to control output power from intermittent renewable generation. Puerto Rico Electric Power Authority (PREPA) for example has suggested limiting the ramp-rate from wind turbines and PV to be within 10% of rated capacity per minute (Gevorgian & Booth, 2013). By having this limit the impact of voltage and frequency fluctuation in grid side could be minimized.

High penetration of intermittent PV cause voltage fluctuations in grid, voltage rise and reverse power flow, power fluctuation in grid, variation in frequency and grounding issues. PV penetration in low voltage distribution network also causes harmonic distortion in current and voltage waveforms (Karimi, Mokhlis, Naidu, Uddin, & Bakar, 2016). PV inverters are the main source of injecting current harmonics into the distribution system. The injected current harmonics can cause voltage harmonics and increases total harmonic distortion level in the system. These harmonics can increase the losses in the distribution system. A review on dynamic and static characteristics on integrating very large scale PV plant with utility is carried out in (Ding et al., 2016). It was found that fluctuations in output power found in large scale grid connected PV

plants can affect the system's primary and secondary frequency regulation resulting from significant real power imbalance on the grid side. Since PV has no inertia, integrating large PV plants as a substitute to conventional generators reduces the effective inertia of the bulk power system, which in turn causes the system to have poor ability to cope with frequency fluctuations caused due to frequent output power changes. A review by (Shah, Mithulananthan, Bansal, & Ramachandaramurthy, 2015) also discussed the impact of very large scale PV when integrated with the utility and grid code requirement which would facilitate interconnection of large scale PV system with the utility grid. Since the regulation varies from one system operator to another the authors insist on developing necessary standards globally to facilitate integration of very large MW (megawatt) scale PV plant with utility grid which helps the PV equipment manufacturers and developers to reduce additional manufacturing cost.

The movement in cloud influences change in output power which also depends on size of the PV plant. The larger the size of PV plant lower the output power fluctuations. Shorter the sampling time higher the significance of the smoothing effect (Marcos, Marroyo, Lorenzo, Alvira, & Izco, 2011). In (Denholm & Margolis, 2007; Eltawil & Zhao, 2010) authors illustrate challenges faced when large scale PV installations interact with existing grid utility. Due to random fluctuations, it is difficult to prepare the scheduling of PV for electricity generation. The PV output fluctuations can be limited by using additional sources like battery, capacitors, diesel generators, fuel cell, controlling maximum power point tracking (MPPT) to control output power from PV generator or by installing dump load to divert excess power. There has been an intense research activity in the field of RES and the problems associated with it.

Installing PV in feeder would contribute to problems like frequency deviation and voltage fluctuation in electric power system. In this section important issues such as (i)

Grid connected voltage fluctuation, voltage rise and reverse power flow, (ii) unintentional islanding, (iii) power fluctuation in grid and (iv) effect in grid frequency are discussed below.

(i) Grid connected voltage fluctuation

Voltage fluctuation is the change in voltage from the prescribed value. It is problematic when it deviates from the specified limit. PV is not only affected by the change in grid voltages but also sometimes cause voltage fluctuation themselves. Movement of clouds is also a source for induced voltage fluctuation however, the magnitude of voltage fluctuation is independent of cloud cover (Woyte, Van Thong, Belmans, & Nijs, 2006). The impact of voltage fluctuations has been explained in (Lim & Tang, 2014; Y. Liu, Bebic, Kroposki, De Bedout, & Ren; Woyte et al., 2006).

Voltage regulation is an issue when power from intermittent sources increases during grid operation. When PV penetration increases the voltage level at the substation also increases. The voltage level at the substation may violate the limits in presence of capacitor bank or voltage regulating devices which are normally installed in substations to boost the voltage. The possible way to solve this issue is to limit the PV real power generation. When cluster of intermittent PV are connected to low voltage (LV) distribution network, the voltage will raise with the reverse flow of power from the intermittent source towards the substation. During this voltage rise the power output from the PV should be restricted and continuing with this problem the intermittent power source has to be disconnected from the LV network (Hara et al., 2009). Figure 2.3 depicts the problem of voltage rise locally. The voltage across the distribution line decreases from sub-station until it reaches the point of PV connection. The voltage rises immediately after connecting PV at points A and B. To avoid further voltage rise beyond its acceptable upper limit the PVs at point C and D are disconnected. In addition

to it reverse power flow destabilizes the control system of voltage regulators since they are designed for unidirectional power flow and also trigger the protection relay which may possibly disconnect the load.

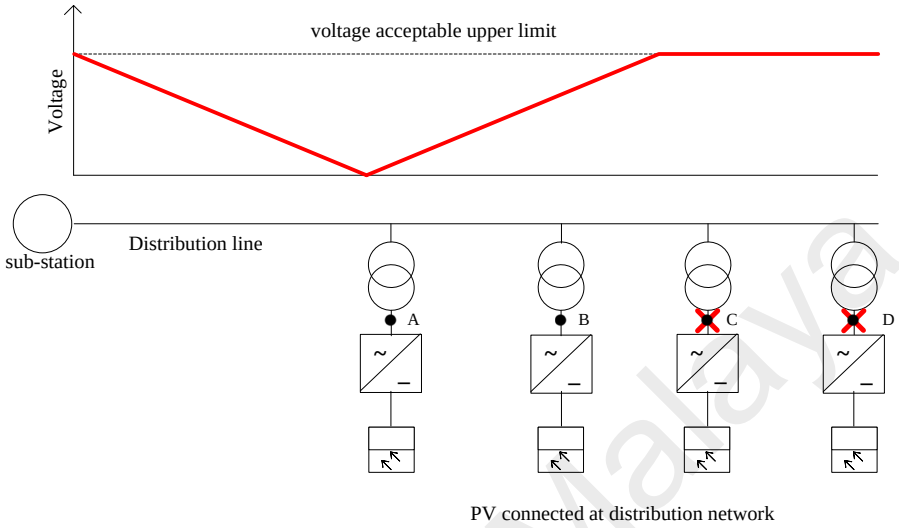

Figure 2.3: Problem of voltage rise at distribution network

Authors in (D. Cheng, Mather, Seguin, Hambrick, & Broadwater) have recommended ways to handle the reverse power flow problem in the distribution network. The authors recommended the use of phase balancing from the utility side to mitigate single phase reverse power flow and use of bidirectional regulators to maintain voltage regulation and check three phase reverse power flows. Reactive power control for PV inverter was suggested by authors in (X. Liu, Cramer, & Liao, 2015) to improve distribution system operation. The reactive power control method mitigates distribution system voltage magnitude fluctuation caused by short term solar power fluctuation. Literatures also suggested the use of dump load and energy storage devices to mitigate the voltage rise problem. Authors in (Weckx, Gonzalez, & Driesen, 2014) suggested curtailment of both active and reactive power by locally controlling the PV inverter to avoid voltage rise.

Another important issue pertaining to variable power output from PV is voltage flicker. Figure 2.4 illustrates voltage flicker where the variation in voltage peaks (waveform

inserted in Figure 2.4) caused by PV output power variation induced by movement of clouds.

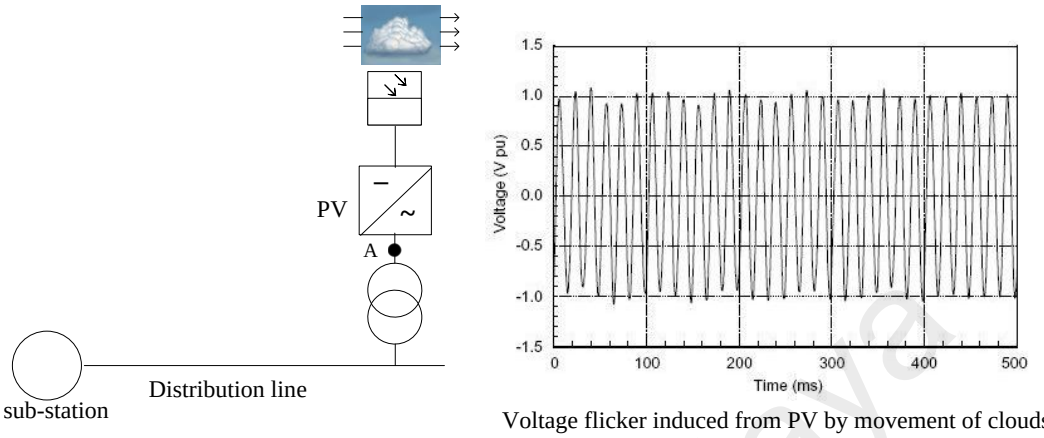

Voltage flicker induced from PV by movement of clouds

Figure 2.4: Voltage flicker induced from PV by movement of clouds

This problem occurs when rapid changes in PV occurs due to clouds passing which will lead to sudden changes in voltage level. Literature has suggested many ways to handle the voltage rise problem (Whitaker, Newmiller, Ropp, & Norris, 2008).

(ii) Unintentional Islanding

Unintentional islanding occurs when a fault occurs in distribution level, during which the power generated from PV is equal to load demand. The power interruption from the grid side cannot be sensed by the PV system and PV continues to generate power to the load. However for safety concerns PV system has to stop generating power. This state is called "Unintentional Islanding" (Hara et al., 2009).

Remote, active and passive are the methods used to detect unintentional islanding. Remote islanding technique is associated with utility side and is based on communication between PV inverter unit and utility. Although it is more reliable than active and passive techniques, it is expensive to implement and involve complex communication techniques (Ku Ahmad, Selvaraj, & Rahim, 2013). During active

method the islanding is detected by inducing an intentional disturbance such as active or reactive power fluctuations to the grid. However these disturbances also contribute to power quality issues. These intentional disturbances may also affect the performance of PVs when connected in cluster. The passive island detection method works on examining a sudden drift in parameters like voltage, current, frequency, active power or reactive power when islanding occurs. The passive method works well for large power system where the huge drift in parameters are easy to detect.

(iii) Power Fluctuations in Grid

Industries are widely affected when there is a grid disturbance. One of the main causes of disturbance is intermittent power output from PV and wind power. These sources do not deliver constant power continuously like nuclear, thermal or gas-fired plants. It is the challenge for the grid operator for the ability to predict the power produced from these intermittent sources. The fluctuation in the grid changes the voltage and frequency parameter which affects sensitive equipments in manufacturing units. Due to this problem battery backup and local generators are commonly used to protect sensitive equipment and control systems.

(iv) Effect to Grid Frequency

Frequency is one of the important factors in power quality. During grid interconnection frequency must be maintained uniformly. Usually load variation causes frequency deviation in the grid and it becomes worse when PV output power changes due to quick change in radiation level (Senjyu, Datta, Yona, Sekine, & Funabashi, 2007). Control of intermittent source output is necessary since increasing share of PV will affect power quality during grid interconnection. At present, frequency deviation due to PV penetration is less as compared to wind turbines. The frequency can be regulated by installing energy storage devices. Distributed storage can be used to regulate system

frequency for the area by charging or discharging the storage on operators command. In future, the frequency deviation due to increase in PV penetration will be noticeable.

2.5 Dispatchable Distributed Energy Resources (DERs)

A dispatchable unit refers to a DER whose output power can be set externally through an external supervisory channel such as the system operator. A dispatchable DER can be either a slow-response or a fast-acting unit (Chowdhury & Crossley, 2009). Batteries, flywheel, fuel cell and capacitors are few examples of dispatchable DERs. These sources can be exploited to bring ancillary services for the power grid (Barnes & Levine, 2011; Carbone, 2011; Divya & Østergaard, 2009; Droste-Franke et al., 2012; Haruna, Itoh, Horiba, Seki, & Kohno, 2011; Nasiri, 2008; Vazquez, Lukic, Galvan, Franquelo, & Carrasco, 2010).

2.5.1 Battery Energy Storage System

Battery energy storage system (BESS) can bring many benefits when they are connected with intermittent sources like solar PV and wind turbines. BESS can be used for mitigating power oscillation by absorbing or injecting required real power. In addition to this BESS is also used for frequency stability, voltage stability, and short and long duration power quality applications. BESS that are utilized for power applications have deep cycle characteristics. Lead acid batteries, sodium sulfur (NaS) batteries, Lithium ion (Li-ion) batteries, redox flow batteries, nickel cadmium and nickel metal hydride batteries are the types of batteries commonly used for power system applications. Use of sodium sulfur (NaS) batteries is limited to small scale utility power and automotive applications. NaS batteries are typically used for short duration power quality applications. NaS batteries are high energy storage devices but the use of ceramic electrolyte induces high heat during its operation. As a result thermal driven mechanical stress is evident in NaS batteries. Therefore the protective circuit of NaS batteries are

complex. Application of lithium ion batteries can be found in (Clark & Doughty, 2005). High cost, complex protective circuit, self discharge, overcharging and overheating are few important disadvantages of lithium ion batteries to mention. The degradation of lithium ion batteries is larger than any other batteries and it was recorded that the degradation is about 2% in 37 cycles (Kan, Verwaal, & Broekhuizen, 2006). Nickel cadmium batteries are ranked alongside lead acid batteries in terms of maturity. High energy density and low maintenance cost are few advantages of nickel cadmium batteries. Nickel cadmium can also be used for renewable integration applications and offers increased system reliability, and longer life. Nickel cadmium batteries are large in size, contain toxic heavy metals and suffer from severe self discharge.

The Use of lead acid batteries for PV and wind system is found in (Chang et al., 2009). Lead-acid batteries are ideal for renewable energy integration applications as they can discharge continuously as much as 80% of their capacity. They are suitable for grid connected energy management applications where users buy or sell power through net metering (Nair & Garimella, 2010). The dominant position of lead-acid batteries in PV systems may decline due to introduction of new battery types, but the demand for lead acid batteries will increase with the rapid development of the PV industry. Lead-acid batteries, especially the floating valve regulated lead acid (VRLA) design or the improved one based on VRLA, and the open flooded types, have a dominant advantage in PV/wind power generation systems at present by virtue of their particular technology and cost advantages. The application of lead acid batteries as backup for PV generators which is used to supply power to communication systems is found in (Chang et al., 2009). One battery pack was 48 V, 300 Ah. Solar energy provided the power to the loads during the day, the excess power is used to charge the battery packs while the battery packs supply power to the loads at night. An application of lead acid battery bank operated parallel with PV system for load following application is found in (Hua,

Zhou, Kong, & Ma, 2006). Here the combination of PV and lead acid battery supply power to varying load. If the output power from PV output power exceeds the load the excess power is used for charging the battery. During the night time the lead-acid battery bank is used to supply power to the load. It was concluded that the lead acid batteries displays good cycling life therefore making ideal choice to stand-alone applications in remote area. Application of lead acid batteries for smoothing PV output power is evident in (Koohi-Kamali et al., 2014). Here the charge controller of the lead acid battery bank is controlled accurately to supply or absorb power in order to stabilize the grid connected microgrid. Here the lead-acid battery also participates in voltage regulation by supplying adequate reactive power to the load. Application of lead acid batteries for hybrid energy system and microgrid can be found in (e Silva & Hendrick, 2016; Khalilpour & Vassallo, 2016; Lujano-Rojas et al., 2016; McKenna, McManus, Cooper, & Thomson, 2013; Mohammedi, Rekioua, Rekioua, & Bacha, 2016). Low self discharge, high unit voltage, cheaper investment cost and less maintenance cost have forced users to choose lead-acid batteries for power system application. Performance at low and high ambient temperature and unfriendly lead content are few limitations of lead-acid batteries to mention. Despite the disadvantages, lead-acid batteries are widely used for large scale power and renewable energy integration applications. As a result lead-acid batteries account for 75% of the PV/wind power system market.

2.5.2 Solid Oxide Fuel Cell (SOFC) System

A fuel cell is an electrochemical device that converts chemical energy for a fuel into electricity and heat as a byproduct without combustion. Like conventional power generation methods fuel cells are not limited by thermodynamic limitations such as the Carnot efficiency. The electricity generated from the fuel cell can be used as residential power stations, transportation and military services. The heat produced as a byproduct from the chemical reaction can be used for any other applications e.g. space heating.

Compared to other distributed sources used for power generation applications, fuel cell have shown their potential for power generation application due to low or almost zero emission, quiet in operation and high reliability over other DGs. Since fuel cell is quiet in operation it can be installed very near to the load centers. Another major advantage of fuel cell is that it can be utilized for long term applications. Despite the advantages fuel cell is one of the emerging distributed generation technologies that have been hindered by high initial costs. However the costs are expected to decline as manufacturing capacity and capability increases and improvement in designs happens. Fuel cell offers high efficiency than conventional power plants. Further the efficiency of the fuel cell can be improved by effectively managing the waste heat.

There are different types of fuel cell available such as polymer electrolyte membrane fuel cell, direct methanol fuel cell, alkaline fuel cell, solid oxide fuel cell, and molten carbonate fuel cells. Due to flexibility in fuel input and high power density, SOFC is widely used for large scale electric power applications. SOFC allow conversion of a wide range of fuels, including various hydrocarbon fuels. SOFC operates at 600-1000'C where ionic conduction by oxygen ions takes place. SOFC systems have demonstrated high efficiencies of any power generation system, combined with low air pollutant emissions. These capabilities have made SOFC an attractive emerging technology for stationary power generation between 2kW to few MW capacity range. SOFC converts chemical energy in hydrogen (H_2) and oxygen (O_2) directly into electrical energy. The basic reactions at the two electrodes of SOFC is described as in equation 2.2 (Blomen & Mugerwa, 2013; Larminie, Dicks, & McDonald, 2003),

$$\text{Anode: } H_2 + O^{=} \rightarrow H_2O + 2e^{-}$$

$$\text{Cathode: } \frac{1}{2}O_2 + 2e^{-} \rightarrow O^{=} \qquad (2.2)$$

DC current in the electrical circuit connected across the two electrodes due to the releasing of the electrons ($2e^{-}$) at the anode. The well-known Nernst equation is used to calculate the internal EMF generated by the SOFC stack and is given in equation 2.3 as,

$$E = N_0 E_0 + E_f \ln\left(\frac{pH_2 pO_2^{0.5}}{PH_2O}\right) \tag{2.3}$$

SOFC can be classified as electronically interfaced DG which is dispatchable. This means that the operator can decide about the amount of power that can be delivered by the SOFC at anytime, satisfying all operational constraints. The feasibility of using SOFC as a stationary power plant along side with other renewable energy source has been studied by researchers in (Blomen & Mugerwa, 2013; Hall & Colclaser, 1999; Hatziadoniu, Lobo, Pourboghrat, & Daneshdoost, 2002; Krumdieck, Page, & Round, 2004; Larminie et al., 2003; Y. Li, Rajakaruna, & Choi, 2007; Padulles, Ault, & McDonald, 2000; Ro & Rahman, 1998; Sedghisigarchi & Feliachi, 2004a, 2004b; Zhu & Tomsovic, 2002). For example, a 100kW SOFC plant was made operational in Netherlands (Hassmann, 2001). The system achieved continuous operation of SOFC for more than 15000hours. During the test it was found that the characteristics of SOFC plant that is electrical efficiency, emission and noise have met or even exceeded the expectations. Similarly analysis of SOFC 220kW plant was also carried out in Pittsburgh, Pennsylvania. The performance of this SOFC plant can be found in (Hassmann, 2001).

SOFC technology fits in the global picture with a variety of power generation technologies. The total market volume in the distributed heat and power generation sector amounts to 100,000MW where SOFC has 5% of this market potential (Hassmann, 2001). Active R&D activities on cost reduction of SOFC power plants are

taking place in a rapid phase. Development is under way to improve the SOFC design in-order to improve the performance of SOFC reformer. By improving the SOFC reformer it is possible to speed up the chemical reaction in generating electricity which could force SOFC fuel cell as ideal candidate for PV output power smoothing applications. In long term applications SOFC can run using liquid fuels which favors SOFC power plants to be used in remote areas and even in remote villages in developing countries. Smaller SOFC units can be used for residential applications for long term use.

2.6 Smoothing PV output power fluctuation using energy storage technologies

Storage devices assist in performing one or more important tasks such as (i) smoothing power fluctuation, (ii) shift peak generation period, (iii) protection during outages when installed along with large PV generation (Omran, Kazerani, & Salama, 2011b). Control strategy for a grid-connected PV, battery storage is proposed by(Daud, Mohamed, & Hannan, 2013) to smooth output power fluctuations from PV. The optimal size of the battery storage is estimated by optimizing a multi-objective function using genetic algorithm for a 1.2 MW PV plant. Operating efficiency of the proposed controller is reported as 84% and the state of charge (SOC) controller reduces the size of battery by 2% from 300 kWh to 294 kWh. It is also observed that the non-linear parameters like battery impedance, self-discharge resistance affect the charging and discharging of batteries. It is also suggested that the proper representation of battery storage contribute to accurate SOC estimation and improves controller design. A day ahead dispatch smoothing model is optimized using linear programming for a PV, wind, battery hybrid system when connected with the grid connection (Akhil et al., 2013). The combined output of PV and wind is smoothed effectively by charging and discharging the battery system. A rule based controller for battery is designed in (Teleke, Baran, Bhattacharya,

& Huang, 2010) for optimal use of lead acid battery storage. The authors achieved effective smoothing of PV output where the battery is dispatched on hourly basis.

A power management system is developed in (Koohi-Kamali et al., 2014) which balance real and reactive power independently with current controller and is capable of smoothing the output power fluctuations from PV. A microgrid consisting of diesel power plant, PV and battery storage is considered in this study. The power management system works on operator decision. The design and size of the lead acid battery is accurately found by following the developed guideline algorithm. The authors observed the reduction in computational burden and the effective smoothing was carried out by applying moving average filtering method. In (Hill, Such, Chen, Gonzalez, & Grady, 2012) presents challenges of operating PV in grid connection mode and explains different modes of operating the battery storage in solar-grid connected mode. The authors focused on ramp rate control, frequency response and reactive power support for a battery storage integrated with PV installed in Hawaiian Islands. They reported that, integrating PV with battery will improve the economics. PV-battery storage also provides voltage and frequency regulation services. The battery storage act as a centralized storage installed in distribution feeder since the control of battery in centralized storage is easy.

Sodium Sulphur (NaS) batteries were used to suppress PV output power fluctuations, where the hybrid method involving moving average and fluctuation center to produce reference set point for NaS battery bank (Akatsuka et al.). Results show the performance of hybrid suppression method is almost same when compared to moving average method and it is also estimated hybrid suppression method requires battery with low power capacity and high energy capacity.

The ramp-rate of PV generators connected to grid can be controlled by electric double layer capacitor (EDLC) where the reference is generated using moving average method (Kakimoto et al., 2009). The capacitors absorb the difference of power between PV and inverter output. The expression for calculating the capacitor size was developed and it was found that the capacitor size decreases when ramp-rate decreases. Moreover the size of the capacitor is reduced by 10% to its projected size when the PV output is smoothed using moving average method. Euler moving average prediction (EMAP) method is applied to a system consisting of PV, fuel cell and EDLC, where the following objectives were achieved: (i) meeting customer power requirement, (ii) effective use of fuel cell, (iii) EDLC to compensate PV output, load demand and to (iv) maintain voltage stability (Monai, Takano, Nishikawa, & Sawada, 2004). EMAP is an effective method for optimal power sharing between fuel cell and EDLC. Furthermore, the size of EDLC is also reduced by 77% when compared to moving average prediction method.

The use of superconducting magnetic energy storage (SMES) with intermittent sources shows its effectiveness in maintaining load side frequency (Jung et al., 2009). It was found that the increase in SMES capacity maintains the frequency within the limit. The SMES is combined with 4 kW PV facility to show that the PV output is fully utilized and is effective in leveling the PV output power fluctuations (Tam et al., 1989). The experimental results conducted at different weather conditions demonstrate that the PV output is effectively enhanced by using SMES.

Similarly, application of diesel generator, fuel cell and power curtailment by MPPT and dump load methods are effectively used to mitigate PV output power fluctuations (Senjyu, Datta, Yona, Sekine, & Funabashi) (Datta, Senjyu, Yona, Funabashi, & Kim, 2009) (Canever, Dudgeon, Massucco, McDonald, & Silvestro) (Senjyu et al., 2007)

(Tesfahunegn, Ulleberg, Vie, & Undeland, 2011) (X. Li, Song, & Han, 2008) (X. Li, Song, & Han) (Ina, Yanagawa, Kato, & Suzuoki, 2004) (Zarina, Mishra, & Sekhar, 2014) (Omran et al., 2011b) (Lim & Tang, 2014) (R Tonkoski, Lopes, & Turcotte) (Reinaldo Tonkoski, Lopes, & El Fouly, 2011).

Limiting PV output power is not recommended since it limits the revenue of the owners even though it is found to be an economical method for smoothing PV output. Effects like voltage fluctuation, reverse power flow and frequency deviation produced due to PV output fluctuations can be reduced by complementing PV with rapid energy storage technologies such as batteries, fuel cell, capacitors with more effective control. Performance comparison among different mitigation methods are summarized in Table 2.1. On comparing the performances based on vital characteristics such as response time, ability to mitigate fast ramp ups and downs and reliability in mitigating PV fluctuations, it was found that diesel generator and fuel cell were not able to mitigate fast ramp ups and downs. This is because the time taken by these sources to respond to this sudden change is slow. They were capable in supporting relatively slower ramp-ups and ramp-downs. On the other hand other mitigating methods were fast enough to mitigate PV ramp-ups and downs. MPPT control method and use of dump load is highly reliable but is not recommended to mitigate PV power fluctuations in large PV plants since it limits the revenue of the owners even though the cost is relatively very low. But they can be applied for relatively smaller PV installation of residential levels or up to community level.

Table 2.1: Comparison between different mitigating methods to mitigate PV power fluctuation using MA and CES methods

Characteristics	Battery	Capacitor/ EDLC/SM ES	Diesel gen	Fuel cell	MPPT method	Dump load
Response time of the source for mitigation problem	Fast	Very fast	Slow	Slightly slow	Fast	Fast
Short/long term storage application	Short	Short	Long	Long	Long	Long
Ability to mitigate fast ramp ups and downs	Yes	Yes very rapid	No	No	Yes	Yes
Efficiency in mitigating short term PV fluctuations	High	High	Low	Low	High	High
Ability to control voltage/frequency fluctuation due to PV power fluctuation in grid side	Yes	Yes	Yes	Yes	Yes	Yes
Reliable in mitigating PV fluctuations	High	Very high	Low	Low	High	High
Cost	High	High	High	High	Low	Low
References	(Akatsuka et al.; Omran et al., 2011a)	(Jung et al., 2009; Kakimoto et al., 2009)	(Datta et al., 2009; Senjyu et al., 2007)	(X. Li et al., 2008; Tesfahunegn et al., 2011)	(Ina et al., 2004; Zarina et al., 2014)	(Lim & Tang, 2014; Omran et al., 2011a)

Energy storage devices like battery, capacitors or SMES are suitable candidates for PV power fluctuation problem. Rapid changes in PV output power may induce unwanted voltage or frequency fluctuation at the point of interconnection. These changes can be efficiently mitigated with the help of battery or capacitors. Battery energy storage is most preferred for MW scale PV installations since batteries have high energy density, it can discharge power for longer duration that is even for hours. On the other hand capacitors or SMES are high power density devices which can discharge power only for few seconds and can be used to mitigate power fluctuation for smaller PV installations.

In addition, the capacitors/SMES have clear advantage over batteries as they are cost effective, have faster charging time and have longer life which proves to be an ideal candidate for small PV installation up to commercial scale. For capacitors or SMES, increasing the energy density is the key and this limitation hinders them from being implemented in multi MW scale PV projects. From the above discussion it can be seen that the battery storage is the ideal choice for mitigating PV output power fluctuations for PV installations of any size. In addition, when using fuel cell for power mitigation problem, the processing time taken by the fuel reformer to convert the necessary input to hydrogen to deliver required power is slow. Therefore this makes the fuel cell the second best choice for the power mitigation problem. Improvement in fuel cell reformer can eliminate the time delay where fuel cell technology can be a potential alternate to batteries in the future.

Moving average (MA) and conventional exponential smoothing (CES) were predominantly used by the researchers to produce appropriate reference values. The difference between the reference and the actual PV output power is the amount of power that is required by the energy storage to supply or absorb. The MA and CES methods depend on older data points. When there is no significant fluctuations in PV output the reference waveform produced using MA and CES methods deviates wider. This is because these methods heavily depend on previous or older data points which are termed as "memory effect". Therefore due to this reason the energy storage will operate unnecessarily even thought there is no significant fluctuation in PV output power.

2.7 Energy Management System (EMS) for microgrid operation

Efficient operation of a microgrid consisting of more than two distributed sources operated either in islanded mode or in grid-connected mode requires a power or energy

management system (Katiraei, Iravani, Hatziargyriou, & Dimeas, 2008). Quick response of EMS is essential for a microgrid because of the following reasons,

(i) microgrid consists of multiple distributed sources with different power, energy capacities and characteristics.

(ii) during it's autonomous operation there is no dominant source i.e., lack of infinite bus.

(iii) swift response of electronically interfaced distributed source may create voltage instability or angle instability when appropriate provisions are absent.

Figure 2.6 shows data or instruction flow of an EMS for a microgrid. The energy management block receives present value and forecasted values of load, generation and also the current market information i.e. utility electricity and energy pricing information. Using this information an appropriate reference output power for the dispatchable generation units in the microgrid are provided.

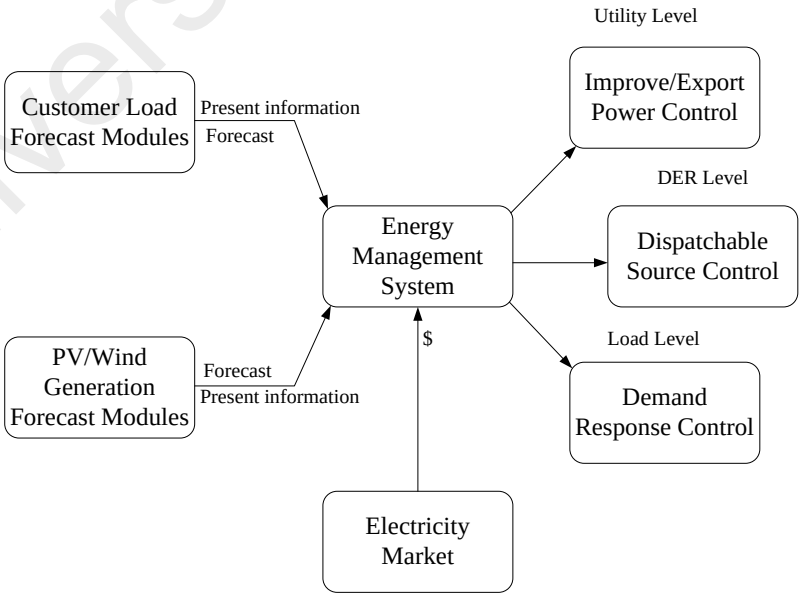

Figure 2.5: Functions of a real-time EMS for a microgrid (Katiraei, Iravani et al., 2008)

The EMS assigns the dispatchable sources present in the microgrid units to,

(i) Appropriately share the real and reactive power among the distributed sources in the microgrid.

(ii) Provide proper response to microgrid disturbances or transients.

(iii) Restore the frequency by balancing the power from the dispatchable sources.

(iv) Minimize the power imported from the utility grid during grid operation.

During the grid-connected operation of microgrid, the utility grid is expected to supply the difference in real or reactive power supply and the load demand within the microgrid. On the other hand during islanded operation of microgrid, the power to the load demand should be effectively managed by the distributed sources within the microgrid. If not, load shedding process is initiated inorder to strike the balance between the generation and load. In addition fast and flexible real/reactive power control strategy is required in order to minimize the impact in microgrid during events like PV output power fluctuations, unintentional islanding and frequency oscillations.

The EMS should be able to manage the microgrid both on short term and long term basis. During short term it is necessary for the EMS to, (i) provide voltage regulation and frequency restoration during transient events by providing smoothing sharing of real or reactive power by the distributed sources within the microgrid, (ii) provide power quality to sensitive loads and (iii) make available of resynchronization scheme to manage reconnection to the main utility grid. On a long term basis the energy management strategy should include, (i) necessities to continue an right level of reserve capacity while rescheduling the operating points of dispatchable source based on an optimization process to minimize power loss, control net power import from the grid

and to maximize the power output from the renewable sources, (ii) to manage the sources in the microgrid to operate economically that is, with minimum daily operating cost for long term basis considering the operating limits and constraints of the distributed sources in the microgrid and (iii) to provide demand response management by shedding of non-sensitive loads during appropriate time and to facilitate reconnection or restoration of the shed loads.

In (Zhou, Bhattacharya, Tran, Siew, & Khambadkone, 2011) a composite energy storage system (CESS) using dual active bridge (DAB) converter is proposed to manage the energy flow within the sources present in the grid connected microgrid. CESS consists of energy storage devices like batteries and ultracapacitors. The proposed dynamic EMS enhances (i) allocation of dynamic and steady power demands to batteries and ultracapacitors, (ii) smooth distribution of power flow between the energy storage devices, (iii) simultaneous charging and discharging of ultracapacitors without affecting normal operation and (iv) effortless allocation of additional energy capacity to CESS without disturbing normal operation. The combined use of energy storage technologies like batteries and ultracapacitors were exploited in (Dougal, Liu, & White, 2002; Glavin, Chan, Armstrong, & Hurley, 2008; Guoju, Xisheng, & Zhiping, 2010) for energy management purposes. In (K. Tan et al., 2013) an EMS algorithm is proposed to coordinate the power flow between the energy sources in the microgrid. The grid-connected microgrid consists of solar PV generator, fuel cell and lithium-ion battery energy storage system (BESS). In the proposed energy management algorithm the fuel cell is used as a backup unit to compensate for the power generated by the PV source. On the other hand the BESS is used for peak shaving applications and to maintain the stability during islanded operation.

In (K. Tan et al., 2012) an efficient EMS was developed for inverter based distributed generators to coordinate the smooth operation of sources in the microgrid in supplying the load. For this purpose the authors proposed a model predictive controller for the distributed sources inverter control. A centralized microgrid EMS is proposed by(Almada, Leão, Sampaio, & Barroso, 2016) to assist the control of electronically interfaced distributed sources of the microgrid during grid connection mode, islanded mode and during the transition between both the modes. The main concern of the proposed EMS is to supply power to the local load while maintaining the power quality of the whole system. The microgrid consists of solar PV generator, fuel cell and BESS and variation in electricity tariff for the whole day is considered while building this model. The disadvantage of the proposed microgrid model is, it does not consider economic operation of microgrid.

A centralized EMS is proposed for a standalone microgird in (Olivares, Cañizares, & Kazerani, 2014). The EMS uses receding horizon control approach and the energy management problem is solved using mixed integer linear programming in-order to reduce the computational burden. In the above references the energy management system does not consider economic operation of microgrid. It is absolutely necessary for the power system operator to operate the microgrid sources in an economical way. In order to operate the microgrid in an economical way that is with reduced daily operating cost or generation cost, economic dispatch of the microgrid sources has to be done.

Researchers have also focused on solving economic dispatch problem of microgrid sources in their EMS. Predominantly numerical methods and metaheuristic methods are used by researchers to solve the economic dispatch problem of microgird for a particular operating strategy as an energy management solution. Therefore the literature

review on EMS is divided into two sections that are, solving the microgrids's economic dispatch problem using numerical methods and metaheuristic methods.

2.7.1 EMS using numerical methods

Solving the economic dispatch of microgrid sources using numerical methods are reviewed in this section.

A model to economically operate the grid-connected microgrid considering the load demand and environmental constraints is presented in (Mohamed & Koivo, 2010, 2012). The constrained optimization problem is solved using mesh adaptive direct search (MADS) numerical optimization method. The schedule of microgrid sources and its optimal capacity is found using linear programming method in (Hawkes & Leach, 2009). A mixed integer linear programming (MILP) model is developed in (Ren & Gao, 2010) to evaluate optimal dispatch of distributed units used in the microgrid. The optimal EMS is proposed by optimizing the total generating cost considering the economic and environmental constraints. A mathematical model of EMS for the microgrid operated both in grid-connected and islanded mode is presented in (Tenfen & Finardi, 2015). The optimal dispatch of the sources present in the microgird is optimized using MILP optimization technique by minimizing the generation cost as the objective function.

A tiered EMS is proposed by(Hooshmand, Asghari, & Sharma, 2014) for grid-connected microgrid where the economic dispatch problem is solved using MILP optimization technique. In order to implement the proposed management strategy in real-time scenario the proposed EMS is solved as a receding horizon economic dispatch (RHED) problem. A double layer coordinated EMS for operating the microgrid in both grid connected and islanded mode is proposed by (Jiang, Xue, & Geng, 2013). The proposed EMS considering economic operation of microgrid is solved using MILP

optimization method. Use of mathematical or numerical method in solving the energy management problem can also be found in (Dai & Mesbahi, 2013; Marzband, Sumper, Domínguez-García, & Gumara-Ferret, 2013).

2.7.2 EMS using metaheurictic methods

Use of metaheuristic methods to solve the energy management problem can be found the literature. However the use of metaheuristic methods like particle swarm optimization (PSO), genetic algorithm (GA) or evolutionary programming (EP) optimization techniques have few implementation issues. The search space of these methods is restricted by the method's boundary condition. In addition the population generated in these optimization techniques is randomly governed and due to this, solving the equality constraint like matching the power flow between generation and load is difficult.

In (Guo, Bai, Zheng, Zhan, & Wu, 2012) the optimal generation dispatch is solved as a multi objective dispatch problem where the generation cost, reserve capacity of the sources and environmental emission of greenhouse gases are minimized using PSO. The energy management problem is solved in (Marzband, Ghadimi, Sumper, & Domínguez-García, 2014) using multiperiod gravitational search algorithm (MGSA) considering system constraints. The objective is to minimize the overall system operation cost. In (Kalantar, 2010) integration of wind turbine, solar PV generator, microturbine and BESS is made feasible by EMS. The EMS of the autonomous microgrid is solved using GA. The objective is to obtain the optimal size and minimize the operating cost of the microgrid. Similarly, GA was used in (Mousavi G, 2012) for systematic operation of autonomous microgrid in order to provide sufficient electrical energy supply for the load demand all the time.

In (Y.-S. Cheng, Chuang, Liu, Wang, & Yang, 2016) PSO based on roulette wheel re-distribution mechanism is proposed to solve the energy management of grid-connected microgrid. The roulette wheel re-distribution mechanism is proposed by the authors to solve the equality constraint that is to match the power flow between the generation and the load. An EMS is proposed for islanded microgrid consisting of wind turbine, solar PV generator, BESS and proton exchange membrane (PEM) fuel cell aided by bioethanol reformer in (Feroldi, Degliuomini, & Basualdo, 2013). The EMS is solved by minimizing the total generation cost using GA optimization technique. Use of metaheuristic methods in solving the microgrid's energy management problem can be found in (Abedi, Alimardani, Gharehpetian, Riahy, & Hosseinian, 2012; Baziar & Kavousi-Fard, 2013; Berrazouane & Mohammedi, 2014; García, Torreglosa, Fernández, & Jurado, 2013; Park, Lee, & Shin, 2005; Sharafi & ELMekkawy, 2014).

A summary on different EMS using metaheuristic and mathematical methods are provided in Table 2.2.

Table 2.2: Summary on different EMS using metaheuristic and mathematical methods

References	Objective function used	Proposed optimization method	Solution time step	Demerits
(Mohamed & Koivo, 2010)	Minimization of microgrid's operating cost	MADS	Hourly	(i) hourly based solution. (ii) one operating strategy or operating algorithm.
(Hawkes & Leach, 2009)		LP	Hourly	
(Dai & Mesbahi, 2013; Ren & Gao, 2010; Tenfen & Finardi, 2015)		MILP	Hourly	
(Hooshmand et al., 2014)		LP	Minute by minute	
(Marzband et al., 2013)		Mixed integer non-linear programming	half hour	
(Baziar & Kavousi-Fard, 2013; Y.-S. Cheng et al., 2016; Guo et al., 2012; Sharafi & ELMekkawy, 2014)		PSO	Hourly	(i) hourly based solution. (ii) one operating strategy or operating algorithm. (iii) random factor solving equality constraint is difficult. (iv) solution restricted by search space constraint. (v) time consuming. (iv) system considered is islanded microgrid.
(Marzband et al., 2014)		GSA	half hour	
(Feroldi et al., 2013; Kalantar, 2010; Mousavi G, 2012)		GA	Minute by minute	
(Feroldi et al., 2013)		GA	Hourly	
(Abedi et al., 2012)	Minimization of microgrid's operating cost + loss of electrical energy	Differential Evolution	Hourly	
(Berrazouane & Mohammedi, 2014)	Levelized energy cost+loss of power supply probability	Cuckoo search	Hourly	

2.8 BESS sizing methods for economic operation of microgrid

Application of battery energy storage system (BESS) in the microgrid influences its performance. Since the power produced from BESS is cheap it contributes to decrease in daily operating costs. Therefore it is important to estimate the energy capacity of the BESS necessary for economic operation of microgrid. The energy capacity of BESS is influenced by its initial capital cost.

A power management system is developed in (Koohi-Kamali et al., 2014) which balance real and reactive power independently with current controller and is capable of smoothing the output power fluctuations from PV. A microgrid consisting of diesel power plant, PV and BESS is considered in this study. The power management system works on operator's decision. The authors also proposed guidelines to estimate the capacity of lead acid BESS. The BESS sizing method is not accurate because the power management strategy does not consider economic operation of microgrid. Sizing of BESS involves finding optimal energy capacity in kWh with the aim of reducing microgrid's daily operating cost. An optimal sizing of BESS for microgrid is presented in (Chen, Gooi, & Wang, 2012). The author focuses on determining the size of BESS for microgrid operation. The optimal size of BESS for microgrid is formulated as a unit commitment problem for both islanded and grid-connected microgrid operation. The authors of this paper also try to find the relationship between the size of BESS and the total operating cost of the microgrid. The microgrid consists of intermittent generating sources like wind turbine and PV installations. Variations in output power from these sources were considered for building this model.

Optimal sizing of BESS using improved bat algorithm is presented in (Bahmani-Firouzi & Azizipanah-Abarghooee, 2014). In this paper authors proposed the new improved bat algorithm (IBA) to obtain the optimal energy capacity of BESS used for microgrid

operation. The grid connected microgrid consists of solar PV, wind turbine, microturbine, fuel cell and BESS to supply power to varying loads. The performance of the IBA algorithm is evaluated with other optimization techniques like artificial bee colony (ABC), conventional bat algorithm (CBA), teaching learning based optimization (TLBO) optimization techniques. It was found that IBA algorithm was robust enough to calculate the BESS size accurately with less standard deviation for more trials. Genetic algorithm based method for sizing BESS is proposed by (Fossati et al., 2015). The EMS employed in the proposed method is based on a fuzzy expert system that is used to set the power output of the BESS. Since the EMS depends on characteristics of BESS, both the EMS and BESS capacities are simultaneously optimized. In order to build adequate knowledge base for the expert system, genetic algorithm was used to set the fuzzy rules and membership functions held in the knowledge base. Since EMS influences the lifetime of the BESS, a lifetime prediction model was incorporated into the algorithm. In addition the genetic algorithm was also used to obtain optimal dispatch of the microgrid's energy sources. The developed model was evaluated on a grid connected microgrid.

In (Changsong Chen, Shanxu Duan, Tao Cai, Bangyin Liu, & Guozhen Hu, 2011) matrix real-coded genetic algorithm (MRCGA) is used to find optimal energy capacity of BESS. The optimization problem is solved by having the net present value (NPV) as the objective function. In (Sharma et al., 2016) grey wolf optimization (GWO) is applied to find the optimal capacity of BESS system by solving the operation cost minimization problem of microgrid. The effectiveness and superiority of the results obtained from GWO is compared with other optimization techniques such as genetic algorithm (GA), particle swarm optimization (PSO), bat algorithm (BA), improved bat algorithm (IBA), tabu search (TS), differential evolution (DE), biogeography based optimization (BBO) and teaching learning based optimization (TLBO) techniques.

Minimization of total daily operating cost of microgrid is considered as the objective function. A detailed comparison of GWO with other optimization techniques based on computational time, convergence speed and performance of the solutions is presented and it was concluded that GWO algorithm may be considered as one of the strongest algorithm to solve different cost minimization related optimization problems of microgrid.

A smart energy management system (SEMS) is proposed by(Ci Chen et al., 2011) to coordinate the power forecasting, BESS and energy exchange between the sources in the microgird. The objective of the developed model is to minimize the daily operation cost. SEMS identifies optimal operating schedules based on available distributed energy resources equipment options and their associated capital and operating and maintenance costs, load forecasting, energy price structures and fuel prices. Matrix real coded genetic algorithm (MRCGA) is applied to minimize the microgrid cost. A method to evaluate optimal power and energy capacity of vanadium redox battery (VRB) was developed in (Nguyen, Crow, & Elmore, 2015). The microgrid consists of solar PV generator, VRB battery bank and a distributed generator operated in parallel with the load. The case studies were performed on microgrid operated both in islanded and grid-connected mode. Like the above mentioned references there are different methods developed by the researchers to find optimal BESS capacity and can be found in (Aghamohammadi & Abdolahinia, 2014; Arun, Banerjee, & Bandyopadhyay, 2008; Bahramirad, Reder, & Khodaei, 2012; Borowy & Salameh, 1996; Elhadidy & Shaahid, 1999; Fossati et al., 2015). A summary of different battery sizing method is provided in Table 2.3.

Table 2.3: Summary on different BESS sizing method

References	Objective function used	Proposed optimization method	Solution time step	Demerits
(Koohi-Kamali et al., 2014)	-	-	Hourly	(i) inaccurate (ii) solution is hourly basis. (iii) sizing is calculated manually.
(Chen et al., 2012)	Minimization of microgrid's operating cost+BESS capital cost	-	Hourly	
(Bahmani-Firouzi & Azizipanah-Abarghooee, 2014)	Minimization of microgrid's operating cost+BESS capital cost	IBA	Hourly	
(Sharma et al., 2016)	Minimization of microgrid's operating cost+BESS capital cost	GWO	Hourly	
(Nguyen et al., 2015)	Minimization of microgrid's operating cost+BESS capital cost	-	Hourly	
(Aghamohammadi & Abdolahinia, 2014)	-	-	Hourly	
(Arun et al., 2008)	Minimization of microgrid's operating cost+BESS capital cost	-	Hourly	
(Bahramirad et al., 2012)	Minimization of microgrid's operating cost+BESS capital cost	-	Hourly	
(Fossati et al., 2015)	Minimization of microgrid's operating cost+BESS capital cost	GA	Hourly	

From the previous studies, some of the researchers try to optimize the operation of microgrid without accurately evaluating the BESS capacity. In most of the literature where the BESS energy capacity is evaluated, the microgrid's economic operation is performed on hourly basis. The evaluated BESS capacity may not be accurate if the microgrid's economic dispatch is performed on hourly basis that too with the presence

of intermittent sources like solar PV generator. The short term variation in PV output power influences the microgrid's operating performance. Therefore it is essential that the BESS capacity and microgrid's economic dispatch is simultaneously optimized on minute-by-minute basis. In addition to that the operating strategy proposed by the researchers also influences the microgrid operating cost and BESS's energy capacity. Majority of the literature focused in single operating strategy of microgrid which may not necessarily incur lower operating cost. Therefore the BESS capacity for the microgird's economic operation should be optimized for the operating strategy which incurs lowest operating cost and the optimization problem should be solved on minute-by-minute basis.

2.9 Summary

It was found that battery storage, capacitors, SMES or EDLC can be idle source used for smoothing PV output power. In addition to it, it was found that MA and CES methods are predominantly used to control PV output power ramp-rates. Both the MA and CES method exhibit memory effect. Memory effect allows the energy storage to operate even though PV output power ramp-rate is within the limit. Therefore a new ramp-rate control strategy which does not exhibit memory effect is essential to limit the significant PV output power fluctuations thereby increasing the lifespan of energy storage technologies.

The efficient operation of two or more distributed sources depends on design on energy management system (EMS). In the literature, microgrid's energy management problem was solved using numerical method and metaheuristic methods. It was found that solving the energy management problem using numerical methods is easy with less computational burden. Solving the microgrid's energy management problem using single operating strategy may not necessarily incur lower operating cost. Therefore it is

necessary to frame an EMS with an operating strategy where the microgrid sources are operated with lowest daily operating cost. Since BESS influences the microgrid operating cost the accurate evaluation of BESS is necessary. In this section different methodology of BESS sizing necessary for economic operation of microgrid is reviewed. There are different optimization approaches used to find optimal value of BESS size. Mostly population based algorithms like PSO, artificial bee colony (ABC) and evolutionary based algorithms like GA were used. In this research the proposed optimal BESS sizing method is solved using grey wolf optimizer (GWO) and the results were compared with metaheuristic techniques like PSO, ABC, GA, gravatitional search algorithm (GSA).

CHAPTER 3: METHODOLOGY OF THE PROPOSED ENERGY MANAGEMENT SYSTEM

3.1 Introduction

The proposed microgrid model is introduced in this chapter. The grid-connected microgrid consists of solar PV generator, solid oxide fuel cell (SOFC) system and battery energy storage system (BESS) supplying power to the load. An energy management system (EMS) which employs a novel "mix-mode" operating strategy to operate the grid-connected microgrid with lowest operating cost is presented. In this research the EMS is solved using receding horizon economic dispatch (RHED) approach. Therefore the concept of RHED operation is explained in detail.

Since BESS is present in microgrid, the methodology to accurately evaluate the size of BESS in kWh is presented in detail. Further the proposed ramp-rate control strategy to limit the PV output power fluctuation is also presented.

3.2 Proposed Microgrid Configuration and Operation

3.2.1 Overview

The proposed microgrid is completely electronically interfaced and is operated in grid-connected mode. Figure 3.1 shows the configuration of the proposed grid-connected microgrid. The microgrid model consists of solar PV installation and two controllable distributed sources which are solid oxide fuel cell (SOFC) and BESS. These sources are operated to supply power to varying load which are considered to be a residential community.

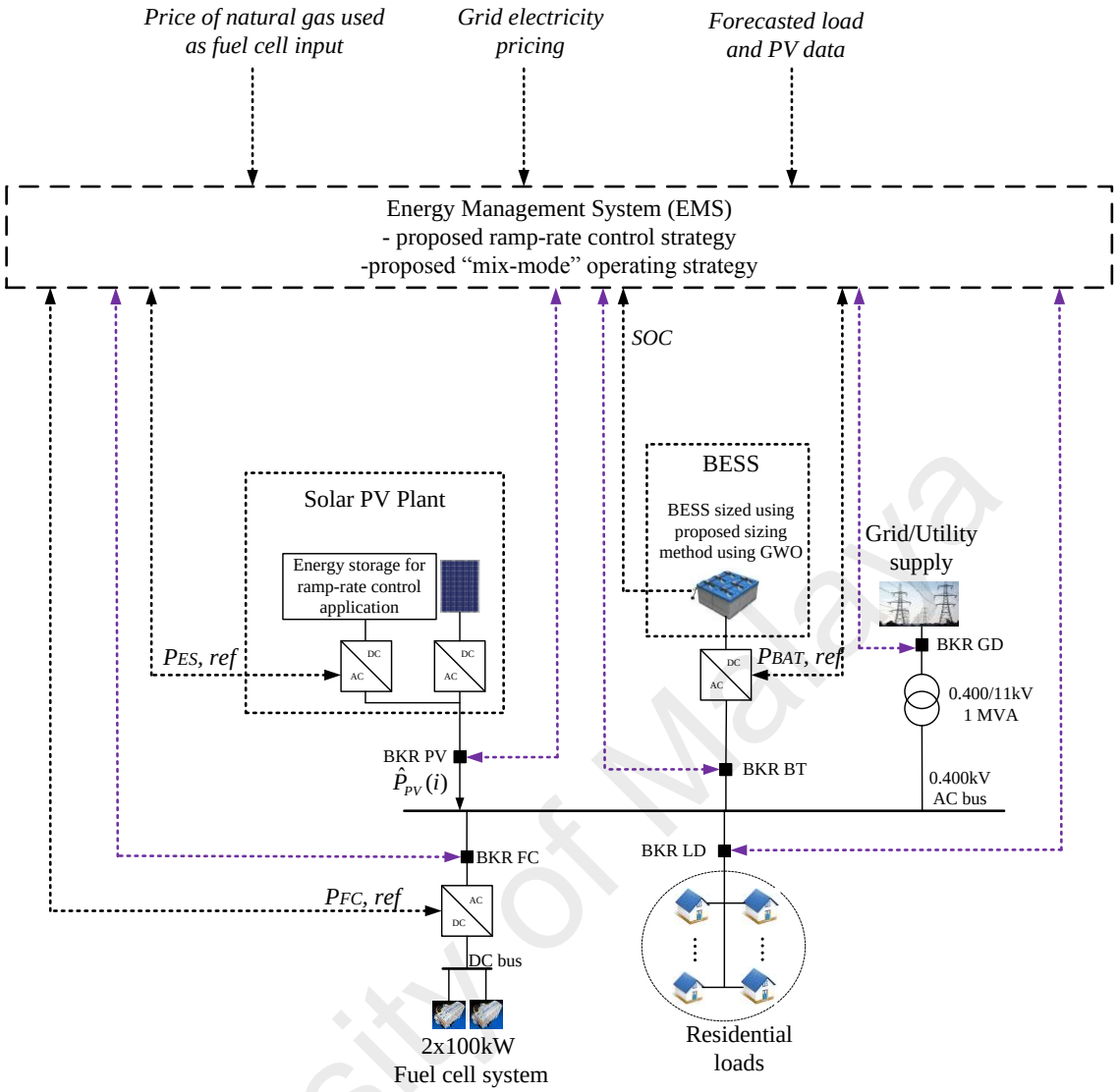

Figure 3.1: Proposed grid-connected microgrid configuration

The output power of 200 kWp PV generator is fluctuating in nature and in order to mitigate the output power fluctuation, the PV plant houses an energy storage which is utilized only to control PV output power ramp rates. The energy storage device can be any rapid storage technology like capacitor, super capacitor, electric double layer capacitors (EDLC), superconductive magnetic energy storage (SMES), or batteries. In this research battery storage is used for the ramp-rate control application. The output power from the solar PV plant is the smoothed one. The microgrid also has two identical SOFC each having the rated capacity of 100kW. In addition to these sources a controllable BESS of 100kW power capacity is connected to the AC bus bar. The

energy capacity of the BESS is evaluated using the proposed sizing method. These sources serve a nearby residential community. The load demand is supposed to vary throughout the day. The entire microgrid is connected to the utility grid through a 0.4/11KVstepup transformer. The excess power generated by the microgrid is not injected into the utility grid, therefore the excess power available in the microgrid is used to charge the BESS. The proposed microgrid is modeled using PSCAD/EMTDC software.

3.2.2 Energy Management System (EMS) module

The microgrid model houses the proposed energy management system (EMS) which has the proposed PV ramp-rate control strategy and "mix-mode" operating strategy. The EMS formulates appropriate reference values to the distributed sources based on the operating strategy. Prices of natural gas and utility grid electricity and forecasted values of PV output power and load power is given as the input. Information on breakers connected to distributed sources and load were also updated by the EMS on regular basis.

From the forecasted PV power, the smoothed PV power is calculated using the proposed ramp-rate control strategy. The difference between the smoothed PV power and the forecasted actual PV power is the required reference for the energy storage ($P_{ES,ref}$) present in the solar PV plant. Further based on the available information such as prices of natural gas and utility grid electricity, smoothed PV power and forecasted load power, appropriate reference values for fuel cell system ($P_{FC,ref}$) and BESS ($P_{BAT,ref}$) is calculated. The EMS calculates the reference values for the distributed sources using mix-mode operating strategy.

3.2.3 Parameters of Solar PV Plant

The basic unit of PV generator is the solar cell which is able to generate electrical power about 1 to 2 watt. Single-diode model of solar PV cell is used for modeling (Rajapakse & Muthumuni, 2009). Series and/or parallel electrically coupled PV cells make PV modules and further PV arrays. A PV array encompasses series and parallel connected modules and hence the single cell equivalent circuit can be scaled up in order to rearrange for any series/parallel configuration. In this work, a 200 kWp PV array is built by connecting 37 parallel strings where each parallel string contains 20 PV modules in series. Parameters of PV module used are this thesis is given in Table 3.1.

Table 3.1: Electrical specification of solar module (HIT-N210A01)("HIT Photovoltaic Module Power 210A," 2010)

Parameter	Value
Rated Power (P_{max})	210 W
Maximum Power Voltage (V_{pm})	41.3 V
Maximum Power Current (I_{pm})	5.09 A
Open Circuit Voltage (V_{oc})	50.9 V
Short Circuit Current (I_{sc})	5.57 A
Temperature Coefficient (V_{oc})	-0.142 $V/^oC$
Temperature Coefficient (I_{sc})	1.95 $mA/^oC$
NOCT (Normal Operating Cell Temperature)	46^oC

3.2.3.1 Maximum Power Point Tracking (MPPT)

The amount of power which can be captured from the solar cell depends on its operating points on *I-V* characteristics. To draw as much power as possible from the PV generator, different MPPT techniques have been introduced in the literature (Bhatnagar & Nema,

2013; Eltawil & Zhao, 2013; Ishaque & Salam, 2013; Salas, Olias, Barrado, & Lazaro, 2006).

A commonly used algorithm is Perturb and Observe (P&O) technique. However, this method has its own limitations. For example, the exact maximum power point (MPP) can never be found and hence the power oscillates around MPP (Rajapakse & Muthumuni, 2009; Yazdani et al., 2011). The MPP method adopted in this work is Incremental Conductance (IC). Figure 3.2 shows the flowchart of this algorithm. The IC algorithm is designed to evaluate Eq.3.1 at the MPP as:

$$\frac{dP}{dV} = \frac{d(VI)}{dV} = I + V\frac{dI}{dV} = 0 \tag{3.1}$$

where I and V are the output current and voltage at the terminal of PV generator. The logic behind this algorithm is given in Table 3.2.

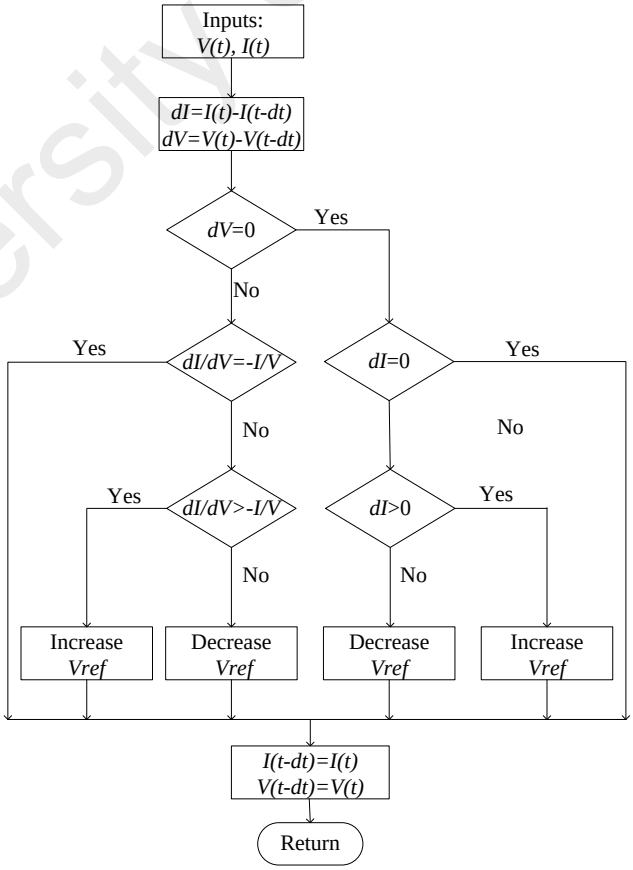

Figure 3.2: IC algorithm in order to estimate V_{ref} for DC bus controller

Table 3.2: Logic behind the IC MPPT algorithm

$\frac{dI}{dV}$	$\frac{dP}{dV}$	Operating point with respect to MPP
$= -\frac{I}{V}$	=0	at MPP
$> -\frac{I}{V}$	>0	Left side
$< -\frac{I}{V}$	<0	Right side

3.2.4 Modeling of Battery Energy Storage System (BESS)

Sheperd model (Moore & Eshani, 1996; Rekioua & Matagne, 2012) of lead-acid battery is used in this thesis. In the PSCAD the battery source is implemented as a DC voltage source connected in series with a variable resistor. The equivalent circuit of the battery model is shown in Figure 3.3.

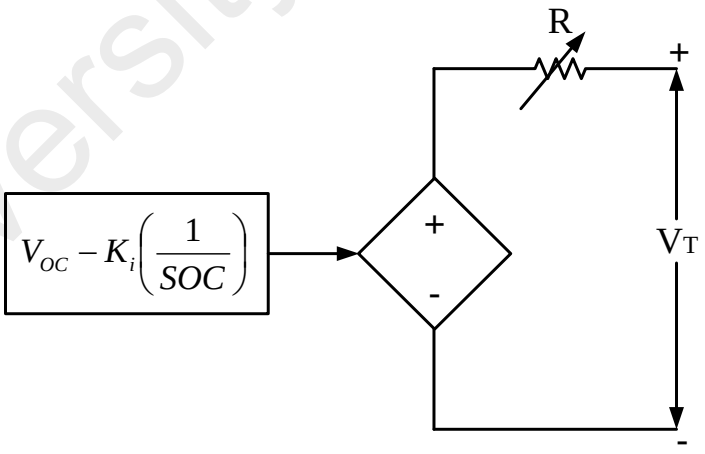

Figure 3.3: Equivalent dynamic model of battery module

The terminal voltage of the battery source is calculated from Peukert equation and is given as,

$$V_T = V_{OC} - R.i - K_i \frac{1}{SOC_i - DOD} \tag{3.2}$$

where V_{OC} is the battery open-circuit voltage, R is the internal resistance in ohm, K_i is polarization coefficient, SOC_i is initial state of charge and DOD is depth of discharge.

The DOD is calculate as:

$$DOD = \frac{1}{Q_{\max}} \int idt \tag{3.3}$$

where Q_{max} is the maximum available capacity of the battery.

SOC_i can vary between 0.2 and 1 while the simulation is started. Instantaneous battery state of charge is formulated as:

$$SOC = \frac{Q_{ini} - Q_{used}}{Q_{\max}} = SOC_i - DOD \tag{3.4}$$

where Q_{ini} is the initial available capacity of the battery and Q_{used} is given as,

$$Q_{used} = \int idt \tag{3.5}$$

Technical specifications of lead-acid battery module utilized to arrange the BESS are given in Table 3.3.

Table 3.3: Technical specification of 12V battery module (RM12-75DC)(RemcoLtd., 2012)

Nominal voltage	V_{OC}	12 V					
Nominal capacity	C_{20} (Q_{max})	75 AH (20hours)					
Internal resistance	R_0	≤4.8mΩ (fully charged battery)					
Polarization coeff.	K_i	0.003					
Electrolyte resistance	K_R	0.7mΩ					
Units in series	N_s	1					
Units in parallel	N_p	1					
Max. Charge Current	$I_{ch,max}$	22.5 A					
Final Voltage		5 mins	10 mins	15 mins	30 mins	45 mins	60 mins
9.6 V	Ampere	265.3	188.2	148.5	92.6	67.9	53.3
	Watt	2501.6	1880.3	1518.7	925.2	698.6	579
10.02 V	Ampere	235.9	176.5	141.5	90	66.7	53
	Watt	2416.7	1822.3	1473.9	896.3	687.4	572.3
10.2 V	Ampere	216.6	167.4	137.3	88.2	66.1	52.4
	Watt	2271	1756.4	1426.3	881.5	675.9	564.5
10.5 V	Ampere	193.1	152	128.1	84	64	51.3
	Watt	2066.5	1620.4	1347.3	863.9	665.6	558
10.8 V	Ampere	174.9	136.4	116.6	77.9	61.6	49.7
	Watt	1820	1491.5	1242.3	836	647	547.8

3.2.5 Modeling of Solid Oxide Fuel Cell (SOFC) system

The microgrid model consists of two identical SOFC where the rated capacity of each fuel cell is 100kW. Figure 3.4 shows the dynamic model of SOFC fuel cell.

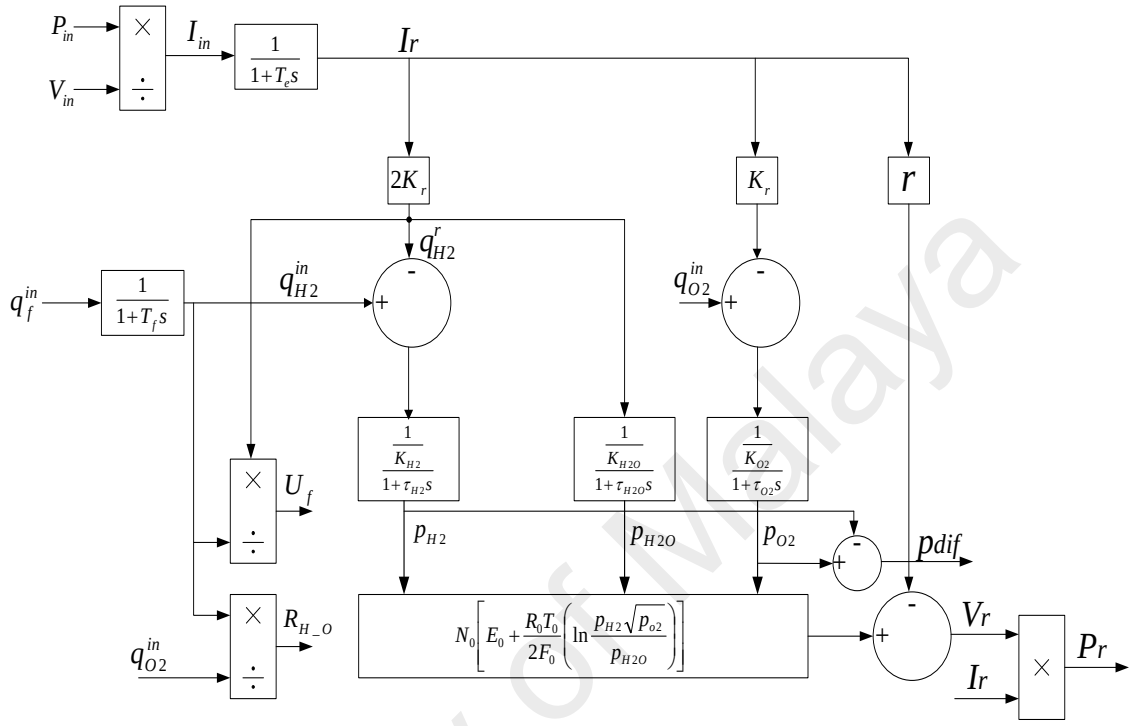

Figure 3.4: SOFC dynamic model(X. Wang, Huang, & Chen, 2007)

The dynamic model is built in PSCAD software and the well known Nernst equation is used to calculate the output voltage produced from the fuel cell stack. The output terminal voltage produced from the SOFC fuel cell stack considering ohmic losses is given by,

$$V_r = N_0\left[E_0 + \frac{R_0T_0}{2F_0}\left(\ln\frac{p_{H2}\sqrt{p_{o2}}}{p_{H2O}}\right)\right] - rI_r \tag{3.6}$$

In this dynamic model the fuel processor is assumed to operate that is convert fuels such as natural gas to hydrogen whenever the SOFC is about to generate the power. The

output power of the modeled SOFC system is 100kW and the nominal voltage at the terminal of the fuel stack is 333.8V and the current demand is 300A.

Fuel utilization factor (U_f) and ratio between inlet hydrogen and oxygen (R_{H_O}) are the important control variables for operation of SOFC system. The typical utilization factor varies between 80% to 90% and for this work the utilization factor is taken as 85% inorder to avoid permanent damage to fuel cells and fuel starvation. Similarly, the R_{H_O} value varies between 0 to 2 and for this work it is taken as 1.145 as this values is optimal to keep the fuel cell pressure less than nominal level (X. Wang et al., 2007; Zhu & Tomsovic, 2002). For PSCAD modeling the entire fuel cell model shown in Figure 3.4 is modeled and the output voltage V_r from the fuel cell stack is given to the controllable voltage source and through the DC-DC converter and VSC the SOFC system is connected to the 400V AC bus bar. The parameters used for dynamically model the SOFC is given in Table 3.4.

Table 3.4: Parameters used for SOFC model (X. Wang et al., 2007)

Parameter	Value	Unit
T_o	1273	K
F_o	96485	C/mol
R_o	8.314	J/(mol K)
E_o	1.18	V
N_o	384	-
K_r	0.996 x 10^-3	mol/(s A)
K_{H2}	8.32 x 10^-6	mol/(s Pa)
K_{H2O}	2.77 x 10^-6	mol/(s Pa)
K_{O2}	2.49 x 10^-5	mol/(s Pa)
τ_{H2}	26.1	s
τ_{H2O}	78.3	s
τ_{O2}	2.91	s
r	0.126	Ω
T_e	0.8	s
T_f	5	s

3.2.6 Voltage Source Converter (VSC)

This section consists of the controller for three phase grid-connected voltage source converter (VSC) system. Figure 3.5 consists of controller scheme for three phase VSC. The controller consists of two main components power controller and current controller. The purpose of using this strategy is to control the active power flow between the microgrid and the utility grid. The power controller consists of two proportional-integral (PI) controllers. The error difference produced from difference of real power and voltage levels are given as the input to the PI controller from which the reference

current vectors I^*_d and I^*_q in the dq-reference frame are generated. These reference current vectors are given as the input to the current controller. The objective of the current controller scheme is to ensure accurate tracking and short transients of the inverter output current. The current control scheme is based on synchronous reference frame. The current control scheme has two PI controllers to eliminate the error in the current. A phase locked loop (PLL) is used to detect the phase angle in-order to implement the park's transformation. The output signal from the controller represent the reference voltage signal in dq-reference frame and is followed by signal transformation from dq to abc frame. Using the reference abc signals as the input the reference control signals are produced using sinusoidal pulse width modulation (PWM) in-order to control the VSC.

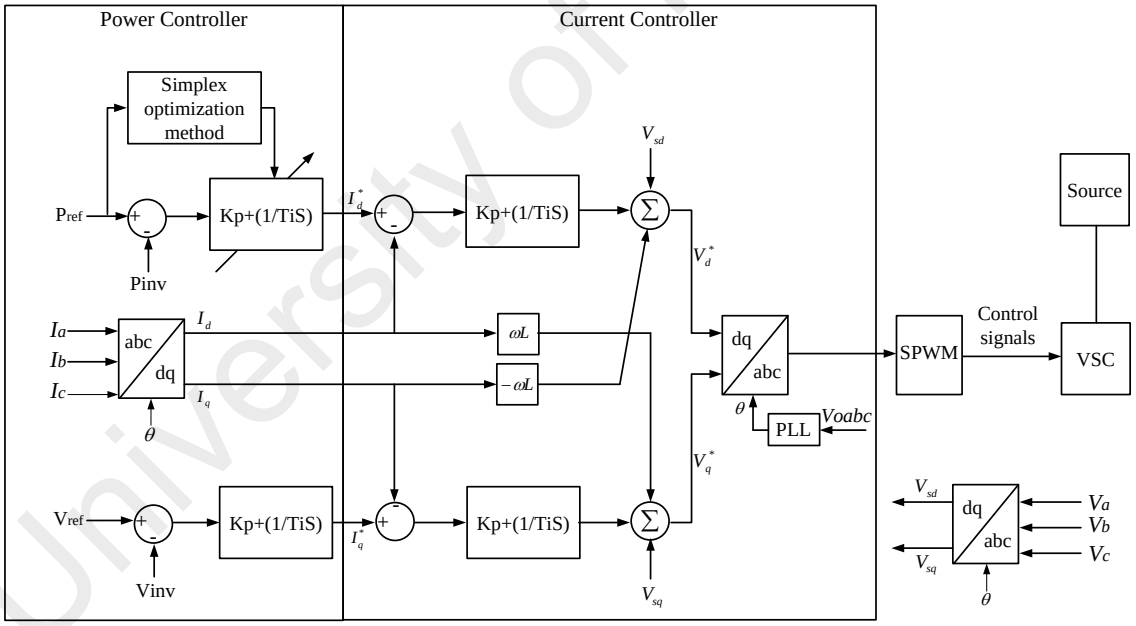

Figure 3.5: Grid-connected mode power controller of VSC

In this research, implementation of simplex optimization method to generate appropriate control values of PI controller implemented in real power controller is carried out. This appropriate value of *Kp* and *Ti* are generated for the VSCs connected to the controllable source like BESS and SOFC power plants. Here the appropriate reference real power

values are provided by the proposed EMS module. The simplex optimization method in turn generates appropriate proportional gain (K_p) and integral time constant (Ti) which is given as input to PI controller.

The PI controller used in the VSCs active power control should be robust in nature when the system is operating under dynamic changes such as PV output and load. Therefore optimal operation of PI controller is necessary. In this work, the controller's objective function is to minimize the error using Integral of Time multiplied by Absolute Error (ITAE) performance criterion. The advantage of using ITAE performance criterion is that it produces smaller overshoot and oscillations (Maiti, Acharya, Chakraborty, Konar, & Janarthanan, 2008). The mathematical expression for ITAE criterion is given as:

$$J = \int_0^\infty (t.|e(t)|).dt \tag{3.7}$$

Where t is the time and $e(t)$ is the difference between reference power and the actual output power from the source.

The PSCAD program is equipped with optimum run search engine module which enables us to perform successive simulations for group of parameters using simplex optimization method. The simplex optimization algorithm is used for simulation program and simultaneously evaluates the objective function given in equation (3.7). The search is terminated when the stopping criterion is met that is when the algorithm completes the maximum number of iteration.

3.3 Analysis of moving average and conventional exponential smoothing methods

In this section analysis of moving average (MA) and conventional exponential smoothing (CES) methods with their limitations is carried out in detail. MA and CES methods are predominantly used by researchers to control PV output power ramp-rate. These methods are used to smooth PV output power shown in Figure 3.6. Output power from solar PV represents time series data, where the data points consist of successive measurement of PV power over a time interval.

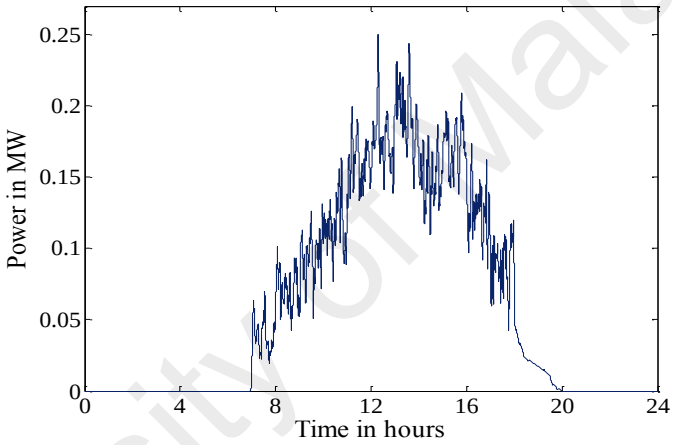

Figure 3.6: Output power of solar PV plant

3.3.1 n-point Moving Average (MA) method

MA is essentially centred on finding out average for the set of input and the assumption is attributed that it represents a constant or level model. Moving averages is made by assuming that the latest '*n*' period is more relevant and others are left out. The principle of operation of MA for '*n*' relevant data points for the input having '*k*' data points is given as,

$$F = \frac{\left(i(k) + i(k-1) + \ldots + i(k-n)\right)}{n} \tag{3.8}$$

where n is number of relevant data points used in MA smoothing, i and F are input (P_{PV}) and smoothed output respectively. For this work 41 data points is used as the

moving average window therefore the value of n=41. The MA window is chosen as 41 since the level of smoothness is found to be satisfactory. Elaborating (3.8) for 41-point MA is given as,

$$F = \left[\frac{i(k) + i(k-1) + ... + i(k-41)}{41} \right] \tag{3.9}$$

As mentioned above for a 41-period moving average, 41 P_{PV} data points which are most relevant for producing smoothed output is used and other data points are left out. A 41-period moving average can be thought of giving weights '*1*' for the relevant data points considered for producing smoothed output and '*0*' weights for the points left out.

MA is able to capture the principle that the most recent data points are important and older points do not contribute for the smoothing. From the above explanation we would like to highlight two main issues that are associated with MA which causes "memory effect",

(i) MA essentially ignores older data points by giving '0' weights.

(ii) The weights associated with relevant data points are equal which is not logical or acceptable.

The limitation of (MA) method is demonstrated using Figure 3.7. For illustration purpose the 41-point MA smoothed waveform during the time period 1.30PM and 6.30PM is presented in Figure 3.7 and it is obtained by smoothing the actual PV output power shown in Figure 3.6.

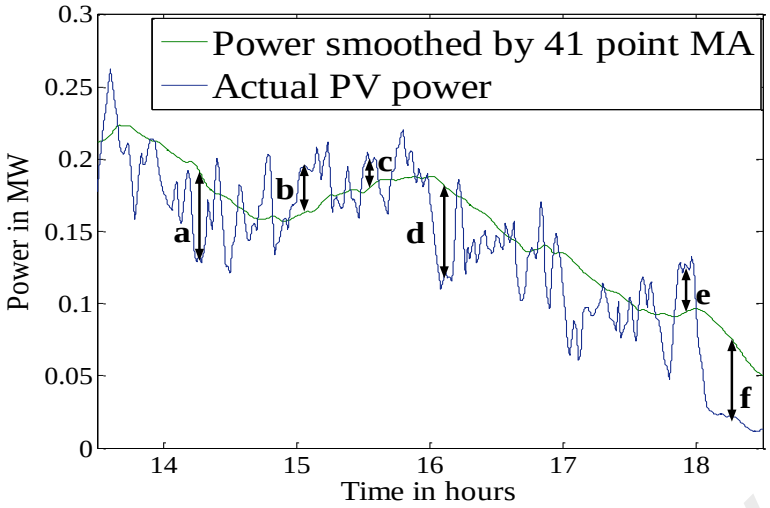

Figure 3.7: Actual PV power and smoothed power using 41 point MA waveform

The actual solar PV power obtained from 1-min radiation data is compared with PV power smoothed by MA method. Noticing portions a,b,c,d,e and f in Figure 3.7, there is no significant fluctuation in PV for which the battery storage supplied or absorbed significant amount of power which is due to memory effect (Alam et al., 2014).

3.3.2 Conventional Exponential Smoothing (CES) method

CES method actually considers all the points in the system and gives progressively increasing weights to more recent data. The fundamental equation for CES is given as,

$$\hat{P}_{PV}(i) = \alpha P_{PV}(i) + (1-\alpha)\hat{P}_{PV}(i-1) \tag{3.10}$$

where $\hat{P}_{PV}(i)$ is smoothed output, $\hat{P}_{PV}(i-1)$ is smoothed output at previous step, P_{PV} is the actual output power from solar PV and *'α'* is the smoothing constant which should be selected between *0* and *1*. Substituting the value of $\hat{P}_{PV}(i-1)$ in (3.10) we get

$$\hat{P}_{PV}(i) = \alpha P_{PV}(i) + (1-\alpha)\left[\alpha P_{PV}(i-1) + (1-\alpha)\hat{P}_{PV}(i-2)\right] \tag{3.11}$$

Likewise substituting the value of $\hat{P}_{PV}(i-2)$ in (3.11) the equation is expanded and if we continue to do this we get,

$$\hat{P}_{PV}(i) = \alpha[P_{PV}(i) + (1-\alpha)P_{PV}(i-1) + (1-\alpha)^2 P_{PV}(i-2) + (1-\alpha)^3 P_{PV}(i-3) + \ldots$$

$$+ (i-\alpha)^n P_{PV}(i-n)] + (1-\alpha)^n \hat{P}_{PV}(i-(n-1)) \tag{3.12}$$

where '*n'* is the number of PV data points in the time window. In (3.12) $\hat{P}_{PV}(i-(n-1))$ is '*zero*' because it the forecast for point *n-1*. Therefore (3.12) can be written as,

$$\hat{P}_{PV}(i) = \alpha[P_{PV}(i) + (1-\alpha)P_{PV}(i-1) + (1-\alpha)^2 P_{PV}(i-2) + (1-\alpha)^3 P_{PV}(i-3) + ...$$

$$+ (i-\alpha)^n P_{PV}(i-n)] \quad (3.13)$$

From (3.13) it is clear that the value of α, $\alpha(i-\alpha)$…, $\alpha(i-\alpha)^n$ is treated as the weights associated with the corresponding PV data points and is progressively decreasing to older data points.

If the value of *'α'* is greater than 0.5 or closer to 1 the contribution of the present value or the most recent value is weighed more and contribution of older terms is less for smoothing. If the value of *'α'* is less than 0.5 or closer to 0, present value or the most recent terms will be weighed less and more older terms start contributing to the smoothing. Therefore smoothing constant *'α'* is the main parameter which helps to smooth PV fluctuations. Choosing the smoothing constant between 0 and 0.5 will over smooth PV output power and choosing smoothing constant more than 0.5 or values nearer to 1 will not smooth PV power effectively. There is no absolute logic present in the literatures on choice of smoothing constant *'α'* pertaining to this PV ramp-rate control problem.

For comparison purpose the value of *'α'* is chosen as 0.2 which is predominantly found in the literature. For illustration purpose the CES method smoothed waveform during the time period 13.5h and 18.5h is presented in Figure 3.8. The areas encircled in dotted lines shows there is no significant fluctuation in PV output. For which the energy storage will supply or absorb significant amount of power which is due to memory effect. In other words the weights α, $\alpha(i-\alpha)$…, $\alpha(i-\alpha)^n$ distributed among the data points are not logically related to PV ramp-rate therefore creating "memory effect". For this reason the energy storage is allowed to operate even though there is not significant fluctuation.

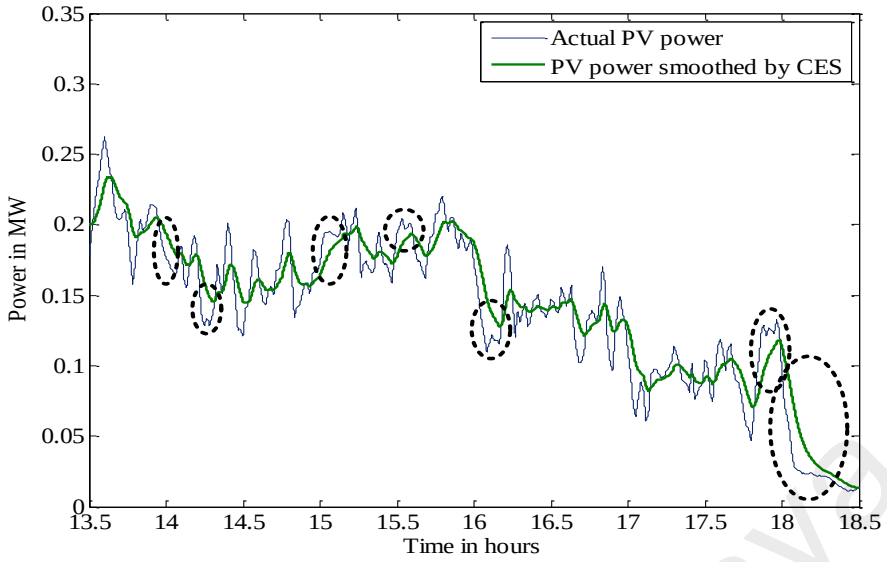

Figure 3.8: Actual PV output and PV power smoothed using CES method

The difference between CES and MA method is, CES method considers all the PV data points in the system and gives progressively increasing weights to more recent data. On the other hand MA method consider only relevant PV data points and give equal weights to it and older data points are left out. Due to this memory effect, CES and MA methods will invariably smooth the PV output power even thought there is no significant fluctuation.

3.4 Proposed Solar PV Ramp-Rate Control Strategy

It is well known that rapid fluctuation in solar PV output power will have negative impact on voltage and frequency on the grid side. Mitigating the fluctuation by a rapid source like capacitors, super capacitors, ultra capacitors, electric double layer capacitors (EDLC), superconductive magnetic energy storage (SMES), or batteries energy storage is a solution to control the solar PV output power fluctuations. In this research the PV ramp-rates are controlled using battery storage. The difference between the smoothed reference waveform and the actual PV output power is where the battery source will absorb or supply power to mitigate the fluctuation problem.

A novel ramp-rate control strategy which does not exhibit memory effect and also limit the PV output power fluctuations within the limit is proposed in this section. The proposed ramp-rate control strategy will allow battery source only to limit the significant PV output power ramp ups/downs and for rest of the hours the battery source is switched off.

The proposed ramp-rate control strategy uses exponential smoothing method with modifications. Therefore the fundamental equation of exponential smoothing method with the proposed smoothing parameter 'σ' is given as,

$$\hat{P}_{PV}(i) = \sigma P_{PV}(i) + (1-\sigma)\hat{P}_{PV}(i-1) \tag{3.14}$$

where $\hat{P}_{PV}(i)$ is the smoothed PV output for the instant '*i*', $\hat{P}_{PV}(i-1)$ is the smoothed PV output for the instant '*i-1*' and $P_{PV}(i)$ is the actual PV output power for the instant '*i*'. Unlike the smoothing parameter in Equation 3.10, the proposed smoothing parameter 'σ' in Equation 3.14 change for every time step depending on the ramp-rate violations. Therefore the ramp-rate has to be checked for any violation for every time step. Based on the level of violation the smoothing parameter 'σ' is calculated. The ramp rate of solar PV output power at instant '*i*' is found by,

$$\frac{dP_{PV}}{dt}(i) = \frac{\left[P_{PV}(i) - P_{PV}(i-1)\right]}{t(i) - t(i-1)} \tag{3.15}$$

where $P_{PV}(i)$ and $P_{PV}(i-1)$ are actual powers at i^{th} and $(i-1)^{th}$ instant. Likewise the difference between actual PV power at instant '*i*'($P_{PV}(i)$) and smoothed PV power at instant '*i-1*'($\hat{P}_{PV}(i-1)$) also denotes the ramp-rate and is expressed as,

$$\frac{d\overline{P}_{PV}}{dt}(i) = \frac{\left[P_{PV}(i) - \hat{P}_{PV}(i-1)\right]}{t(i) - t(i-1)} \tag{3.16}$$

For this work 10% of solar PV's rated capacity per minute is taken as ramp-rate limit. This ramp-rate limit was considered reasonably safer in order to avoid voltage and frequency fluctuations. The ramp-rate beyond the prescribed limit is noted as violation. Therefore, Equations 3.15 and 3.16 are checked for ramp violation using a ramp-rate function *f(RR)* which is basically used to limit the PV ramp-rate. The *f(RR)* is illustrated as follows,

$$f(RR) = \begin{cases} \dfrac{d\overline{P}_{PV}}{dt}(i), \ if \left|\dfrac{dP_{PV}}{dt}(i)\right| \le |RR_{\lim}| and \left|\dfrac{d\overline{P}_{PV}}{dt}(i)\right| < |RR_{\lim}| \\ \\ RR_{\lim}, \qquad\qquad otherwise \end{cases} \tag{3.17}$$

The proposed ramping function *f(RR)* is added with smoothed power at previous instant '*i-1*' ($\hat{P}_{PV}(i-1)$) to obtain the smoothed power at instant '*i*' $\hat{P}_{PV}(i)$ and is given in Equation 3.18.

$$\hat{P}_{PV}(i) = \hat{P}_{PV}(i-1) + f(RR) \tag{3.18}$$

By equating the Equations 3.14 and 3.18 the proposed smoothing parameter (σ) is given as,

$$\sigma = \left|\frac{f(RR)}{P_{PV}(i) - \hat{P}_{PV}(i-1)}\right| \tag{3.19}$$

The calculated smoothing parameter (σ) is substituted in Equation 3.14 to find out smoothed output $\hat{P}_{PV}$ for every time instant. A discrete switching function *S(i)*, based on the smoothing parameter 'σ' is given in Equation 3.20 to obtain optimal battery operation.

$$S(i) = \begin{cases} 0, & for \ \sigma = 1 \\ \\ 1, & for \ \sigma < 1 \end{cases} \tag{3.20}$$

By introducing the switching function *S(i)* in equation 3.14, the equation 3.14 is updated as follows,

$$\hat{P}_{PV}(i) = \sigma P_{PV}(i) + \left[(1-\sigma)\hat{P}_{PV}(i-1)\right]S(i) \tag{3.21}$$

Equation 3.21 is the final control equation from which the smoothed PV output power ($\hat{P}_{PV}(i)$) for instant '*i*' is obtained.

The difference between the smoothed power ($\hat{P}_{PV}$) and the actual PV output power (P_{PV}) gives the target power required by the battery energy storage ($P_{ES,ref}$) to absorb or inject in order to control the PV ramp-rate within the limit and is given by,

$$P_{ES,ref}(i) = \hat{P}_{PV}(i) - P_{PV}(i) \tag{3.22}$$

If $P_{ES,ref}$ is positive the battery will discharge, and if negative the battery will operate in charging mode. A simple illustration for generation of target power ($P_{ES,ref}$) from the energy storage is given in Figure 3.9.

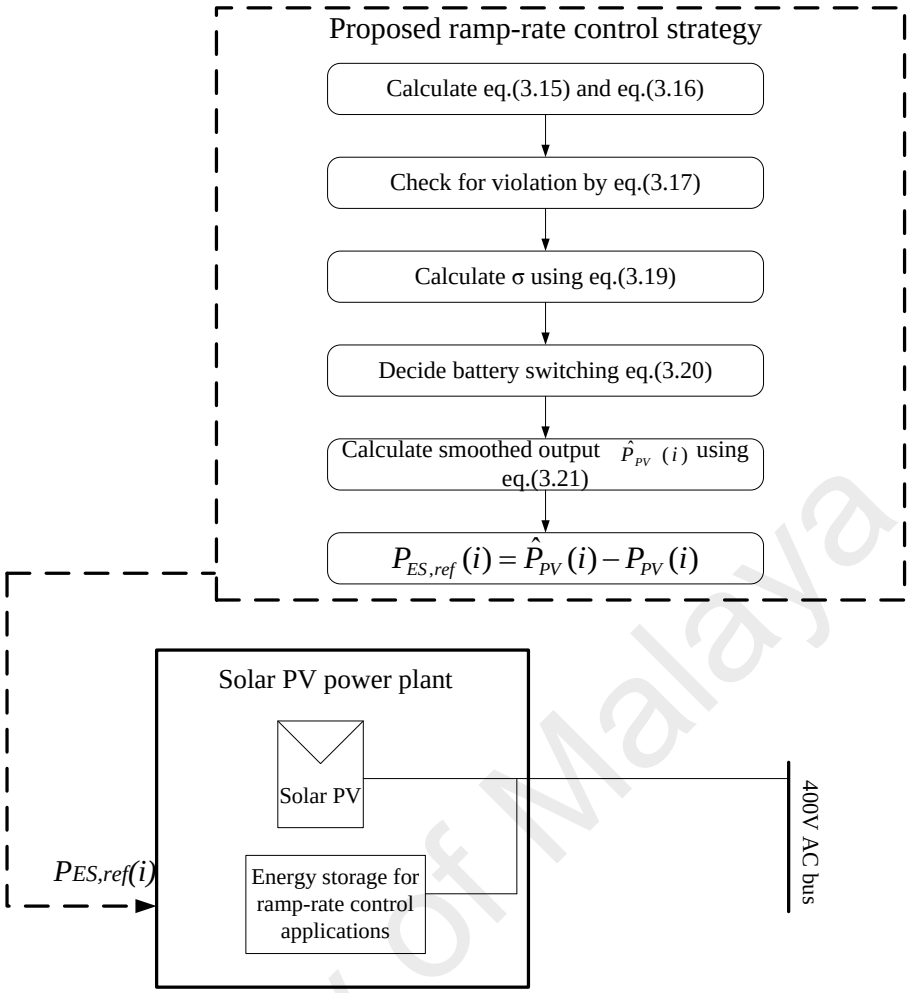

Figure 3.9: Calculating P_{ES} for battery energy storage and working of proposed ramp-rate control strategy

3.5 Illustration of the Proposed Ramp-Rate Control Strategy

The illustration of the proposed ramp-rate control strategy is provided in Figure 3.10. During the time period *t1* to *t4*, the ramp-rates are calculated using equations 3.15 and 3.16. The calculated ramp-rates are checked for any violation using equation 3.17 and the appropriate ramping function *f(RR)* is calculated. Since there is no violation in ramp-rates the smoothing parameter 'σ' calculated using equation 3.19 is *1* (see Figure 3.11) for which the battery is also switched OFF. Therefore the values of smoothed PV power ($\hat{P}_{PV}$) and actual PV output (P_{PV}) are same for the time period *t1* to *t4*. From t4 to t5 there is a significant fluctuation in PV output power (P_{PV}). Therefore the ramp-rates are calculated and checked for violation. Using the ramping function *f(RR)* the appropriate

value of smoothing parameter 'σ' is calculated from which the battery switching is also decided. Finally, the smoothed output $\hat{P}_{PV}$ is calculated from equation (3.21) and since actual PV power (P_{PV}) is more than the smoothed power ($\hat{P}_{PV}$) the battery has to be operated in charging mode in order to limit the ramp-rate.

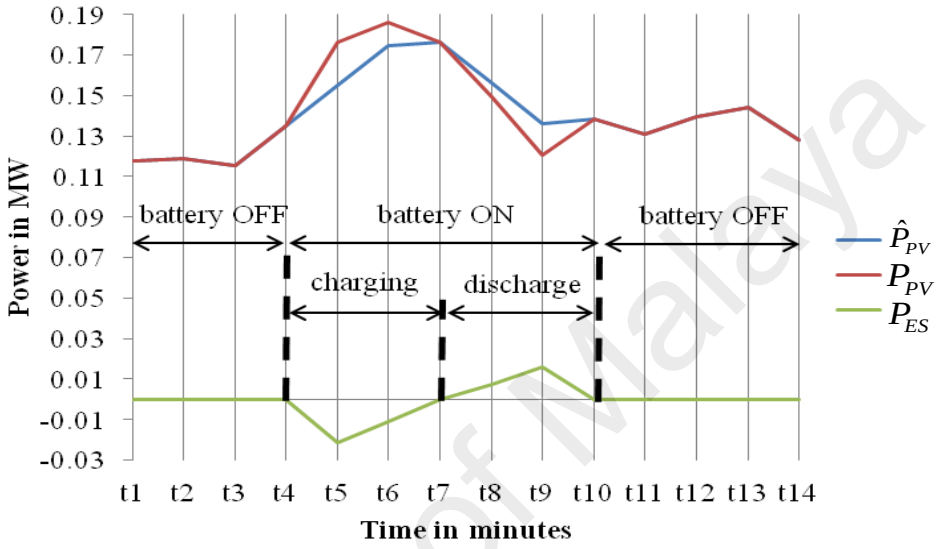

Figure 3.10: Illustration for proposed ramp-rate control strategy

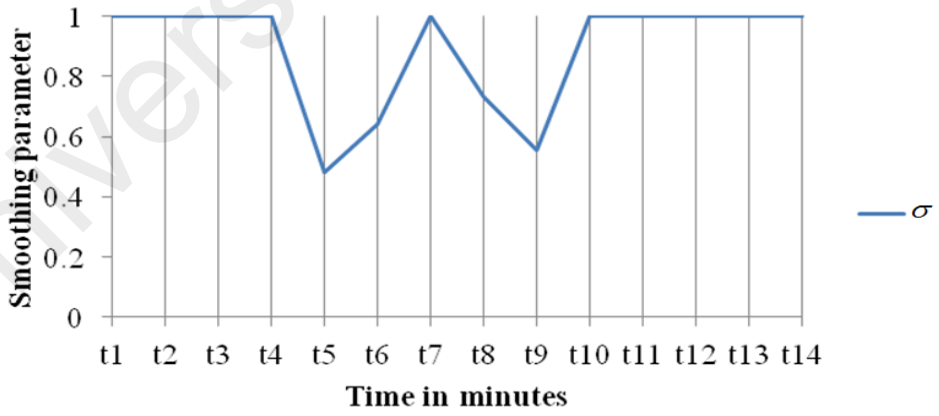

Figure 3.11: Variation in smoothing parameter for the proposed ramp-rate strategy

There is no significant power fluctuation in actual PV power from t5 to t6 but $\frac{d\overline{P}_{PV}}{dt}$ exceeds the ramp limit. Therefore the ramp-rate for the smoothed waveform is limited

and the smoothed reference to time instant *t6* is calculated ($\hat{P}_{PV}(t6)$). During this time period the battery is charged. Between *t6* to *t7* the ramp-rates are within the limit therefore $\hat{P}_{PV}(t7)$ is equal to P_{PV} (t7). Therefore the smoothing parameter 'σ' for the time period *t7* reaches *1* for which the battery is switched OFF. Similarly the ramp-down is controlled by discharging the battery between the period *t7* to *t10* where the variation in the smoothing parameter 'σ' during this period is presented in Figure 3.11. From *t10* to *t14* there is no significant fluctuation in PV output (P_{PV}), therefore the smoothed output ($\hat{P}_{PV}$) and actual PV output (P_{PV}) remains the same. During this time period the value of smoothing parameter 'σ' is also '1' and the battery is also switched OFF. It is clear from Figure 3.10 that battery is used only to smooth out the ramp ups and downs.

3.6 Proposed Optimal BESS Sizing Method and Operating Strategy to Reduce Microgrid's Daily Operation Cost

The present work is based on a hypothesis that, optimizing the daily operation cost of the hybrid system for a single operating strategy may not necessarily incur lower operating cost as the majority of the articles found in the literature. Different from the idea presented by researchers the present research is focused on developing an operating strategy which incurs the lowest operating cost of the hybrid system by combining two or more operating strategies. Therefore for this purpose a novel operating strategy namely "mix-mode" is proposed.

The size of BESS influences the microgrid's operating cost. Therefore it is necessary to evaluate the energy capacity of BESS necessary in kWh for operating the microgrid in mix-mode operating strategy. For this purpose a method to evaluate the BESS in kWh is also proposed. Therefore in this section the mix-mode operating strategy and accurate

BESS method necessary for reducing the microgrid's overall daily operating cost is presented in detail. Since the BESS sizing method is influenced by the microgrid's operating strategy, first we will explain the "mix-mode" operating strategy and then the methodology for evaluating the BESS size is presented in detail.

3.6.1 Proposed "Mix-Mode" Operating Strategy

Operating the microgrid under more than one operating strategy is referred as mix-mode operating strategy. For this purpose three operating strategies namely "continuous run mode", "power sharing mode" and "ON/OFF mode" are proposed and explained in the following.

3.6.1.1 Strategy 1: Continuous Run Mode

In this operating mode the power drawn from the utility grid is always zero. The fuel cell is operated continuously during 24h time period. The output power from the fuel cell depends on load demand and output powers from PV and BESS. During this strategy initially output power from PV and BESS is used to supply the load demand. If demand not met the fuel cell is optimally dispatched to satisfy the load demand. There are chances where the output power from PV is greater than load demand, in this case the BESS is charged and fuel cell is forcibly switched OFF. The objective function for this mode is to reduce the daily operating cost which can be expressed as,

$$obj1 = Minimize\left[C_{gi} \sum_{i \in T} \frac{P_{FCi}}{\eta_i} + \beta\left(P_{BATi}\right) \right] \qquad \forall i \in T \tag{3.23}$$

In this research the optimal schedule is calculated on minute-by-minute basis where the 24hours time horizon is divided into 1440 minutes. The scheduling horizon is denoted by $T \equiv \{1,2...1440\}$.

where,

C_{gi} is natural gas price to supply the fuel cell in dollars per kilowatt-hour

P_{FCi} is fuel cell power at time interval 'i'

β is taken as 1×10^{-6} in order to obtain the dispatch solution of P_{BATi}

P_{BATi} BESS power at time interval 'i';

If P_{BATi} is positive BESS discharge, if P_{BATi} is negative BESS operates in charging mode

η_i is cell efficiency of SOFC at time interval 'i' which is given as,

$$\eta_i = \frac{\left(\frac{V_{stack(i)}}{N}\right)}{E^o} \qquad \forall i \in T \tag{3.24}$$

E^o is electrochemical standard potential which is 1.482 volt/cell

V_{stack} is fuel cell output stack voltage at instant 'i'

N is number of cell in fuel cell stack

At any given time instant 'i', the sum of power generated from the distributed sources should be equal to the load which can be expressed as,

$$P_{PVi} + P_{BATi} + P_{FCi} = P_{Li} \qquad \forall i \in T \tag{3.25}$$

The power produced from PV is uncontrollable. Fuel cell and BESS is modeled as variable controllable source which should be operated within prescribed limits for 24h time period. The constraints for controllable source is given as,

$$P_{FC\min} \le P_{FCi} \le P_{FC\max} \qquad \forall i \in T \tag{3.26}$$

The constraints related to BESS energy level and allowable charge/discharge power considered for this work is explained section 3.6.4.

3.6.1.2 Strategy 2: Power Sharing Mode

In this power sharing mode the utility grid, BESS and fuel cell is optimally utilized to supply power to the load demand. BESS source is charged when output power from PV is greater than the load demand. The objective function for the power sharing mode is to reduce the daily operating cost which can be expressed as,

$$obj2 = Minimize\left[C_{gi} \sum_{i \in T} \frac{P_{FCi}}{\eta_i} + C_{ei}\left(P_{Li} - P_{neti}\right) + \beta\left(P_{BATi}\right) \right] \forall i \in T \tag{3.27}$$

where,

C_{ei} tariff of electricity purchased in dollar per kilowatt-hour

P_{Li} is the load demand at interval 'i'

$P_{net\,i}$ is the net power produced at interval 'i'

At any instant of time 'i', the summation of total generated power from PV, fuel cell, BESS and utility grid should be same as the total load demand.

$$P_{PVi} + P_{BATi} + P_{FCi} + P_{Gi} = P_{Li} \qquad \forall i \in T \tag{3.28}$$

Since the microgrid is operated at the distribution level, the excess power from the microgrid is utilized for charging the BESS. This is necessary to avoid power injected to grid that will activate the reverse power flow relay installed at point of common coupling (PCC). The power imported from the grid at time instant 'i' can be used to

charge the BESS or supply the load. Therefore considering the power drawn from the grid as a constraint which can be expressed as,

$$P_{Gi} \geq 0 \qquad \forall i \in T \tag{3.29}$$

In addition to it, the boundary constraints for fuel cell given in equation 3.25 are considered for this strategy. The limitations related to BESS energy level and allowable charge/discharge power considered for this work is explained section 3.6.4.

3.6.1.3 Strategy 3: ON/OFF Mode

In this strategy the objective is to obtain an optimal ON/OFF schedule for fuel cell, utility grid and BESS source thereby minimizing the microgrid's operating cost. Here the output power from PV and BESS supplies the load demand. Any deficit in power required by the load is delivered by optimally dispatching fuel cell and utility grid. In this operating strategy when the fuel cell is switched ON it is forced to run at its rated output power. For the rest of the time the fuel cell is switched OFF. Since the fuel cell is switched ON/OFF, a binary switching variable is introduced to enhance control over fuel cell. The objective function for this ON/OFF mode is given as,

$$obj3 = Minimize\left[S(i)\left(C_{gi} \sum_{i \in T} \frac{P_{FCi}}{\eta_i} \right) + C_{ei}\left(P_{Li} - P_{neti}\right) + \beta\left(P_{BATi}\right) \right] \qquad \forall i \in T \tag{3.30}$$

where *S(i)* is a switching function which takes the value of *0* or *1*. When *S(i)* is *1* the fuel cell is operated at its rated capacity. When *S(i)* is *0* the fuel cell is switched OFF. Therefore during the time of fuel cell operation its output is constant.

At any given time instant '*i*', the sum of power generated from the distributed sources and utility grid should be equal to the load which can be expressed as,

$$P_{PVi} + P_{BATi} + \left(P_{FCi}\right)S(i) + P_{Gi} = P_{Li} \qquad \forall i \in T \tag{3.31}$$

Since fuel cell is forced to run at it rated capacity the operating range of fuel cell is either zero or at its rated capacity. The boundary constraint for utility grid power equation 3.29 is also considered. The limitations related to BESS energy level and allowable charge/discharge power considered for this work is explained section 3.6.4.

3.6.2 Development of "Mix-Mode" Operating Strategy

In this section development of "*mix-mode*" operating strategy is explained. The primary objective of mix-mode operating strategy is to dispatch power from the distributed sources to the varying load with lower daily operating cost. The idea of mix-mode strategy is presented in Figure 3.12.

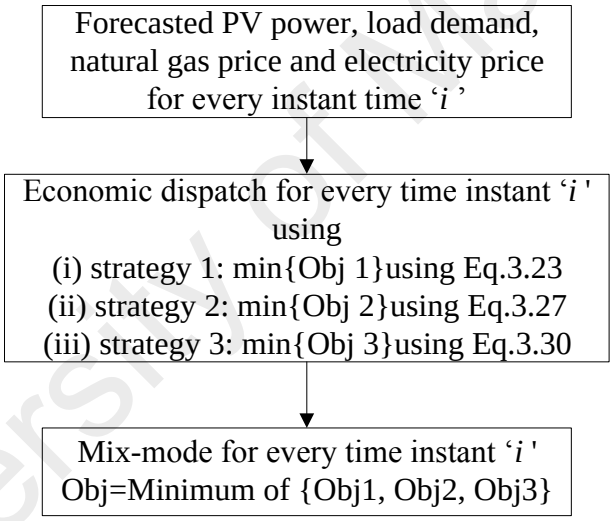

Figure 3.12: Mix-mode operating strategy

Initially the forecasted PV output power and load demand for the time instant '*i*' is considered. For the given time instant with the PV power, load demand, prices of electricity and natural gas at as input, the economic dispatch problem is solved for the three proposed strategies. *Obj1, Obj2* and *Obj3* are the obtained objective functions for strategy 1, strategy 2 and strategy 3 respectively for the given time instant '*i*'. The lowest value of the three objective functions should deliver lowest operating cost. Therefore the optimal dispatch values corresponding to the lowest objective function is

selected and provided as reference to the distributed generators present in the microgrid. The above steps are repeated for every time instant '*i*' that is for 1440 instants for 24h time period.

3.6.3 Proposed Algorithm to Solve the Mix-Mode Operating Strategy

The economic dispatch problems proposed bythe three strategies are solved using linear programming and mixed-integer linear programming optimization techniques. The objective functions for the strategy 1 and strategy 2 that is continuous run and power sharing mode has been modeled as a linear function of microgrid's distributed sources output power. Therefore for strategy 1 and strategy 2 the linear optimization problem is solved using "*linprog*" solver in MATLAB which can be expressed as

$$\min_{x} f^{T} obj \text{ subjected to } \begin{Bmatrix} A.x \le b \\ Aeq.x = beq \\ lb \le x \le ub \end{Bmatrix} \tag{3.32}$$

where: *f, x, b, beq, lb* and *ub* are vectors; *A* and *Aeq* are matrices.

The objective function for strategy 3 has been modeled as a mixed integer linear function of microgrid's distributed sources output power where the switching function for fuel cell generator in equation 3.30 is an integer. Therefore the objective function is modeled as mixed integer linear programming (MILP) one. This MILP problem can be solved using "*intlinprog*" solver function from MATLAB optimization toolbox. The "*intlinprog*" finds minimum of a problem considering the constraints specified by,

$$\min_{x} f^{T} obj \text{ subjected to } \begin{Bmatrix} x(\text{int } con) \\ A.x \le b \\ A_{eq}.x = b_{eq} \\ l_b \le x \le u_b \end{Bmatrix} \tag{3.33}$$

where: *f, x, intcon, b, beq, lb* and *ub* are vectors; *A* and *Aeq* are matrices.

3.6.4 Proposed BESS Sizing Method: Problem Formulation

In addition to the proposed operating strategy, optimal sizing of BESS is also formulated. In order to obtain the optimal BESS sizing the initial capital cost (CC) of BESS should be considered. Total cost per day for BESS source ($TCPD_{BAT}$) is the function of initial capital cost of BESS source. The optimal BESS sizing is obtained by minimizing a total cost function which is summation of daily operating cost of microgrid and $TCPD_{BAT}$ for BESS. Daily operating cost of microgrid (Obj) is obtained from section 3.6.2 by operating the microgrid in mix-mode operating strategy. The total cost function formulated for this problem can be given as,

$$MinF(X) = \sum_{i \in T} Obj(i) + TCPD_{BAT} \qquad \forall i \in T \tag{3.34}$$

Here the $TCPD_{BAT}$ for a particular BESS energy rating will be same for all the three strategies. The expression for $TCPD_{BAT}$ is given as,

$$TCPD_{BAT} = \frac{1}{365}\left(\frac{r.(1+r)^{Lt}}{(1+r)^{Lt} - 1}.CC \right) \tag{3.35}$$

$$CC = C_P.\overline{P} \; + C_E.\overline{E} \tag{3.36}$$

where CC is the capital cost of the BESS source. C_P and C_E are specific costs associated to BESS source's power and energy capacities respectively. 'r' is interest rate for financing the BESS. Lt is the battery source's lifetime. $\overline{E}$ and $\overline{P}$ are rated energy and power capacities of the BESS.

The proposed sizing problem is solved subjected to constraint as given below,

(i) BESS constraints:

The charge in the battery energy storage system (BESS) must be bounded between,

$$E_{BAT}^{\min} \le E_{BAT,i} \le E_{BAT}^{\max} \qquad \forall i \in T \tag{3.37}$$

where E_{BAT} is the energy stored in the BESS at the end of instant '*i*' in kWh.

$E_{BAT}^{\min}$, $E_{BAT}^{\max}$ are minimum and maximum charge to be maintained for BESS

Discharging mode:

Constraint limited to release of energy from BESS is given as,

$$E_{BAT,i} = \max\left\{\left(E_{BAT,i-1} - \Delta t.P_{BAT,i} / \eta_{discharge}\right), E_{BAT}^{\min}\right\} \quad \forall i \in T \tag{3.38}$$

Charging mode:

Constraint limited to energy stored in the BESS is given as,

$$E_{BAT,i} = \min\left\{\left(E_{BAT,i-1} - \Delta t.P_{BAT,i}.\eta_{charge}\right), E_{BAT}^{\max}\right\} \quad \forall i \in T \tag{3.39}$$

In addition to the limitation in charging/discharging levels, the maximum and minimum discharging/charging power is also given as,

$$P^{c}{}_{BAT,t} \le P_{BAT,i} \le P^{d}{}_{BAT,t} \qquad \forall i \in T \tag{3.40}$$

where,

$$P^{c}{}_{BAT,t} = \max\left\{P_{BAT,\min}, \left(E_{BAT,t-1} - E_{BAT}^{\max}\right)/\eta_{charge}, \Delta t\right\} \quad \forall i \in T \tag{3.41}$$

$$P^{d}{}_{BAT,t} = \min\left\{P_{BAT,\max}, \left(E_{BAT,t-1} - E_{BAT}^{\min}\right)\eta_{discharge}/\Delta t\right\} \quad \forall i \in T \tag{3.42}$$

The proposed BESS sizing problem should fulfill the constraints mentioned above in Equations 3.37-3.42 for solving the mix-mode operating strategy.

(ii) Dispatchable distributed generator constraints

PV source is uncontrollable and the output depends on solar radiation. The operating output of other dispatchable sources should be limited within the minimum and maximum limits. The operating limits of fuel cell and utility grid for the proposed strategies are provided in corresponding sections 3.6.1.1, 3.6.1.2 and 3.6.1.3.

3.6.5 Proposed Algorithm for Solving the BESS Sizing Problem

In the ordinary form solving the optimal BESS sizing for the proposed mix-mode operating strategy is a complex non-linear optimization problem. Therefore metaheurictic method like grey wolf optimizer (GWO) is used to solve the BESS sizing problem. The BESS sizing problem is also solved using other optimization techniques like particle swarm optimization (PSO), genetic algorithm (GA), artificial bee colony (ABC) and gravatitional search algorithm (GSA). The performance of these algorithms in solving the proposed BESS sizing method is analyzed in chapter 4. Before going in hand with the description, Figure 3.13 depicts the general flowchart for application of optimization technique in solving the BESS sizing problem. The steps presented in the flowchart is very general where the common optimization steps like declaration of initial population maximum number of iteration are declared during start of the optimization process. Then using the initial population the mix-mode operating strategy

is carried out for 24hours that is for 1440 time instants. Finally the overall objective function that is addition of total operating cost per day and BESS's total cost per day is evaluated. This process is repeated for all the initialized particles or population. Then the best solution is updated after which the condition for the stopping criteria that is the iteration number is checked. If the maximum number of iteration is not reached, the whole process is repeated. If the iteration number reaches its maximum limit the optimization process is stopped and the final optimal value of BESS capacity in kWh is obtained. The BESS sizing problem is solved using five different optimization techniques and the results obtained from them are utilized for comparative study. The optimization techniques used for solving the BESS problem are explained below.

The flowchart shown in Figure 3.13 is the genetic flow in solving the optimization problem. In this research, this BESS sizing optimization problem is solved using GWO, PSO, ABC, GA and GSA. The optimization steps depicted in the figure is highlighted and respective optimization steps were followed when these techniques are implemented. The explanation of the utilized optimization techniques were elaborated between sections 3.6.5.1 to 3.6.5.5.

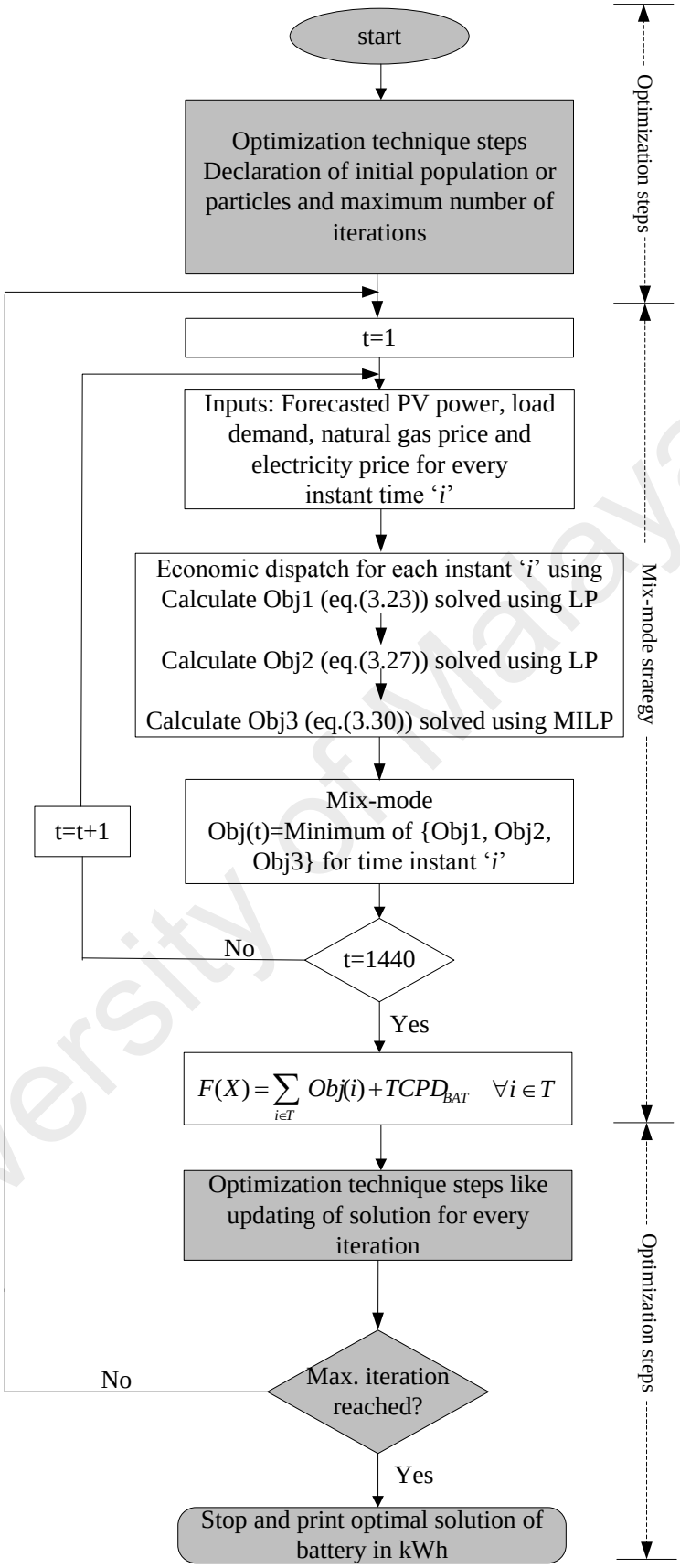

Figure 3.13: Flowchart of the proposed sizing method for mix-mode operating strategy

3.6.5.1 Grey Wolf Optimizer (GWO)

Grey Wolf Optimizer (GWO) optimizer mimics the hierarchy and hunting mechanism of grey wolves in the nature (Mirjalili, Mirjalili, & Lewis, 2014). Four types of grey wolves namely; alpha, beta, delta, and omega are employed for simulation of GWO optimizer. Searching for prey, encircling, and attacking the prey are the three main steps involved in GWO optimizer. In GWO the hunting is guided by alpha, beta and delta wolves. Omega wolves follow the three wolves. The grey wolves encircle the prey during the hunt where the encircling behavior is mathematically modeled as,

$$\vec{D} = \left|\vec{C}.\vec{X}_p(t) - \vec{X}(t)\right| \tag{3.43}$$

$$\vec{X}(t+1) = \vec{X}_p(t) - \vec{A}.\vec{D} \tag{3.44}$$

The vectors $\vec{A}$ and $\vec{C}$ are the coefficient of encircling model. $\vec{X}_p$ and $\vec{X}$ are the position vectors of prey and grey wolf and *t* indicates current iteration.

Vectors $\vec{A}$ and $\vec{C}$ are calculated as,

$$\vec{A} = 2a.r_1 - a \tag{3.45}$$

$$\vec{C} = 2.r_2 \tag{3.46}$$

In the above equations, r_1 and r_2 are random numbers between 0 and 1 and the value of '*a*' decreases linearly from 2 to 0 as the iteration increases.

The hunting ability of the grey wolves in the pack is guided by alpha. Beta and delta wolves also participate in hunting. In order to mimic the hunting behavior it is identified that the alpha wolf attains the best solution, beta and delta wolf have better knowledge about the potential location of prey. First three solution obtained is saved and using

these solution the position of other wolves in the pack is updated. The following equations are used for updating the positions of the wolves,

$$\vec{D}_{\alpha} = \left|\vec{C}_1.\vec{X}_{\alpha} - \vec{X}\right| \tag{3.47}$$

$$\vec{D}_{\beta} = \left|\vec{C}_2.\vec{X}_{\beta} - \vec{X}\right| \tag{3.48}$$

$$\vec{D}_{\delta} = \left|\vec{C}_3.\vec{X}_{\delta} - \vec{X}\right| \tag{3.49}$$

$$\vec{X}_1 = \vec{X}_{\alpha} - \vec{A}_1.(\vec{D}_{\alpha}) \tag{3.50}$$

$$\vec{X}_2 = \vec{X}_{\beta} - \vec{A}_2.(\vec{D}_{\beta}) \tag{3.51}$$

$$\vec{X}_3 = \vec{X}_{\delta} - \vec{A}_3.(\vec{D}_{\delta}) \tag{3.52}$$

$$\vec{X}(t+1) = \frac{\vec{X}_1 + \vec{X}_2 + \vec{X}_3}{3} \tag{3.53}$$

To sum up, the search process starts with initialization of the population of grey wolves. Over the course of iterations, alpha, beta and delta wolves update their position and using the updated best solution, the position of other wolves in the pack is also updated. The value of *a* is decreased linearly from 2 to 0 in order to enable exploration. The solution tend to diverge from the prey when $\left|\vec{A}\right| > 1$ and converge towards the prey when $\left|\vec{A}\right| < 1$. The GWO is terminated when the stopping criteria is reached.

3.6.5.2 Particle Swarm Optimization (PSO)

Particle Swarm Optimization (PSO) is a population based stochastic optimization technique and is inspired by social behavior of bird flocking or school of fish (Kennedy, 2011; Poli, Kennedy, & Blackwell, 2007). In PSO, the particles are placed or initialized in the search space of some problem. The initial position of the particles is updated and

for each particle in the swarm the objective function is evaluated. Each particle then determines its movement within the search space using the individual particles's best solution (*pbest*), best solution from the swarm that is global best (*gbest*). The next iteration takes place after all the particles have been moved. Like this the swarm as a whole will move towards the optimum solution like a flock of birds searching for food. The equations 3.54 and 3.55 are the general equations used to update the velocity and new position of each particle for every iteration.

$$v_i(t+1) = v_i(t) + c_1 r_1(pbest - x_i(t)) + c_2 r_2(gbest - x_i(t)) \quad (3.54)$$

$$x_i(t+1) = x_i(t) + v_i(t+1) \quad (3.55)$$

where r_1 and r_2 are random number between 0 and 1, c_1 and c_2 are inertia parameters which influence the search more locally or globally, $x_i(t)$ is the position of the particle in *t* iteration. Using *pbest* and *gbest* the velocity of each particle is update using equation 3.54. After calculating the updated velocity the new position of the particle is updated. PSO have wide range of applications like images and video analysis, design and restructuring of electricity networks, load dispatching, electronics and electromagnetic, antenna design and even in biological, medical, and pharmaceutical applications. Advantages of using PSO are it is simple in implementation, has very few algorithm parameters and very efficient global search algorithm.

3.6.5.3 Artificial Bee Colony (ABC)

Collective intelligence of honeybee swarms leads to the emergence of artificial bee colony (ABC) algorithm(Karaboga & Akay, 2009). The ABC algorithm is tailored to simulate the foraging behavior of a honeybee colony. A typical honeybee swarm consists of three fundamental components: food source/employed foragers/unemployed foragers (bees). Employed foragers are the bees that are employed at, and currently

exploiting, a certain food source. They carry information about the (distance, direction and the profitability) of the food source and communicate the information with other bees waiting at the hive. Unemployed bees are classified either as an onlooker bee, or as a scout bee. The former tries to find a food source by means of the information given by an employed bee; while the latter randomly searches the environment to find a new (better) food source. Presumably, an employed bee whose food source is depleted becomes a scout bee, and starts to search for a new food source. Furthermore, it assumes the number of employed bees in the colony to be equal to the number of food sources. Conceivably, the position of a food source represents a possible solution to the optimization problem; whereas the amount of a food source corresponds to the quality (fitness) of the associated solution.

Initially, the ABC generates a randomly distributed population of SN solutions (food source positions) in the search space, where SN denotes the size of employed bees or onlooker bees. Assuming the number of optimization parameters to be D, then each solution $x_i(i=1,2,...,SN)$ will essentially be a D-dimensional vector. All solutions generated at this stage can be obtained from the following equation,

$$x_{ij} = x_{\min.j} + rand[0,1](x_{\max,j} - x_{\min,j}) \tag{3.56}$$

where x_{min} and x_{max} are the lower and upper boundry parameters for the solution x_i. The D-dimensional solutions (food source positions) generated in the initialization step (C=0) are subject to repeated cycles (C=1, 2 …, MCN), until a termination criterion is satisfied. Both global as well as local probabilistic search/selection are implemented in a single ABC cycle. Each cycle entails a number of tasks performed by different bee types.

3.6.5.4 Genetic Algorithm (GA)

Genetic algorithm (GA) is a heuristic optimization technique which mimics the process of natural evolution. The basic components of GA are random number generator, objective function evaluation and genetic operators like reproduction, crossover and mutation operators.

The initial population required at the start of algorithm is a group of random number or population generated from the random generator. The generated population string represents a string of solution to the optimization problem. For the each string in the population the associated fitness value or the objective function is calculated. The fitness value is the measure of quality of the solution represented. The objective of the GA is to transform the set of string into the set of high quality string or the values of best solution. The reproduction operator performs the natural selection function. Individual string are copied from one set to the other set depending on the obtained objective function values. Better the solution higher the probability of selecting the string to the next level. The crossover operator matches the pair of strings randomly and produces new gene or new pair. The number of crossover operations is governed by a crossover rate. The mutation operator randomly mutates or reverses the values of bits in a string. The number of mutation operation depends on mutation rate. For every iteration the genetic phase of GA consists of the above mentioned steps that are evaluation, reproduction, crossover and mutation operations. Therefore for every iteration the genetic phase produces new population and the process is repeated until the stopping criterion is reached.

3.6.5.5 Gravitational Search Algorithm (GSA)

Gravitational search algorithm (GSA) optimization technique is based on Newton's gravitational force behaviors (Rashedi, Nezamabadi-Pour, & Saryazdi, 2009). In GSA

algorithm, agents are considered as objects and their performance is measured by their masses. The gravity force causes all the objects to attract each other and this force causes a global movement of all objects towards the objects with heavier masses. Hence the communication between the masses is through gravitational force. Here the heavy mass corresponds to good solution and move slowly than lighter ones. Each mass presents a solution, and the algorithm is guided by properly adjusting the gravitational and inertia mass. As the algorithm progress the masses are being attracted by heavier mass. At last, this mass will present an optimum solution in the search space. Therefore the principle of GSA is works on generating random agents in the search space. By calculating the objection function for each agents the gravitational constant, best and worst solution and inertial masses are updated. Then using the updated information the total force of attraction from different directions for each agent is calculated. The acceleration and velocity for each agent is calculated and by adding the updated velocity with the current position of the agent the new position of the agent is calculated. The above process is repeated until the stopping criteria are reached.

For the iteration '*t*' the force acting on mass '*i*' from mass '*j*' is given as,

$$F_{ij}^{d}(t) = G(t)\frac{M_{pi}(t) \times M_{aj}(t)}{R_{ij}(t) + \varepsilon}(x_j^d(t) - x_i^d(t)) \tag{3.57}$$

where M_{aj} and M_{pi} are active and passive gravitational masses, $G(t)$ is gravitational constant at iteration t, ε is constant and R_{ij} is the Euclidian distance between the agents i and j. The total force F^d_i that acts on agent i can be given as,

$$F_i^d(t) = \sum_{j=1, j\neq i}^{N} rand.F_{ij}^d(t) \tag{3.58}$$

where *rand* is the random number between 0 and 1 and therefore by the law of gravity, the acceleration of the agent *i* at iteration *t* is given as,

$$a_i^d(t) = \frac{F_i^d(t)}{M_{ii}(t)} \tag{3.59}$$

where M_{ii} is the inertial mass of the agent *i*.

The next velocity of the agent *i* can be calculated by adding the fraction of the current velocity with the acceleration and therefore the updated velocity and position of the agent is given as,

$$v_i^d(t+1) = rand[0,1] \times v_i^d(t) + a_i^d(t) \tag{3.60}$$

$$x_i^d(t+1) = x_i^d(t) + v_i^d(t+1) \tag{3.61}$$

3.7 Development of Energy Management System (EMS)

The proposed EMS module has the proposed ramp-rate control strategy and "mix-mode" operating strategy. Forecasted load power and PV power, prices of natural gas and utility grid electricity are the input to the EMS module. The forecasted data are obtained one day ahead and fed into the EMS. From the actual PV power, the smoothed PV output power values are prepared using the proposed ramp-rate control strategy. Using other input information along the smoothed PV output power values the mix-mode operating strategy is solved from which the EMS is able to send dispatch directives or dispatch reference values for the fuel cell and BESS.

In the proposed EMS the mix-mode operating strategy is solved using receding horizon economic dispatch (RHED) approach (Kwon & Han, 2006).

3.7.1 Receding Horizon Economic Dispatch (RHED) Approach for mix-mode operating strategy

In the receding horizon economic dispatch problem initially, the optimal solution is found for finite horizon *N* starting from *1* (Figure 3.14). The resulting optimal value for point *1* is selected and the solutions for remaining horizon are ignored. The solution for point *1* is implemented in the system and the system's response is saved and given as an initial condition for next optimization horizon. Now the finite horizon is moved by one step and held between *2* to *N+1*. Then the aforementioned optimization procedure is repeated. This optimization is repeated for 24hours for every step.

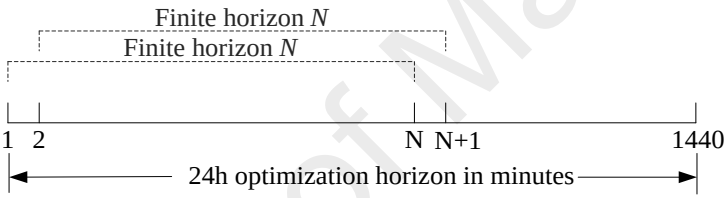

Figure 3.14: Receding horizon economic dispatch approach

Here the receding horizon economic dispatch problem is solved to find the optimal generation dispatch values for *K* generators including utility grid which incurs the lowest operating cost from the proposed strategies. With the forecasted profile of load and smoothed PV power fed into the system, the economic dispatch problem considering the constraints is solved for the horizon between *1* to *N* for strategy 1, 2 and 3 as mentioned above. The output of the economic dispatch is the optimal dispatch values for *K* generators for three proposed strategies which can be summarized in equations 3.62, 3.63 and 3.64 as,

$$P^1(K\times N)=\begin{bmatrix} P^1(1,1) & P^1(1,2) & . & . & P^1(1,N) \\ P^1(2,1) & P^1(2,2) & . & . & P^1(2,N) \\ . & . & . & . & . \\ . & . & . & . & . \\ P^1(K,1) & P^1(K,2) & . & . & P^1(K,N) \end{bmatrix} \tag{3.62}$$

$$P^2(K\times N)=\begin{bmatrix} P^2(1,1) & P^2(1,2) & . & . & P^2(1,N) \\ P^2(2,1) & P^2(2,2) & . & . & P^2(2,N) \\ . & . & . & . & . \\ . & . & . & . & . \\ P^2(K,1) & P^2(K,2) & . & . & P^2(K,N) \end{bmatrix} \tag{3.63}$$

$$P^3(K\times N)=\begin{bmatrix} P^3(1,1) & P^3(1,2) & . & . & P^3(1,N) \\ P^3(2,1) & P^3(2,2) & . & . & P^3(2,N) \\ . & . & . & . & . \\ . & . & . & . & . \\ P^3(K,1) & P^3(K,2) & . & . & P^3(K,N) \end{bmatrix} \tag{3.64}$$

Where matrices $P^1(K\times N), P^2(K\times N), P^3(K\times N)$ contain the optimal solution for strategy 1, strategy2 and strategy 3 respectively for horizon held between *1* and *N*. The corresponding values of the objective function for three strategies for *1* to *N* horizon is presented in Figure 3.15.

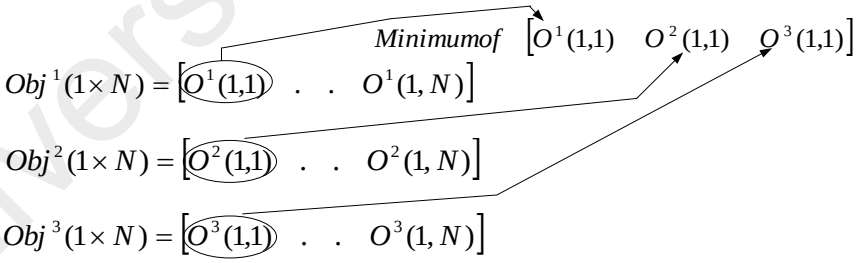

Figure 3.15: Development of mix-mode operating strategy

The matrices $Obj^1(1\times N), Obj^2(1\times N), Obj^3(1\times N)$ contain values of the objective functions for three strategies for *1* to *N* horizon. Here the values of objective functions for the three strategies for initial step are given as $O^1(1,1), O^2(1,1), O^3(1,1)$. The minimum of the three values should incur the lowest operating cost. Therefore, the optimal generation dispatch corresponding for the lowest value of objective function for the initial step is selected and rest of the optimal solution will be ignored. The optimal dispatch values for

K generators is shown in equation 3.65 for instant *1* is implemented in the system, and the system's response is saved and given as the initial condition for next step.

$$P^{optimal}{}_{(K\times 1)}(1) = \left[P(1,1) \quad . \quad . \quad P(K,1)\right]^T \tag{3.65}$$

Since the receding horizon optimization approach is solved for every minute, the horizon moves by one step between *2* to *N+1* for which steps above are repeated. The optimal elements for any time instant *i* in the horizon is given by,

$$P^{optimal}{}_{(K\times 1)}(i) = \left[P(1,i) \quad . \quad . \quad P(K,i)\right]^T \tag{3.66}$$

This receding horizon economic dispatch approach is repeated for 24hours

to optimally schedule the energy sources to incur the lowest operating cost. There are three advantages in implementing mix-mode operating strategy through receding horizon economic dispatch approach.

(i) The receding horizon economic dispatch problem helps in finding the optimal dispatch values online.

(ii) Using other optimization techniques for the economic dispatch problem for every minute requires significant computation time. Since RHED approach shortens the optimization horizon, the computational burden is reduced.

(iii) Implementing RHED approach for mix-mode operating strategy not only reduces the computational time but also finds optimal solution with lowest operating cost for every minute.

3.7.2 Implementation of mix-mode strategy using RHED approach

The flowchart for implementing the mix-mode strategy using RHED approach is shown in Figure 3.16.

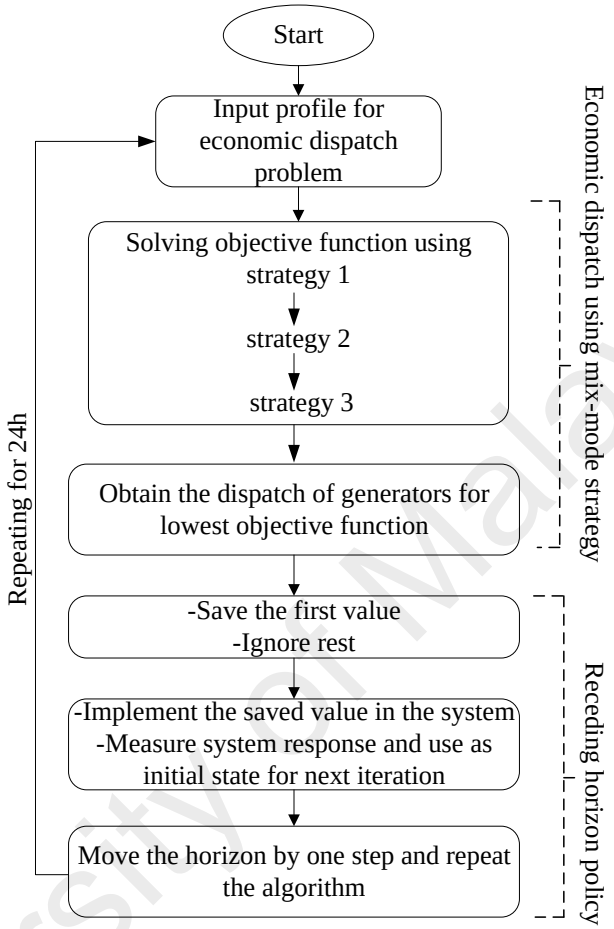

Figure 3.16: Mix-mode operating strategy using RHED approach

In order to implement the RHED approach, as the first step the forecasted profile of load, smoothed PV power, daily grid electricity price pattern, the price of the natural gas and BESS initial state of charge (SOC) and minimum and maximum SOC limits for the BESS should be provided as input. From the given input profiles the economic dispatch is performed for continuous run, power sharing and ON/OFF mode.

The output of the economic dispatch is the optimal dispatch values for three proposed strategies optimized during *1* and *N* horizon which can be summarized in equations 3.67, 3.68 and 3.69 as,

$$P_{EDS1} = \begin{bmatrix} P_{FC}(1) & P_{FC}(2) & . & . & P_{FC}(N) \\ P_{bat}(1) & P_{bat}(2) & . & . & P_{bat}(N) \\ P_{Grid}(1) & P_{Grid}(2) & . & . & P_{Grid}(N) \end{bmatrix} \tag{3.67}$$

$$P_{EDS2} = \begin{bmatrix} P_{FC}(1) & P_{FC}(2) & . & . & P_{FC}(N) \\ P_{bat}(1) & P_{bat}(2) & . & . & P_{bat}(N) \\ P_{Grid}(1) & P_{Grid}(2) & . & . & P_{Grid}(N) \end{bmatrix} \tag{3.68}$$

$$P_{EDS3} = \begin{bmatrix} P_{FC}(1) & P_{FC}(2) & . & . & P_{FC}(N) \\ P_{bat}(1) & P_{bat}(2) & . & . & P_{bat}(N) \\ P_{Grid}(1) & P_{Grid}(2) & . & . & P_{Grid}(N) \end{bmatrix} \tag{3.69}$$

The matrices $Obj^1(1\times N), Obj^2(1\times N), Obj^3(1\times N)$ contain values of the objective function for three strategies for *1* to *N* horizon. As explained before the value of the objective function for the first step from three strategies are compared, and the minimum of three objective functions and its corresponding optimal generation values are saved. Based on the receding horizon approach only the first dispatch elements are saved, and the rest are ignored. The decision variables from the mix-mode strategy for the economic dispatch problem are P_{FC}, P_{Grid} and P_{bat}. The optimal dispatch solution for the first step in the horizon *1* to *N* is found as,

$$P^{optimal}(1) = \begin{bmatrix} P_{FC}(1) & P_{bat}(1) & P_{Grid}(1) \end{bmatrix}^T \tag{3.70}$$

Then the optimal solution is implemented into the system, and the response of the system is saved and used as the initial values for solving the next iteration. Now the economic dispatch optimization window moves by one step, and the optimization horizon is held between *2* to *N+1*. To guarantee the reliability of the solution, the optimization is performed for every minute. If moved every minute for 24hours time horizon the optimization window is performed for 1440 sampling time. Therefore, the algorithm is repeated for 1440 times for 24hours of the day. The results of optimal dispatch for 1440 values can be summarized in a matrix as shown below,

$$P_{RHED}^{optimal} = \begin{bmatrix} P_{FC}(1) & P_{FC}(2) & . & . & P_{FC}(1440) \\ P_{bat}(1) & P_{bat}(2) & . & . & P_{bat}(1440) \\ P_{Grid}(1) & P_{Grid}(2) & . & . & P_{Grid}(1440) \end{bmatrix} \quad (3.71)$$

Equation 3.71 presents the optimal dispatch solutions for the fuel cell, utility grid and energy sources present in the microgrid for 24hours time horizon using mix-mode operating strategy.

3.8 Summary

On analyzing the MA and CES smoothing methods exhibit memory effect. As a result of memory effect the energy storage is allowed to operate even though the PV ram-rates are within the limit. This will eventually contribute to increase in size of energy storage and decrease in its life span. The proposed ramp-rate control strategy checks for ramp-rate violation for every time step. As a result, the energy storage is allowed only for ramp-rate violation events and for rest of the time it will be switched off or the power from the energy source will be zero. The proposed ramp-rate control strategy will eventually contribute to reduction in size of energy storage on the other hand increasing its life span.

The EMS module consists of the proposed ramp-rate control strategy and "mix-mode" operating strategy to operate the microgrid sources with lowest operating cost. The "mix-mode" operating strategy will utilize the microgrid sources optimally with lowest operating cost. An accurate method to evaluate the size of the BESS with lowest capital cost is realized using different optimization techniques. The idea of solving the EMS using RHED approach is also realized because using RHED approach shortens the optimization horizon, therefore reducing the computational burden.

CHAPTER 4: VALIDATION OF PROPOSED RAMP-RATE CONTROL STRATEGY AND MIX-MODE OPERATING STRATEGY

4.1 Introduction

In this chapter the proposed ramp-rate control strategy and the proposed mix-mode operating strategy is validated. For validation purpose the performance of the proposed ramp-rate control strategy is compared with moving average (MA) and conventional exponential smoothing (CES) methods.

4.2 Test system for validation of the proposed ramp-rate control strategy

In this section the proposed solar PV ramp-rate control strategy is validated. For ramp-rate control any energy storage devices like capacitors or batteries are used to limit the PV output power fluctuations. In this research battery energy storage is used to limit the PV output power fluctuations. In order to validate the effectiveness of the proposed technique, the test system in chapter 3 is considered where the fuel cell and BESS are disconnected. Figure 4.1 presents the test system considered where the energy management system (EMS) module except the proposed ramp-rate control strategy is disabled.

The test system consists of a 200kWp solar PV plant and the energy storage consists of 200kWh battery storage. The sources are grid connected and operated parallel with the load.

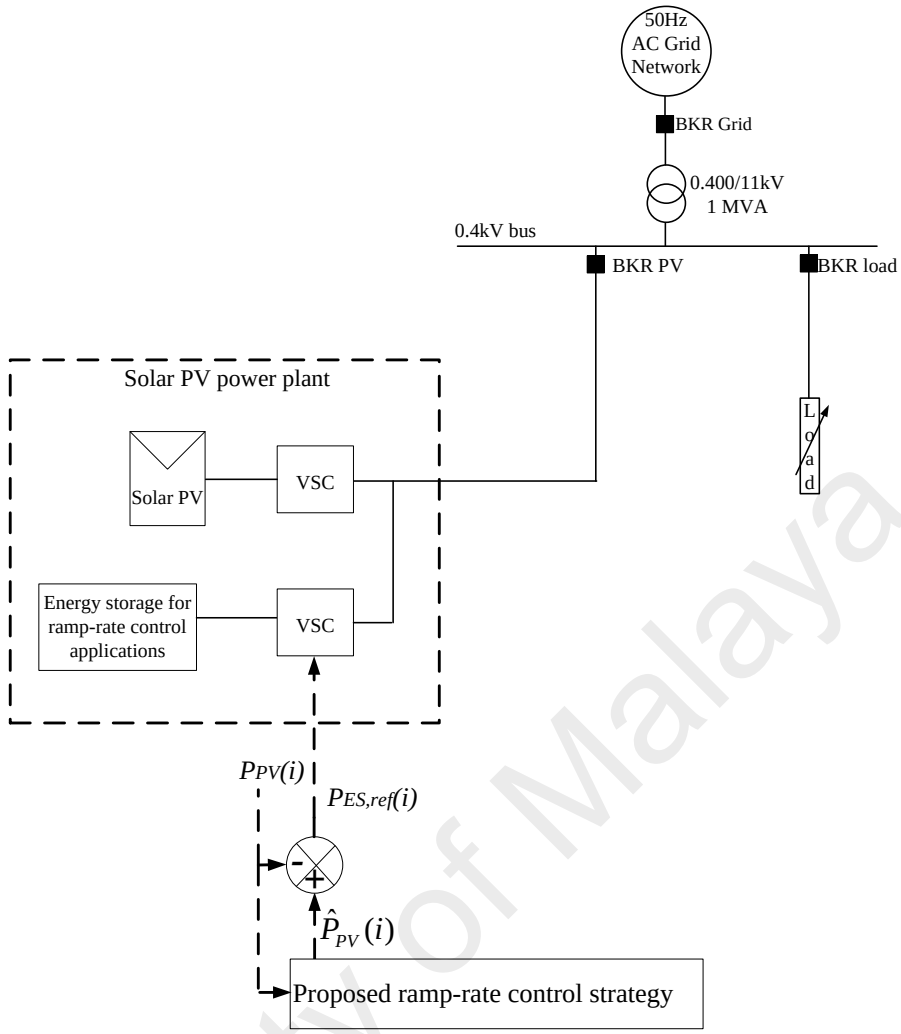

Figure 4.1: Schematic of grid connected PV-energy storage for proposed ramp-rate strategy

4.3 Solar radiation data

Load and generation forecasting are both beyond the scope of this research. However, to examine the impacts of load and generation variations on dynamics of system, it is necessary to collect the real load, solar PV irradiation, and temperature data. In here, the solar irradiation and the daily load profiles are assumed to be forecasted by a data centre or a forecasting module one day ahead.

A typical location in Malaysia in the city of Kuala Lumpur with latitude of 3',7'N and longitude of 101',39'E is chosen as the sampling point. The solar radiation pattern is extracted through the HOMER software which is a Micropower optimization model

developed and supported by Homer Energy LLC. This software is able to estimate the average hourly irradiation profile using the method suggested by (Graham & Hollands, 1990). Homer creates a set of 8760 solar radiation values for each hour of the year.

On the other hand, to study the dynamic behavior of microgrid in presence of solar PV generator plant, solar irradiation profile is needed with higher precision than the hourly data (Katiraei & Agüero, 2011). For example, to see the power flow changes in the system, followed by solar PV unit output power variation (ramp-rate) within 1 minutes, the solar irradiation profile should be sampled in every 1 minutes during a day. In this case, the battery source can absorb or supply the power difference between smoothed waveform and actual PV output power during the period solar PV plant ramp ups or down, respectively.

The abrupt changes in generated power are the main concerns for the system planners and operators. A passing cloud can lead to more than 60% change in PV plant's output power in a matter of seconds (Mills, 2012). Figure 4.2 shows average hourly solar radiation profile G for a day in May for a typical location in Malaysia is extracted using HOMER software. Twenty four hours radiation data have been interpolated to obtain 1440 values by adding normal distribution random noise with '0' mean and standard deviation as '1' (Koohi-Kamali et al., 2014). The solar radiation is then redrawn to create 1min radiation profile (G_n) and is utilized as the input to PV plant.

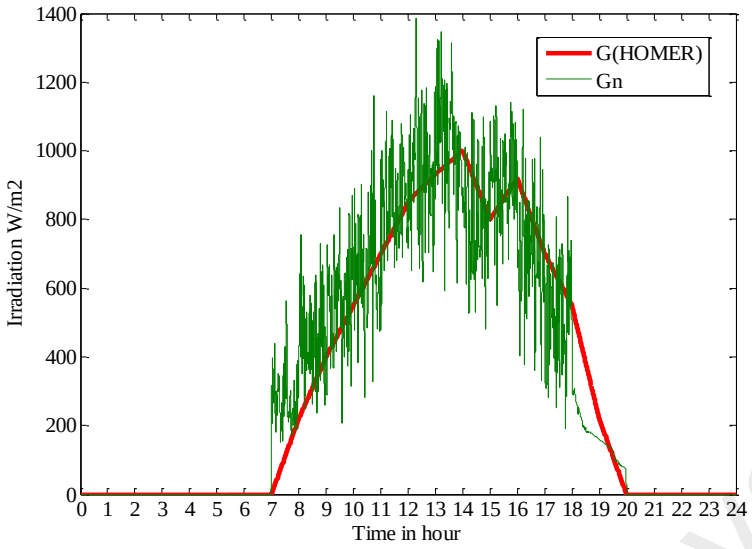

Figure 4.2: Forecasted solar irradiation profile by HOMER in sampling location in Peninsular Malaysia on May and the noise applied on it

4.4 Application of the proposed ramp-rate control strategy

Output power from solar PV represents time series data, where the data points consist of successive measurement of PV power over a time interval. The output power from solar PV plant modelled is section 3.2.3 using 1-minute radiation data as its input is shown in Figure 4.3. Rapid fluctuations in PV output power is found where the proposed ramp-rate control strategy is applied to control the ramp-rate from solar PV within the desirable level.

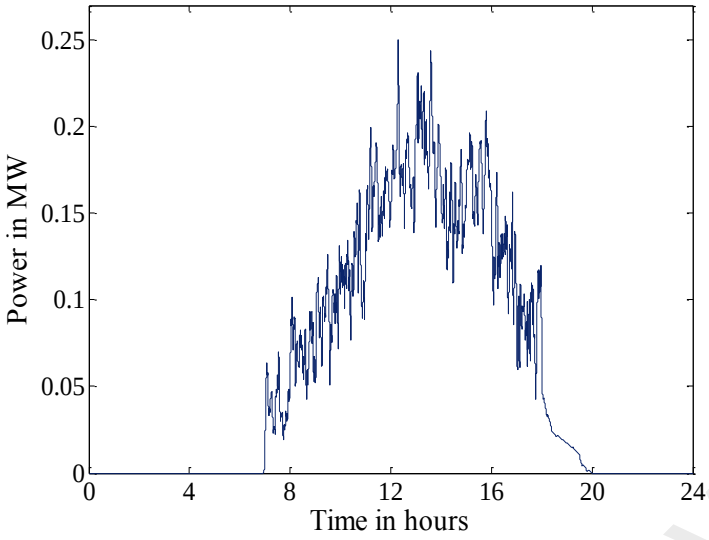

Figure 4.3: Solar output power obtained from 1-min radiation data

The proposed ramp-rate strategy is compared with MA and CES method. The battery storage is permitted to operate between 30% to 100% state of charge (SOC). At initial condition the SOC of the battery is set to 70% to allow the battery to charge and discharge. Results for mitigation of PV output power fluctuation using MA, CES and proposed ramp-rate control strategy are shown in Figures 4.4, 4.5 and 4.6 respectively. In these figures the actual PV power from solar plant is denoted as (P_{PV}) and the power from the energy storage is denoted as (P_{BES}).

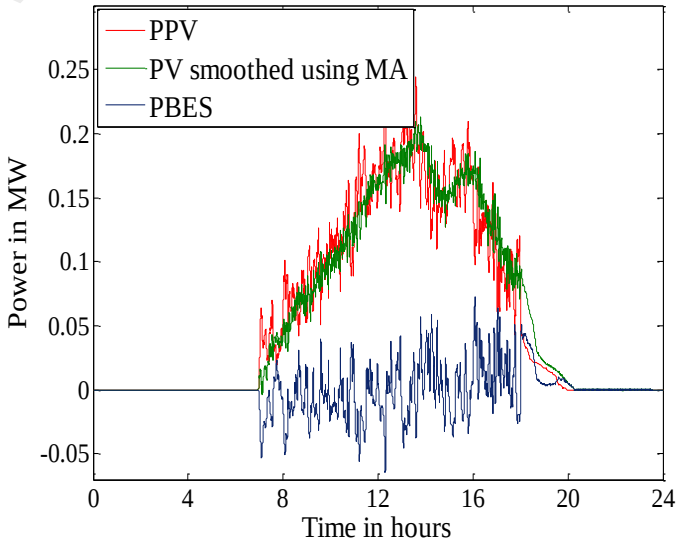

Figure 4.4: Smoothing PV output power by using MA method

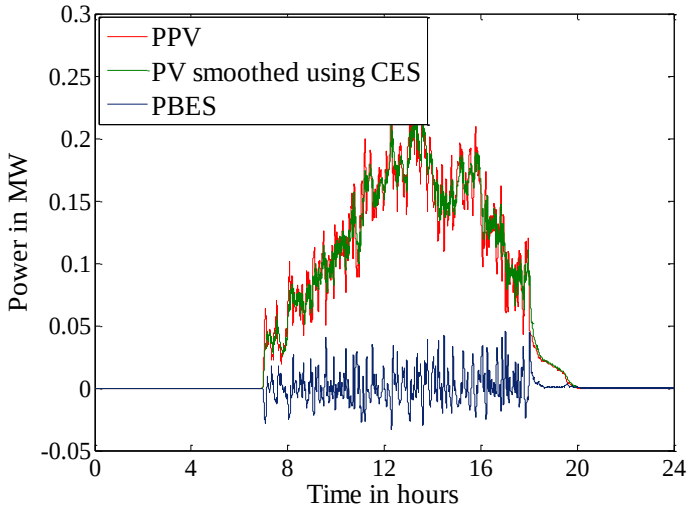

Figure 4.5: Smoothing PV output power by using CES method

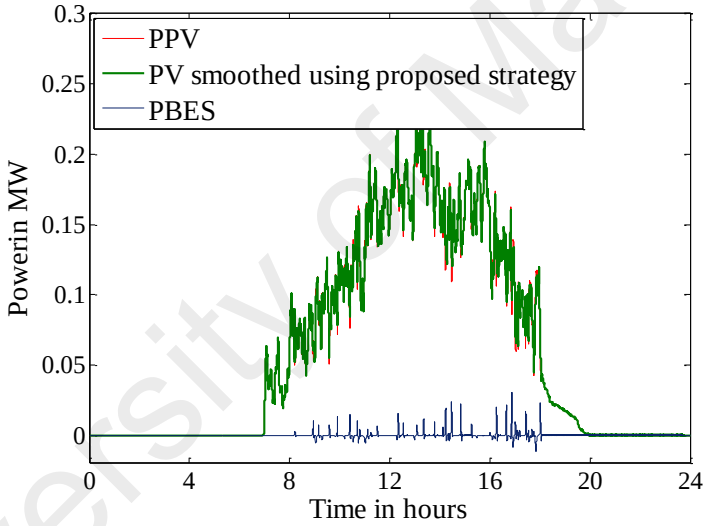

Figure 4.6: Smoothing PV output power by using proposed ramp-rate control strategy

The advantage of the proposed ramp-rate control strategy can be illustrated from Figure 4.7. Figure 4.7 presents actual PV power with smoothed power using MA, CES and the proposed method during the time period 13.5hours and 18.5hours. The corresponding energy source utilization for the three methods is plotted in Figures 4.8, 4.9 and 4.10.

We would like to highlight the waveforms particularly between 18hours and 18.5hours. Between this time period, in Figure 4.7 it can be noticed that there is no significant fluctuation in actual PV power. When MA or CES methods are applied, the energy

storage is discharged unnecessarily in order to smooth the actual PV power as a result of memory effect. The battery discharge for MA and CES methods for time period 18hours-18.5hours can be viewed in Figure 4.8 and 4.9 respectively. These types of non-significant fluctuating events are present over the stretch of PV operation for which the battery will continuously charge or discharge power to smooth the PV output which is actually unnecessary. As a result the energy capacity required for the energy storage will increase when MA or CES methods are applied which will eventually contribute to increase its capital cost. In addition, when MA and CES methods are applied, the battery is continuously switched ON which will affects its lifespan. Deep discharging and frequent charging decreases battery life (Amiri, Esfahanian, Hairi-Yazdi, & Esfahanian, 2009).

On the other hand when using the proposed ramp-rate control strategy the ramp-rates are checked for any violations using the ramping function *f(RR)* for every time step. Furthermore based on the ramping function *f(RR)* the smoothing parameter 'σ' and battery switching is decided. If the ramp-rates are within the limit the battery is switched OFF and during the ramp violation cases the battery is switched ON only to limit the ramp-rate within its desirable level. This is evident from Figure 4.10 where the battery is switched ON only during ramp violation events and for rest of the time it is switched OFF (encircled in Figure 4.10).

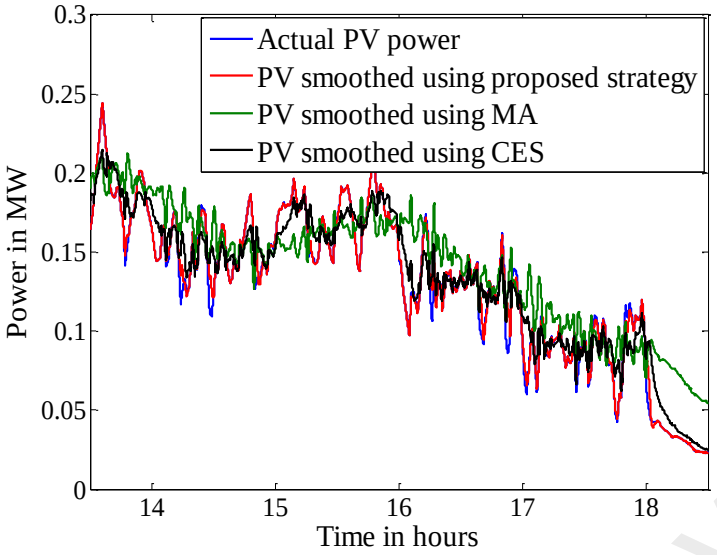

Figure 4.7: Actual power and smoothed power profiles for different methods for specific time period

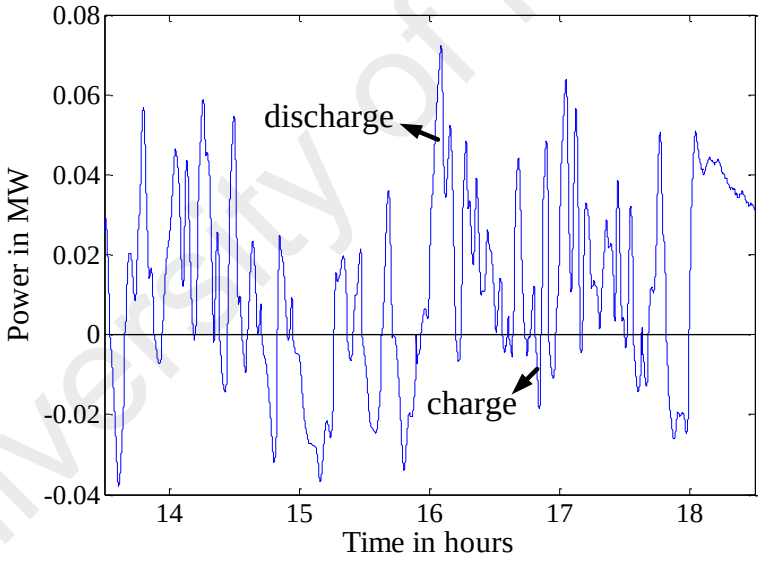

Figure 4.8: Battery utilization for MA method

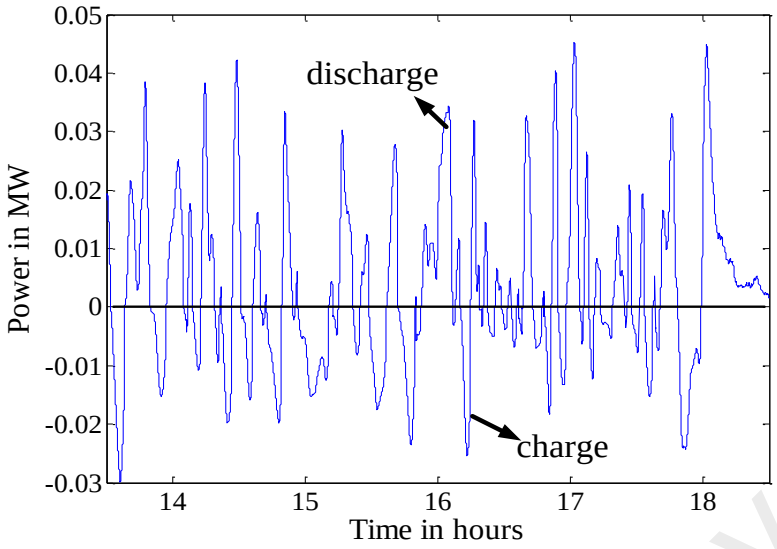

Figure 4.9: Battery utilization for CES method

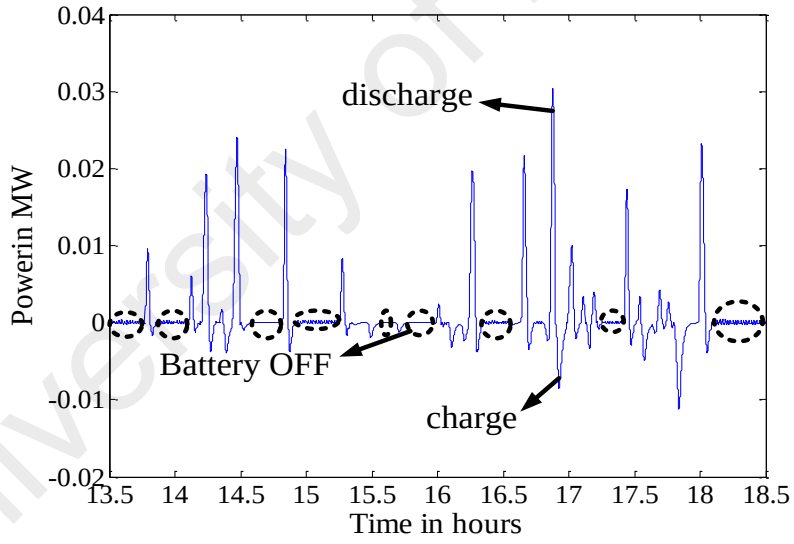

Figure 4.10: Battery utilization for proposed ramp-rate strategy

The ramp-rate profile of the smoothed PV output for the proposed method is presented in Figure 4.11 which indicates the ability of the proposed method to limit the ramp-rate within the desirable range.

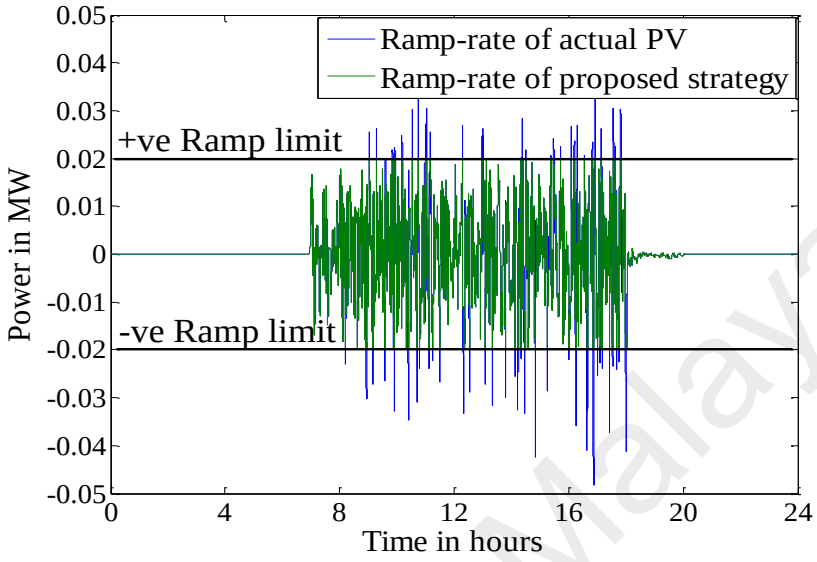

Figure 4.11: Control of PV ramp-rate using proposed strategy

Figure 4.12 gives clear picture of variation of smoothing parameter 'σ 'for entire time of operation. It can be observed that the value of smoothing parameter is '1' when the ramp-rate is within the limits. The value of smoothing parameter will be less than '1' for ramp-rate violations.

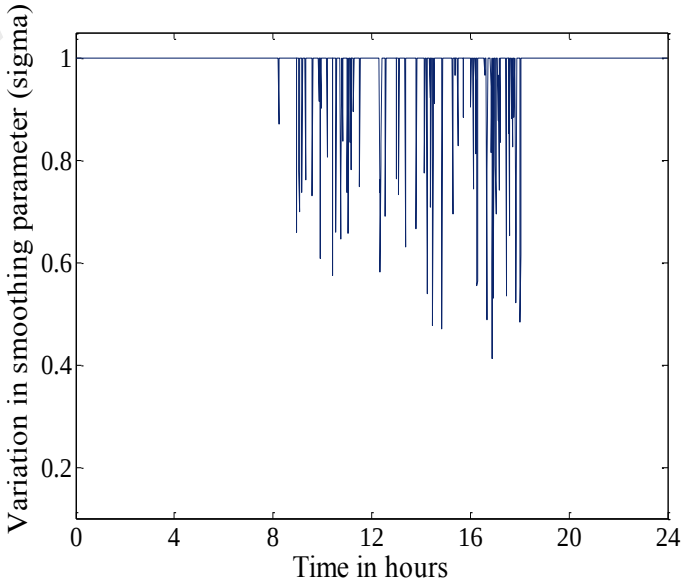

Figure 4.12: Variation of smoothing parameter 'σ 'for proposed ramp-rate strategy

Table 4.1 shows a comparison between the three methods for the number of instances battery storage is switched ON. It was noticed that there are 85 instances of ramp-rate violation events. Using the proposed ramp-rate control strategy the battery storage is switched ON only during those instances. The smoothing parameter calculated will be less than '1' for those instances. During remaining instances the battery storage is switched OFF since the PV ramp-rate is within the limit. Here the value of smoothing parameter is '1'. On the other hand when MA or CES method is used to smooth PV output power fluctuation the battery storage is never switched OFF or the battery storage is switched ON all the time.

Table 4.1: Comparison on battery storage (BS) operation for the three methods

Method	Number of charging instances of BS	Number of discharging instances of BS	Number of instances BS is switched 'ON'
MA method	370	448	All the time
CES method	347	444	All the time
Proposed strategy	36	49	85

From Table 4.1 it is evident that when the proposed ramp-rate control strategy is used the number of charging and discharging instances of battery storage is very less because the battery source is switched ON only during ramp-rate violation events.

It was noticed that the PV output power variability and the power injected or absorbed by the battery storage to smooth PV power affects the voltage at distribution side. Therefore the changes in voltage are measured in terms of total harmonic distortion (THD) at phase voltage at phase A at the load side. The total harmonic distortion (THD) level in voltage waveform at phase A without and with battery storage for three methods is compared in Figure 4.13.

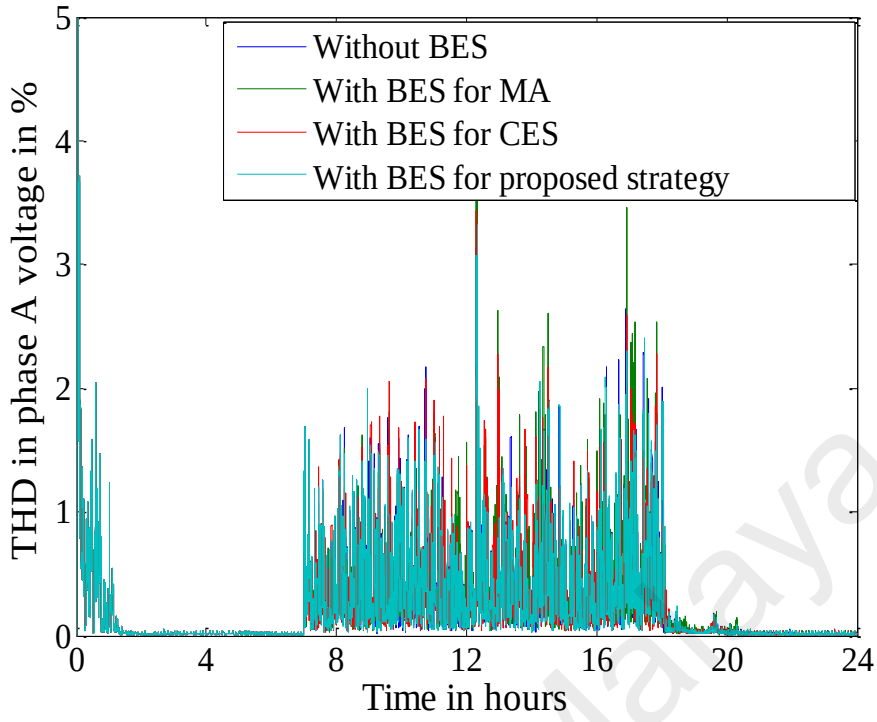

Figure 4.13: THD at phase A voltage without and with battery storage for 3 methods

As per the standards the THD level for the entire system with or without battery storage is maintained below 5%. It is noticed that the THD level is very less when PV power is absent and harmonics injected into phase A voltage increases drastically when PV power fluctuates rapidly. It should also be noticed that during sunset when PV power comes to zero the harmonics injected in phase A voltage is insignificant. The battery storage is operated only during the presence of PV output power. It was further noticed that the THD level varies with and without operation of battery storage. The THD level when the system is operated with battery storage is slightly higher than THD level when system is operated without battery storage. In addition when compared among the three smoothing methods, the THD level is found higher when battery storage is operated using MA method. The THD level is least for most of the time when battery storage is operated using proposed ramp-rate control strategy. As a comparison, Table 4.2 shows average THD level in percentage obtained only when PV and battery storage is operated.

Table 4.2: Average THD level when PV and battery storage is operated

Method	Average THD in %
Without BES	0.3599
MA method	0.4059
CES method	0.3804
Proposed ramp-rate strategy	0.3671

The THD level for all the three method is higher than THD level when the system is operated without battery storage. This is because the battery storage operation for smoothing PV output power contributes to higher THD level. The average THD level is lower for the proposed ramp-rate control strategy because the battery storage is switched ON only during the ramp violation events and rest of the time it is switched OFF. On the other hand the battery storage is switched ON all the time for MA or CES methods.

It is evident that the proposed ramp-rate control strategy controls the PV ramp-rate to desirable level. Since the battery is operated in ON/OFF mode there is no frequent charging/discharging events, therefore the proposed method can contribute to increase in battery storage lifetime. Since battery storage is switched ON for particular time interval for the proposed method the level of voltage distortion on load side is also less.

4.5 Relation between smoothing parameter 'σ' and ramp-rate

For understanding the relation between the proposed smoothing parameter 'σ' and ramp-rate, PV ramp rate is plotted in Figure 4.14 together with its corresponding smoothing parameter.

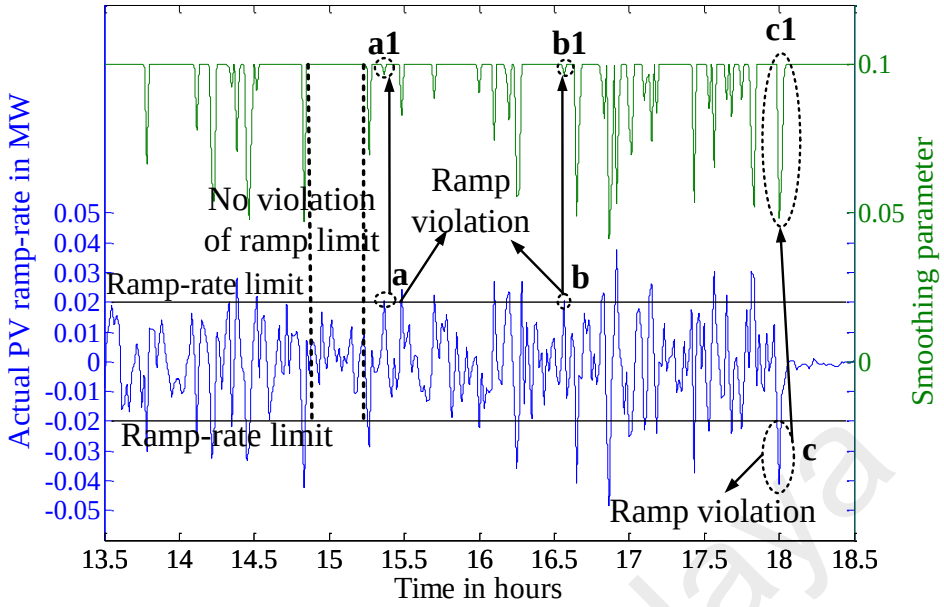

Figure 4.14: Variation of smoothing parameter with ramp-rate violation

The smoothing parameter varies from 0 to 1 and for the purpose of comparing it with ramp-rate, the smoothing parameter is scaled down to 0 to 0.1. Therefore to obtain the actual value of *'σ'*, the scale reading need to be multiplied by 10. For every time instant, the smoothing parameter is calculated. It can be observed in Figure 4.14, if the ramp-rate is within the limit, the value of smoothing parameter *'σ'* is set to '1'. The proposed control strategy controls the ramp-rate even for a slightest violation. For examples, small ramp rate violation at point 'a' and 'b' in Figure 4.14 causes small changes in smoothing parameter from '*1*' as shown in point 'a1' and 'b1' respectively. The small change of the smoothing parameter requires less power from the battery to control the ramp-rate within the limit. On the other hand, a large ramp violation as shown in point 'c' in Figure 4.14 causes large changes in smoothing parameter from '1' as shown in point 'c1'. As a result, the power required from the battery to maintain the ramp-rate within the limit is also large.

4.6 Data used for validation of the proposed mix-mode operating strategy

To evaluate the performance of the proposed mix-mode operating strategy, a low voltage grid connected microgrid presented in chapter 3 is considered. The grid connected microgrid consists of 200kWp solar PV, two identical 100kW solid oxide fuel cell, and BESS operated parallel with the load. The minimum and maximum operating range of the single fuel cell unit is fixed as 10kW and 100kW respectively. Outside the operating range will reduce the fuel cell life (Y. Li et al., 2007).

The load characteristic is one of the main factors in power system modeling for dynamic stability and transient studies. Similar to the stochastic generation, load also varies during the day. In some hours in a day the load profile is in its maximum value. In this thesis residential customer are investigated. The residential loads are considered to be non-vital load. The daily load pattern of a residential area from (Koohi-Kamali et al., 2014) is used for this work. The load pattern is scaled down up to maximum load demand of 200kW as shown in Figure 4.15. The load profile of the residential customers is provided where the load varies during the day.

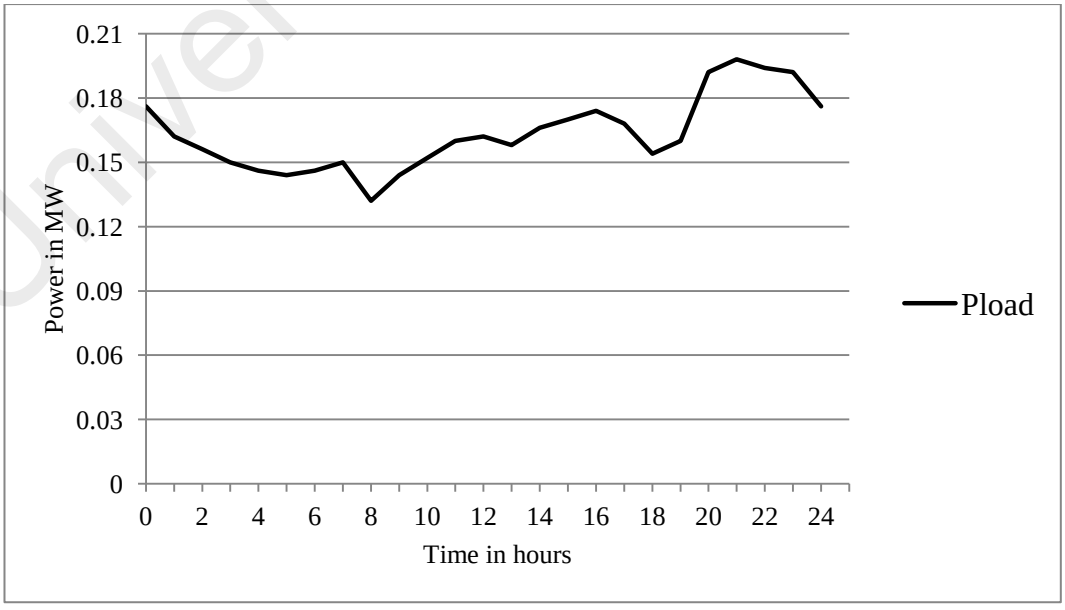

Figure 4.15: Residential customer load profile in Malaysia

The support of utility grid connection for the grid connected microgrid increases the reliability of microgrid system. There may me instances where the microgrid is unable to supply power to the load demand. In this case the power to the load demand is supplied by the utility grid. For energy management it is necessary to maximize the distributed generators and utility grid with less generation cost. In this thesis apart from PV generator there are two distributed generators they are BESS and fuel cell. The operation cost of the PV and BESS is considered negligible in this work. The operation cost of fuel cell with expense on power drawn from the utility grid adds to the total generation cost or operation cost of the grid connected microgrid. The power generated from fuel cell system depends upon the input fuel that is natural gas price. Similarly, the cost of power drawn from the utility depends upon the utility grid electricity price. Therefore the cost of natural gas and utility grid's electricity price considered for this work is given in Figure 4.16. The energy costs considered for this work are taken from (MalaysiaGasAssociation, 2015; Nazar, Abdullah, Hassan, & Hussin, 2012).

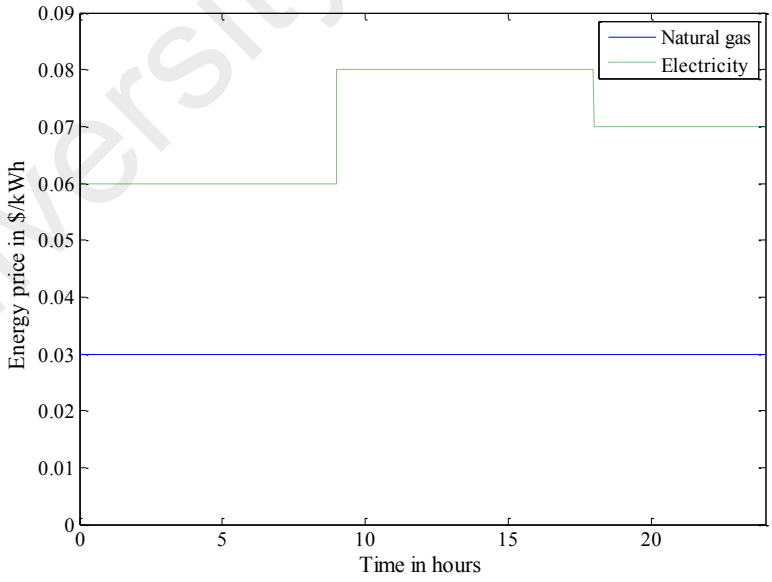

Figure 4.16: Energy prices in ($/kWh)

4.7 Validation of the proposed mix-mode operating strategy

In this section, the superiority of the proposed mix-mode operating strategy is validated for the microgrid model. For this study since BESS is considered, the optimal size of the BESS is found out using the proposed sizing method presented in section 3.6.4. The initial SOC level of the BESS during the start of the day is maintained at 90%. The BESS size is optimized within the range [100kWh, 3000kWh] considering all the BESS and distributed sources constraint. The optimal total BESS capacity for this case is found to be 2350.8kWh. The results of optimal dispatch values for the distributed sources in the microgrid for mix-mode strategy are presented in Figure 4.17. Figure 4.18 show the BESS state of charge (SOC) level maintained within its limit.

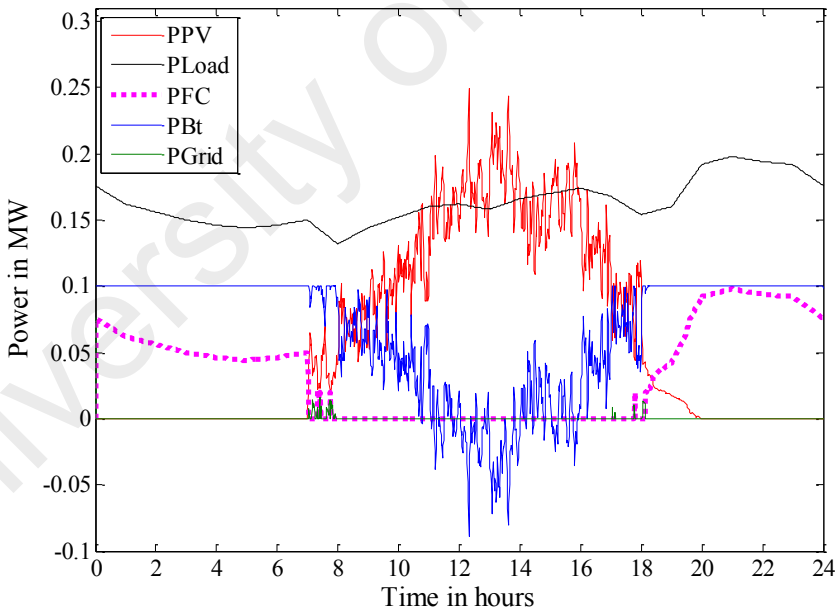

Figure 4.17: Optimal output of distributed source in microgrid for mix-mode strategy

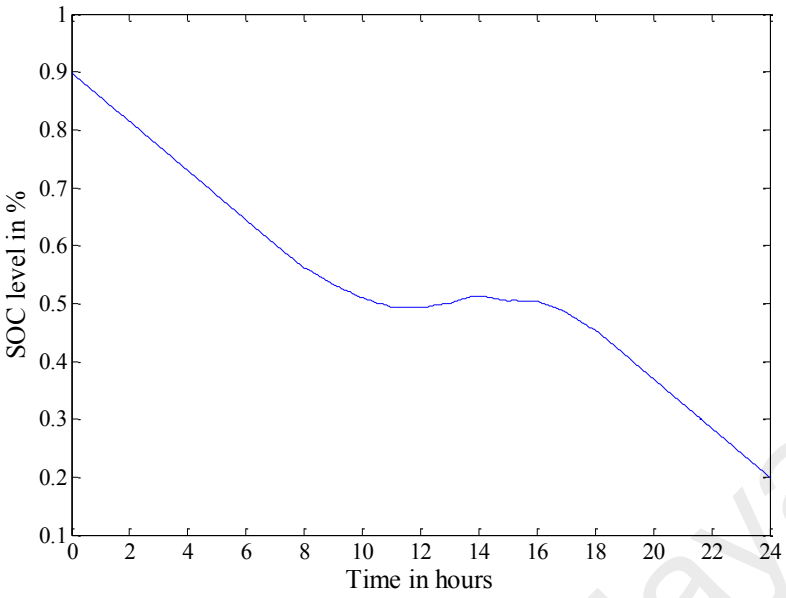

Figure 4.18: BESS SOC level for mix-mode operating strategy

A comparison on daily operating cost for the proposed mix-mode strategy with other strategies is presented in Table 4.3.

Table 4.3: Comparison of daily operating cost

	Strategy 1: Continuous run mode	Strategy 2: Power sharing mode	Strategy 3: ON/OFF mode	Mix-mode
Operating cost in $	1,650.5	837.0528	909.8441	833.8566
BESS operating hours	19.76	20.93	20.93	20.93
FC operating hours	24	13.58	4.46	13
Grid operating hours	0	0.03	9.16	0.61
PV operating hours	12.96	12.96	12.96	12.96

Results from Table 4.3 shows that operating the microgrid in continuous run mode is costlier. In addition, the fuel cell is also forced to run for the 24hours time period. This is because of absence of utility grid participation in the continuous run mode. Operating cost of microgrid is found to be less when the microgrid is operated under power

sharing mode when compared to ON/OFF mode. However, the fuel cell is operated for 13.58hours which is higher than ON/OFF mode where the fuel cell is forced to run at its rated capacity for 4.46hours only. The advantage of operating the microgrid in ON/OFF mode is, when the fuel cell is forced to run at ON/OFF mode the excess power can be used for charging the BESS. Moreover since the run time of fuel cell is less during ON/OFF mode which can contribute to increase in its calendar life. The overall operating cost of the microgrid for the proposed mix-mode operating strategy is less than other operating strategies. This proves the point that operating a microgrid in different operating strategies for 24hours time period will incur lowest operating cost. The operating hours of fuel cell and utility grid is found to be 13hours and 0.61hours respectively.

4.8 Summary

In this section, simulation results of the proposed ramp-rate control strategy and mix-mode operating strategy are presented.

A new method to control the PV output power ramp-rate to desirable level using ES is proposed in this research. From the results it is clear that the MA or CES method may be effective in smoothing PV output power but results in larger ES capacity and reduction of its life span. On the other hand, the proposed ramp-rate control strategy does not exhibit memory effect. The proposed ramp-rate control strategy allows the BES to operate only during ramp violation events for which the BES optimally charges/discharges to control the ramp-rate to desirable level. Therefore when the proposed approach is used, the size of BES can be reduced considerably which will result in reduction of capital cost. During the time of the day the PV power is available for 13 hours. When the proposed method is applied, the BES is switched ON for 85 minutes which constitutes to only 10.9% of BES operation when compared to MA or

CES methods. This selective ON/OFF operation of BES will also contribute to increase in its life span.

With this the validation of proposed mix-mode operating strategy is also carried out. From the results it is confirmed that operating the microgrid with two or more operating strategy its operating cost can be minimized. Majority of the researcher applied power sharing mode for their EMS and compared to the power sharing mode the operating cost of the microgrid is reduced by 0.5% when mix-mode is applied. Similarly, compared to continues run mode and ON/OFF mode, the operating cost of the microgrid is reduced by 49% and 8.5% respectively when mix-mode strategy is applied.

CHAPTER 5: VALIDATION OF BESS SIZING METHOD AND EMS USING RECEDING HORIZON ECONOMIC DISPATCH APPROACH

5.1 Introduction

In this chapter the validation of the proposed BESS sizing method is presented in this chapter. In addition to it the proposed Energy Management System (EMS) using Receding Horizon Economic Dispatch (RHED) approach is also validated. The proposed BESS sizing method is solved using Grey Wolf Optimizer (GWO), Particle Swarm Optimization (PSO), Artificial Bee Colony (ABC), Genetic Algorithm (GA) and Gravitational Search Algorithm (GSA) optimization techniques. Finally a comparative study among these algorithms in solving the proposed BESS sizing problem is also presented. The BESS sizing method is carried out operating the microgrid in mix-mode operating strategy. Therefore the problem of mix-mode operating strategy and BESS sizing is simultaneously optimized.

The proposed energy management system is solved using receding horizon economic dispatch approach (RHED). The proposed EMS module consists of ramp-rate control strategy and mix-mode operating strategy. The EMS delivers the directives or appropriate dispatch values to the distributed source present in the microgrid. For comparative purpose the EMS is also solved using metaheuristic methods like PSO and Evolutionary Programming (EP) optimization techniques. The EMS is validated for the proposed microgrid configuration presented in chapter 3.

5.2 Data used for validation of the proposed BESS sizing method

The load profile and energy prices profile shown in Figure 4.15 and Figure 4.16 is considered for this BESS sizing problem. The microgrid uses lead-acid BESS and the

specific costs associated to BESS's power capacity (C_P) and energy capacity (C_E) are set as \$234/kW and \$167/kWh respectively (Fossati et al., 2015). The lifetime and interest rates of BESS are selected to be 3 years and 6% respectively. The charging and discharge efficiency are the same and are set to 95%. $P_{BAT,min}$ and $P_{BAT,max}$ of the BESS is set as -100kW (charging) and 100kW (discharging) respectively. The minimum and maximum level of SOC for the BESS should be maintained within 20% and 100% respectively. To reflect this in the optimization, $E_{BAT}^{\min}$ and $E_{BAT}^{\max}$ are minimum and maximum level of charge that should be maintained which is set as 20% of $\overline{E}$ and 100% of $\overline{E}$ respectively.

For the BESS sizing method the population or particles in the optimization method is declared between the range,

$$\overline{E}_{\min} < \overline{E} < \overline{E}_{\max} \tag{5.1}$$

The value of $\overline{E}_{\min}$ and $\overline{E}_{\max}$ is set accordingly to the microgrid characteristics. In this thesis the value of $\overline{E}_{\min}$ and $\overline{E}_{\max}$ is considered as 100kWh and 3000kWh respectively. It means the search space for optimization techniques are set between the ranges [100kWh, 3000kWh]. The power capacity of the BESS $\overline{P}$ is fixed as 100kW in this thesis.

5.3 Validation of the proposed BESS sizing method

In this section the validation of the proposed BESS sizing method is carried out. The proposed BESS sizing method is validated with the "trade-off" method. Trade-off method can be used to find the approximate BESS capacity in kWh. For this purpose the operating cost (OC) of microgrid, BESS's TCPD and sum of OC and TCPD cost is plotted for different values of BESS's energy capacity. Since the minimum and maximum range of the BESS energy capacity for this research is [100kWh,3000kWh], the *OC*, $TCPD_{BAT}$ and ($OC+TCPD_{BAT}$) is plotted in Figure 5.1 for different energy

capacities between these ranges on regular intervals. Figure 5.1 is plotted considering the initial charge of the BESS is equal to 100% of the BESS capacity that is the initial State of Charge (SOC) level of the BESS during start of the day is considered as 100% for this case.

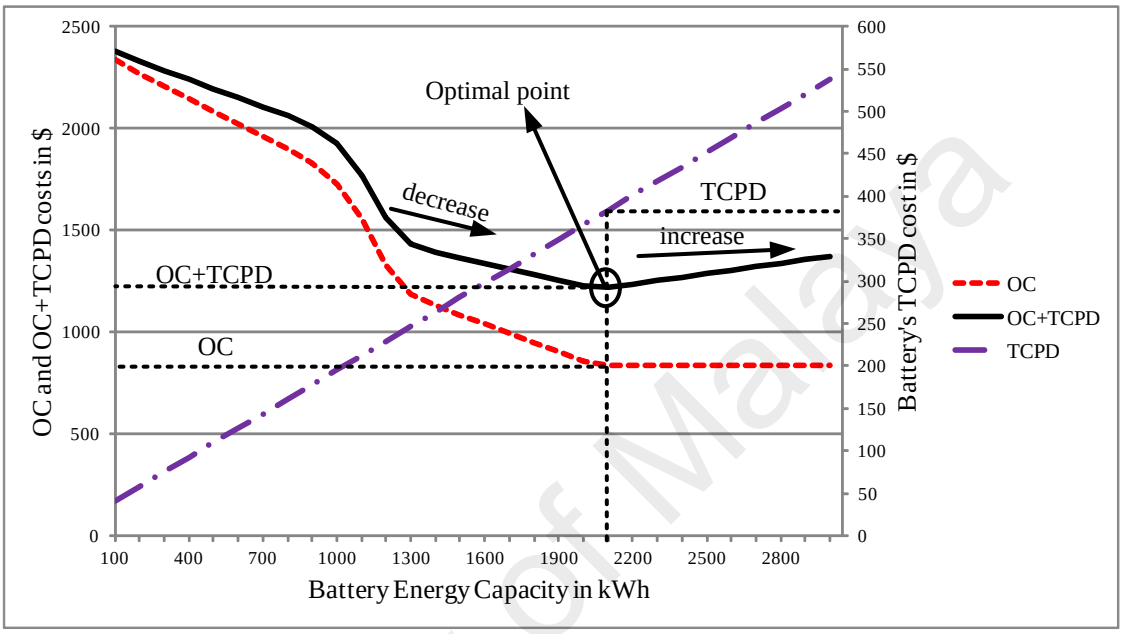

Figure 5.1: Optimal value of energy capacity in kWh using trade-off method

From the Figure 5.1, the operating cost (OC) of the microgrid is very high for lower BESS capacity. As the BESS capacity increases the OC of the microgrid also decreases. This is due to the availability of sufficient BESS source for economic microgrid operation. On the other hand, as the BESS capacity increases the BESS's TCPD cost also increases. This is because the TCPD of the BESS is directly associated with BESS's installation cost. Therefore, with an increase in the BESS capacity starting from 100kWh, the sum of operating cost (OC) and BESS's TCPD that is the combined cost of *OC* and *TCPD* tends to decrease.

With the increase in BESS capacity at one point, the OC of the microgrid attains a minimum value from where it does not decrease and remains constant for further

increment in BESS capacity. At this instant, the readers can notice a sudden change from decrease to an increase in trend in the combined cost of *OC* and *TCPD* costs. The point where a sudden change in the trend happens to be the optimal point, where the combined cost OC+TCPD is very less. The point where the combined cost of OC and TCPD is less is encircled in Figure 5.1 for which the corresponding BESS capacity is found to be 2100kWh. Here the optimal BESS capacity is obtained by a trade-off between microgrid's OC and BESS's TCPD costs. The operating cost (OC) of the microgrid for the optimal value is plotted, and it is found to be $834.06, and the TCPD cost associated with the BESS is $383.43. Therefore, the total combined cost of OC and TCPD from the Figure 5.1 is closer to $1,217.49 per day. That is the point encircled in Figure 5.1 is closer to $1,217.49 per day. It can be noticed from Figure 5.1 that further increase in BESS capacity beyond the 2100kWh increases the combined cost of OC and TCPD, this is due to increase in BESS's TCPD cost. On the other hand, it can be noticed that the OC of the microgrid remains constant for further increase in BESS capacity beyond 2100kWh. Choosing any value below 2100kWh will increase the microgrid's operating cost.

In this research we propose an accurate method to find optimal BESS size using GWO necessary for the economic operation of the microgrid. In addition to it PSO, GA, ABC and GSA is also used to solve the proposed BESS sizing problem. A comparative study on the effectiveness of solving the BESS sizing problem using GWO with another optimization method is also made. The microgrid is operated in mix-mode operating strategy. In this case, the BESS size and operating cost of the microgrid are optimized simultaneously. The BESS capacity is optimized considering the initial SOC level during the start of the day as 100%. The optimal value of BESS capacity optimized using GWO is found to be 2056.80kWh. Table 5.1 provides a comparison between the optimal value of BESS capacity obtained using the trade-off method and proposed

sizing method. In the table, the OC, TCPD, and OC+TCPD costs obtained from the proposed sizing method is compared with the trade-off method. The capacity of BESS and costs tabulated for the proposed sizing method is very close to the values obtained using trade-off method. From the table, it is clear that the proposed BESS sizing method is accurate enough to calculate the BESS capacity in kWh for economic operation of the microgrid.

Table 5.1: Comparison between optimal value obtained using trade-off method and proposed sizing method

	Trade-off method	Proposed sizing method using GWO
Optimal BESS capacity (kWh)	2100	2056.80
OC ($)	834.06	833.94
TCPD ($)	383.43	376.04
OC+TCPD ($)	1,217.49	1,209.98

Table 5.2 shows a comparison between different optimization techniques in solving the proposed BESS sizing method. For comparison purpose, the proposed BESS sizing problem is solved using GWO, PSO, ABC, GA and GSA optimization techniques. The optimization is run for 50 iterations and for each optimization methods 10 trial runs were conducted. One trial run for one particular optimization technique for all 1440 point is time consuming. As a result, the simulation time is not considered for this comparison study.

Table 5.2: Comparison between operation cost of microgrid obtained using various optimization techniques for 10 trial runs

Optimization method	Best solution, $	Average solution, $	Worst solution, $	No. of hits to optimum solution	Median	Standard deviation
GWO	1,209.98	1,210.11	1,210.44	5	1,210.02	0.17
PSO	1,210.13	1,210.15	1,210.27	9	1,210.13	0.04
ABC	1,210.13	1,210.13	1,210.13	10	1,210.13	0
GA	1,210.41	1,212.69	1,222.01	4	1,212.17	3.47
GSA	1,210.27	1,211.08	1,212.03	3	1,210.96	0.74

During this comparative study, it was observed that solving the proposed BESS sizing method using GWO gives the best solution. The best solution represents the combined costs that are microgrid's operating cost (OC) and BESS's total cost per day (TCPD). Using GWO the optimal solution is obtained as 2056.80kWh where the combined cost OC+TCPD is reduces to $1,209.98. PSO and ABC optimization method produce next best solution of 2057kWh where the overall objective function is reduced to $1210.13. Solving the BESS sizing problem using GSA gives a better solution that using GA, but the solution is not as better compared to other optimization methods.

From the Table 5.2 it can be observed that the solution obtained by using ABC and PSO optimization methods were consistent but the solution is not better than solution obtained using GWO. Out of 10 trial runs, GWO is able to obtain the best solution only 5 times and for the remaining number of trials the answers were very close to the best solution. Due to this reason the average solution obtained for GWO is very less compared to other optimization techniques. The solution obtained for all the trial runs using ABC algorithm is same therefore the best solution and average solution remains same. The convergence characteristics for different optimization techniques is shown in Figure 5.2.

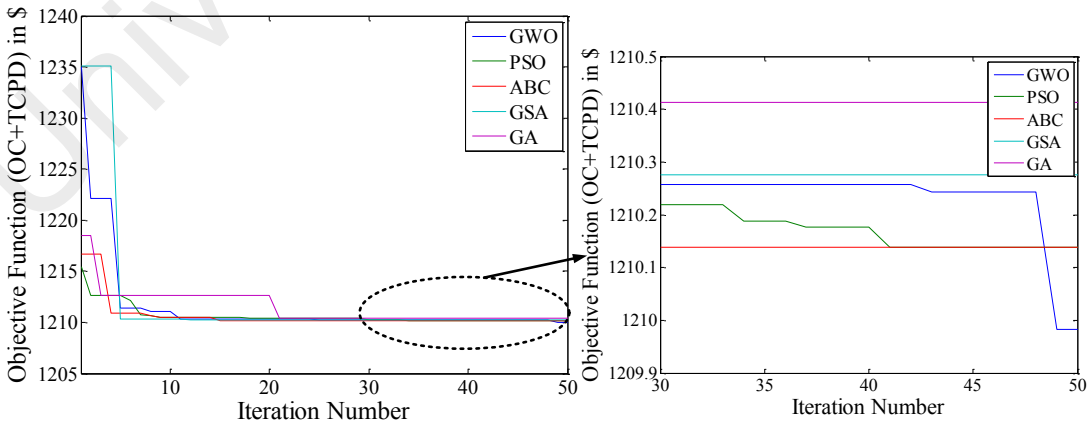

Figure 5.2: Convergence characteristics of GWO with other optimization techniques

From the above comparison table it evident that GWO optimization technique is robust enough in achieving the best solution when compared with other optimization techniques. This comparative study is made to show the effectiveness of GWO technique in solving the proposed BESS sizing problem. There are case studies carried out in this research to obtain the optimal BESS size in kWh for different BESS initial SOC levels. Therefore for these further case studies, GWO optimization technique is used.

5.4 Analysis of variation in optimal energy capacity of BESS

The main advantage of adding BESS in the microgrid is to maintain stability, improve power quality and facilitate the integration of renewable sources (Al-Saedi, Lachowicz, Habibi, & Bass, 2012; Gu et al., 2014; X. Tan, Li, & Wang, 2013). In this case, the optimal BESS capacity required for the economic microgrid operation is evaluated considering the initial SOC of the BESS to be 100%, 90% and 80% during the start of the day. Therefore, the optimal BESS capacity $\overline{E}$ for each of the initial SOC level is optimized within the range [100kWh,3000kWh] using the proposed BESS sizing method.

The optimal values of the BESS energy capacity optimized using GWO technique are found to be 2056.80kWh, 2350.80kWh and 2742.60kWh when the BESS initial SOC levels are 100%, 90% and 80% respectively during the start of the day. This is validated using trade-off method by plotting various costs against different BESS capacity ranging between [100kWh,3000kWh]. The results for optimal energy capacity using trade-off method when the microgrid is operated under mix-mode strategy considering the BESS with initial SOC levels as 100%, 90% and 80% during the start of the day are presented in Figure 5.3. The optimal values are attained for the lowest value of combined cost of OC and TCPD is found to be 2100kWh, 2400kWh and 2800kWh for initial SOC cases of 100%, 90%, and 80% respectively.

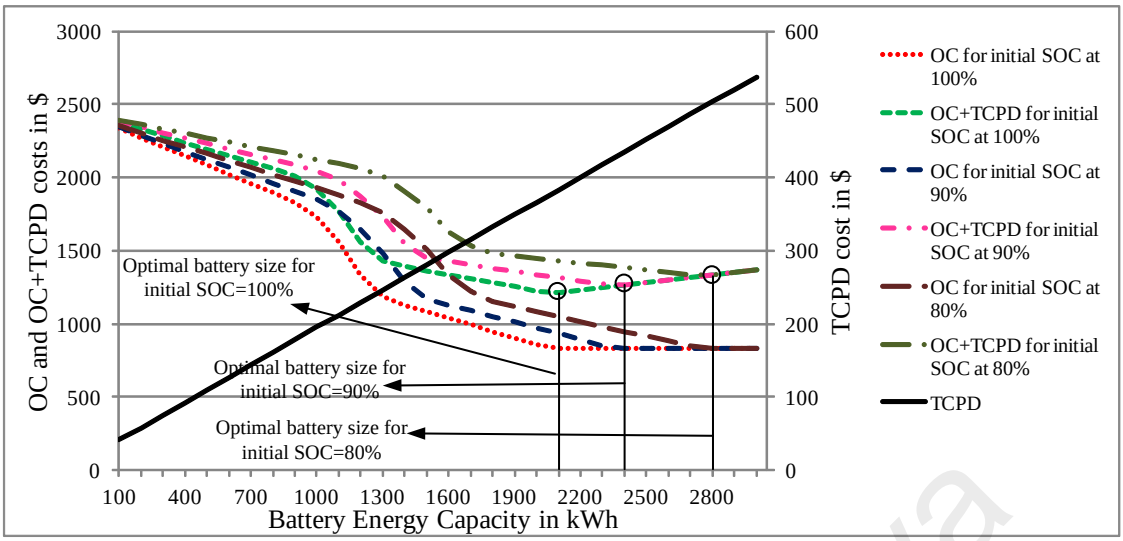

Figure 5.3: Optimal value of energy capacity in kWh using trade-off method for initial BESS SOC at 100%, 90% and 80%

From Figure 5.3 it should be noticed that the microgrid's OC and the combined cost of OC and TCPD are not same when BESS initial SOC levels during the start of the day are 100%, 90% and 80%. The OC and combined cost of OC and TCPD is reduced very much when the BESS initial SOC level during the start of the day is 100%. In other words, if the BESS initial SOC level is very large the operating cost of the microgrid is reduced to its lowest value. From Figure 5.3 it can be noticed that the operating cost of the microgrid settles to a constant value for BESS's optimal capacity value. For example for the case of BESS initial SOC level 100%, the operating cost settles at a value of $834.06 at 2100kWh. Similarly, for the cases of initial SOC levels at 90% and 80%, the operating cost settles down to a constant value of $834.06 at optimal values are 2400kWh and 2800kWh respectively. A clear comparison between the optimal values obtained for different BESS initial SOC levels for trade-off method and the proposed sizing method solved using GWO is presented in Table 5.3.

Table 5.3: Comparison between optimal value obtained using trade-off method and proposed sizing method for BESS initial SOC levels 100%, 90% and 80%

	Trade-off method			Proposed sizing method		
Initial SOC at	100%	90%	80%	100%	90%	80%
Optimal BESS capacity (kWh)	2100	2400	2800	2056.80	2350.80	2742.60
OC in $	834.06	834.06	834.06	833.94	833.85	833.85
TCPD in $	383.43	434.78	503.25	376.04	426.36	493.42
OC+TCPD in $	1,217.49	1,268.84	1,337.31	1,209.98	1,260.22	1,327.28

From the above table, it is also worth to notice that with decreasing level of BESS initial SOC level during the start of the day, the BESS's optimal capacity increases. Therefore in order to reduce the microgrid's operating cost to its lowest value with less BESS initial cost, it is advised to use the optimal BESS capacity with higher initial SOC during start of the day. This will reduce the microgrid's operating cost with less BESS initial cost.

5.5 Analysis of variation of microgrid's operating cost for different initial SOC levels

In this section variation in microgrid's operating cost for different initial SOC levels during the start of the day is analyzed. Before going in hand with the analysis, it is necessary to evaluate the microgrid's operating cost in the absence of BESS. Hence, this section is divided into two sub-sections, (i) microgrid operation without BESS and (ii) microgrid operation with BESS having initial SOC levels at 100%, 70% and 50% during the start of the day.

5.5.1 Microgrid operation without BESS

In this section, the grid connected microgrid is operated without battery source. All the distributed sources present in the microgrid including utility grid should satisfy the forecasted load demand for the 24hours period. In this case, there may be instances where output power from PV may exceed the load demand. Since BESS is not available for charging the excess power, a load resistor is modeled to ground the excess power. By load demand and maximum available power from the distributed sources, the results of the microgrid operation for mix-mode are presented in Figure 5.4.

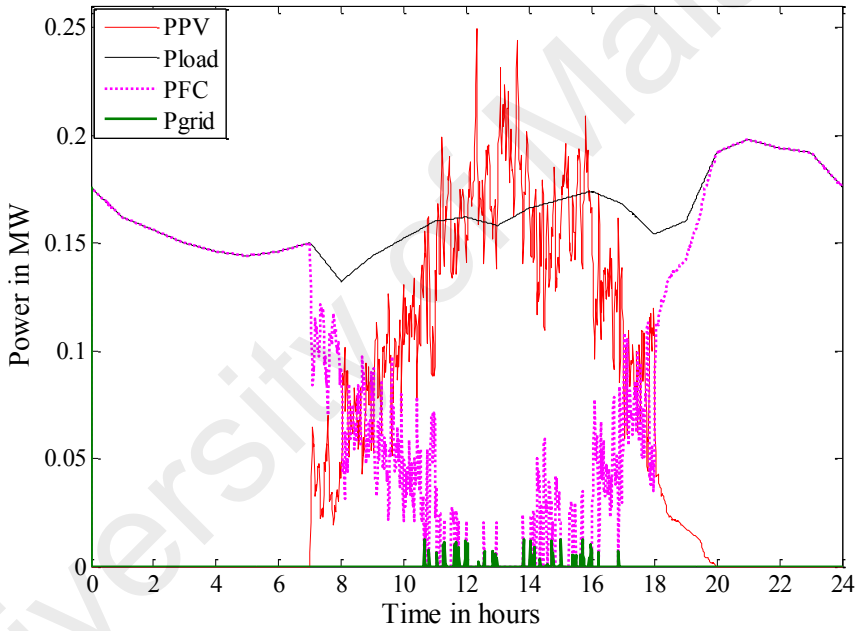

Figure 5.4: Optimal operation of microgrid without BESS

The total operating cost of the microgrid in this case is $2,855.60/day. Since there is no BESS available to deliver ancillary service, the maximum available power from the fuel cell and utility grid is drawn by the load. This forces fuel cell to extend its operating hours by 20hours. Overall, since no BESS is employed, the microgrid rely on power from the fuel cell and the utility grid. Further, the fuel cell operating hours is more than utility grid operating hours. This is because the power drawn from the fuel cell is cheaper than power purchased from the utility grid. There are instances where utility

grid is scheduled instead of the fuel cell. During the entire 24hours operating time the utility grid is optimally scheduled for approximately 1hour.

5.5.2 Microgrid operation with BESS having initial SOC levels of 100%, 70% and 50%

Now the BESS is added to the microgrid test system for this case study. During the early morning hours since BESS is cheap, it will be effectively used to supply the varying load. There is no chance of BESS charging during early morning hours that is before the sunrise. Therefore keeping the initial BESS cost in mind, the initial SOC of the BESS that is during the start of the day is set as 100%. Results in Figure 5.5 portray the optimal dispatch values of the distributed sources in the microgrid when BESS initial SOC level is 100% at the start of the day. The optimal BESS capacity for this case is found as 2056.80kWh. During the early morning hours that are before the sunrise, the power to the load is managed by BESS, fuel cell, and the utility grid. During the day time that is when PV power is present, the BESS is efficiently managed to supply the load or charged when PV power is more than the load demand. During this period of operation, the power from the fuel cell and utility grid are very low or even maintained zero for the majority of the time period. This is due to the availability of cheaper BESS power. During the evening hours along the side of BESS the fuel cell is also used to supply the load. The power drawn from the utility grid is zero during this time because the power purchase cost from the utility grid is very high than power drawn from BESS and fuel cell. From Figure 5.6 it is clear that BESS SOC level is maintained within the limits.

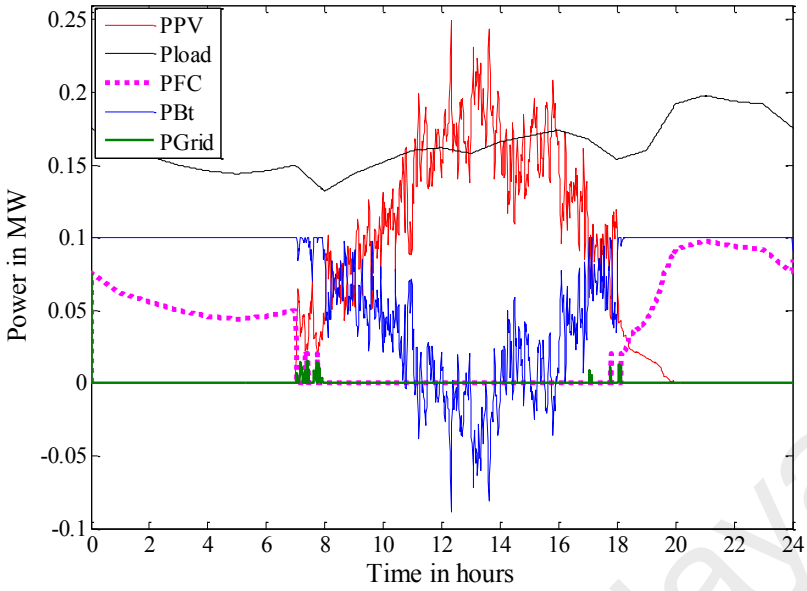

Figure 5.5: Optimal output of distributed source in microgrid for when BESS initial SOC at 100% of 2056.80kWh

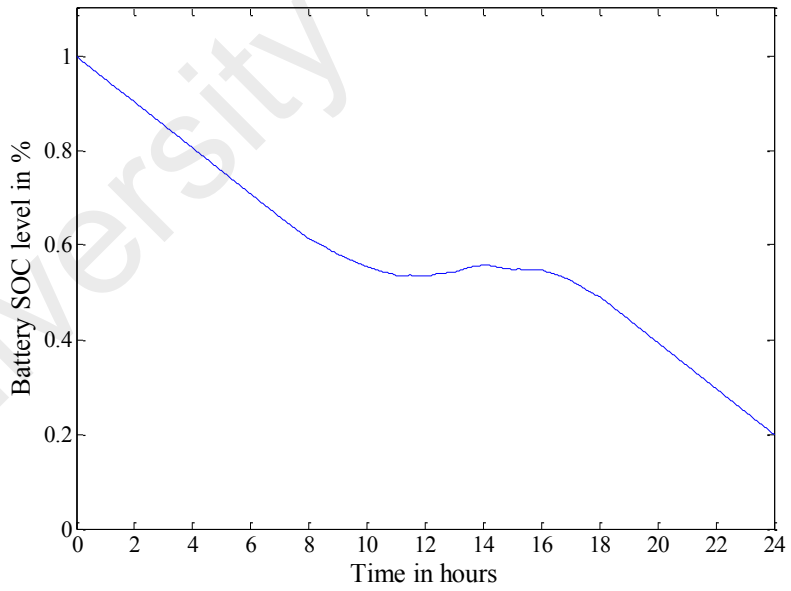

Figure 5.6: BESS SOC level for mix-mode operating strategy when BESS initial SOC at 100% of 2056.80kWh

BESS size of 2056.80kWh is the optimal capacity when initial SOC is at 100% during the start of the day. It is our interest to set the initial SOC level to 70% and 50% during the start of the day for the BESS size of 2056.80kWh and observe the operation of microgrid and calculate its operating cost. Figure 5.7 and Figure 5.8 are the optimal dispatch values and BESS SOC level when the BESS initial SOC level is set to 70% of 2056.80kWh during the start of the day. Similarly, Figure 5.9 and Figure 5.10 are optimal dispatch values and BESS SOC level when the BESS initial SOC level is set to 50% of 2056.80kWh during the start of the day. The discharging action of BESS in each time step of the day is restricted to how much it charges in previous hours. It can be noticed from Figure 5.5, Figure 5.7 and Figure 5.9 that when the initial SOC is high during the start of the day the BESS operates for longer hours. On the other hand, when the initial SOC level of the BESS is set low the BESS operating hours is less because of the less availability of charge in the BESS. When the initial SOC is 70% in Figure 5.7 the BESS operating hours is found to be less and the BESS is completely switched OFF during the night hours. Similarly, when initial SOC is 50% in Figure 5.9 the BESS is switched OFF during night hours and even for few hours during the daytime. For the cases of lower initial SOC levels particularly during the night hours the second unit of the fuel cell is switched ON to supply power to varying load since power drawn from utility grid becomes costlier. A brief comparison of microgrid's operating cost without and with BESS with different initial SOC levels are presented in Table 5.4. The operating cost of microgrid without BESS is calculated as $2,855.60/day. The microgrid operating cost with optimal BESS of 2056.80kWh having initial SOC at 100% at the start of the day is $833.94/day. That means operating the microgrid with optimal BESS sizing reduces the overall operating cost by 70% for a single day. This is because of the availability of BESS and therefore, the BESS operating hours is increased to 21hours.

On the other hand with the same optimal BESS size where the initial SOC is set at 70% during the start of the day will reduce the overall operating cost only by 58% for a single day. Moreover, this increases the fuel cell operating hours to 13.38hours and reduces the BESS operating hours to 14.6hours. For the initial SOC of 50% during the start of the day case, the operating cost of the microgrid is $ 1,916.80/day where the savings is only 33% for a single day which is even less than higher initial SOC cases. For this case, the fuel cell operating hours are increased to 18.18hours and the BESS run time is reduced to 8.68hours.

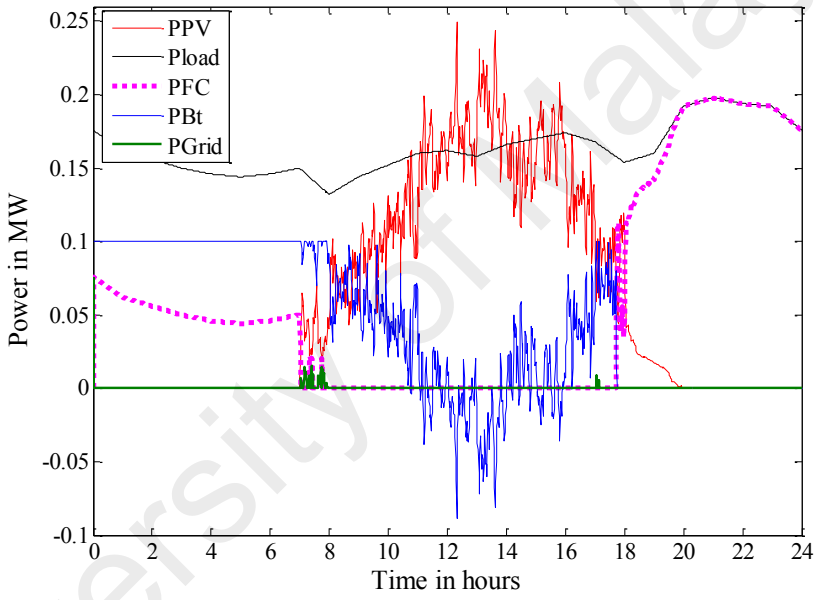

Figure 5.7: Optimal output of distributed source in microgrid for when BESS initial SOC at 70% of 2056.80kWh

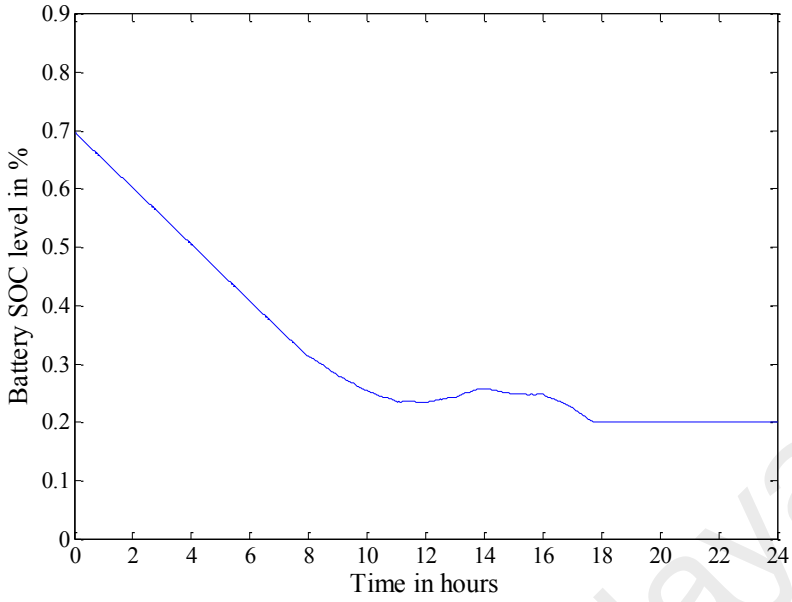

Figure 5.8: BESS SOC level for mix-mode operating strategy when BESS initial SOC at 70% of 2056.80kWh

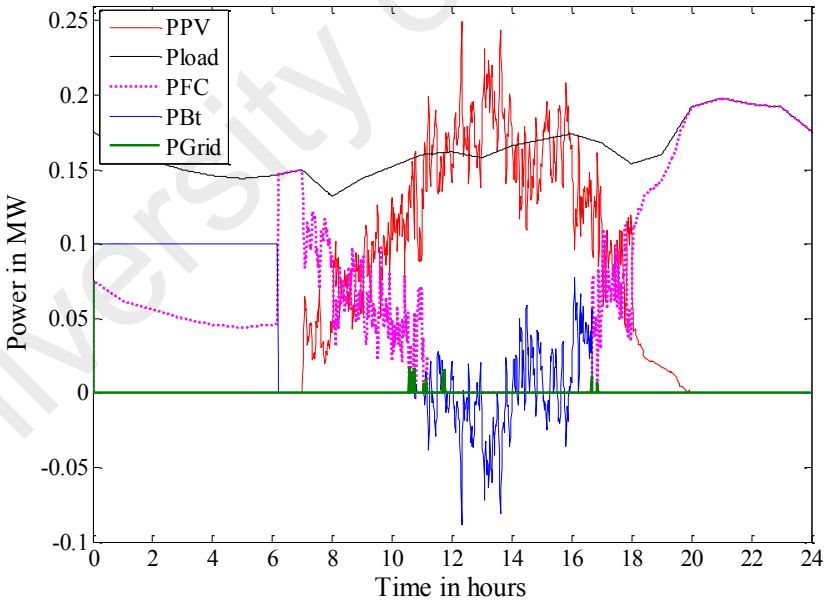

Figure 5.9: Optimal output of distributed source in microgrid for when BESS initial SOC at 50% of 2056.80kWh

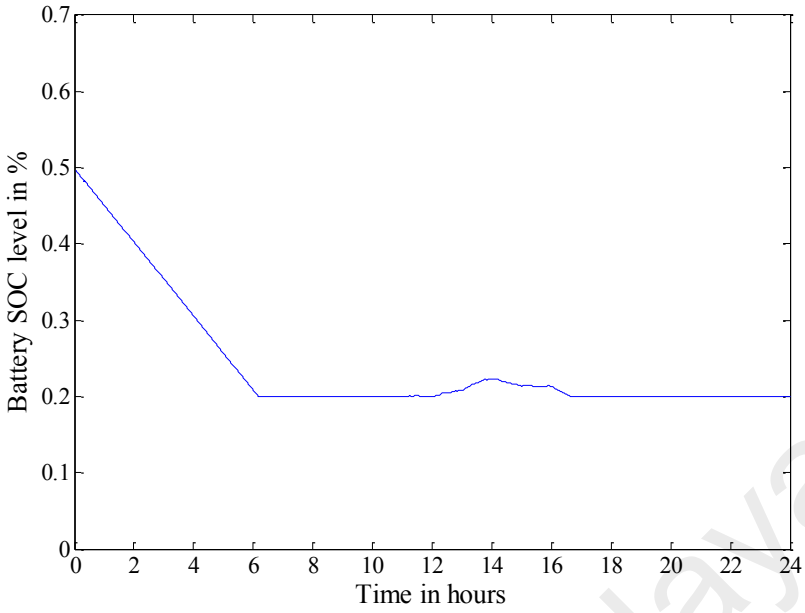

Figure 5.10: BESS SOC level for mix-mode operating strategy when BESS initial SOC at 50% of 2056.80kWh

Table 5.4: Comparison between operating cost with and without BESS case

	With BESS			Without BESS
Optimal BESS capacity (kWh)	2056.80			-
BESS initial SOC level	100%	70%	50%	-
Operating cost in ($/day)	833.94	1,202.40	1,916.80	2,855.60
Fuel cell operating hours	13	13.38	18.18	20
Grid operating hours	0.61	0.5	0.31	1
BESS operating hours	21	14.6	8.68	-
Savings in operating cost in %	70%	58%	33%	-

From the above table, it is clear that if the BESS is optimal with higher initial SOC during the start of the day, there is a significant reduction in microgrid's operating cost. Moreover, the fuel cell operating hours is also reduced which will contribute to increasing in its calendar life. During the microgrid mix-mode operation, the utility grid operating hours is less because the power purchase cost from the utility grid is very high.

From the above results, it can be concluded that:

(i) Including BESS in the microgrid will contribute to a reduction in daily operating cost.

(ii) Installing optimal BESS capacity with higher initial SOC is highly recommended because optimal BESS capacity with higher initial SOC will reduce the daily operating cost with lowest BESS's capital cost.

(iii) Installing BESS capacity with higher initial SOC reduces fuel cell and utility grid operating hours.

5.6 Recommendation on BESS initial SOC level for effective microgrid operation

There is no recommendation found in the literature on the setting of the initial BESS SOC level for microgrid operation. Based on the results depicted in section 5.4 and 5.5 it is highly recommended to use the BESS capacity with higher initial SOC during the start of the day. This will reduce the microgrid's operating cost with less BESS capital cost that is BESS's TCPD. When there is no possibility of BESS charging during the start of the day's operation, it is highly recommended to set the initial SOC of the BESS to 100%. If there are any possible charging events, then the BESS initial SOC can be set to 90% to 95%.

5.7 Validation of EMS using RHED approach

In this section the validation of results in solving the EMS using RHED approach is carried out. The main aim of the EMS is to deliver appropriate dispatch values to the microgrid sources. The proposed EMS is enabled with solar PV ramp-rate control functionality. The inputs to the EMS module are forecasted PV and load demand, the price of electricity and the price of natural gas. The input is fed into the EMS module a day ahead and from the PV forecasted values, the smoothing reference is generated.

From the reference, appropriate dispatch reference is generated for energy storage present in solar PV plant. This energy storage is used only to limit the PV output power fluctuations. From the smoothed PV power and other input values, appropriate dispatch values are calculated based on mix-mode operating strategy. The EMS module generates these reference values to the microgrid sources.

The size of the BESS is evaluated for economic operation of microgrid using the proposed sizing method solved using GWO. Since there are no charging instances during the start of the day, the initial SOC level of the BESS is set at 100%. The optimal energy capacity in kWh of the BESS is found to be 2047kWh. Therefore the BESS is sized to the evaluated capacity.

The EMS layer prepares the dispatches for the fuel cell, BESS and grid utility using mix-mode operating strategy using RHED approach. Figure 5.11 presents the output power profiles for PV, fuel cell, BESS, and power drawn from utility grid for the sunny day using mix-mode strategy. From Figure 5.11 it can be noticed during early morning hours that is when power output from PV is zero, fuel cell, BESS and grid are optimally scheduled to deliver power to the load using mix-mode operating strategy.

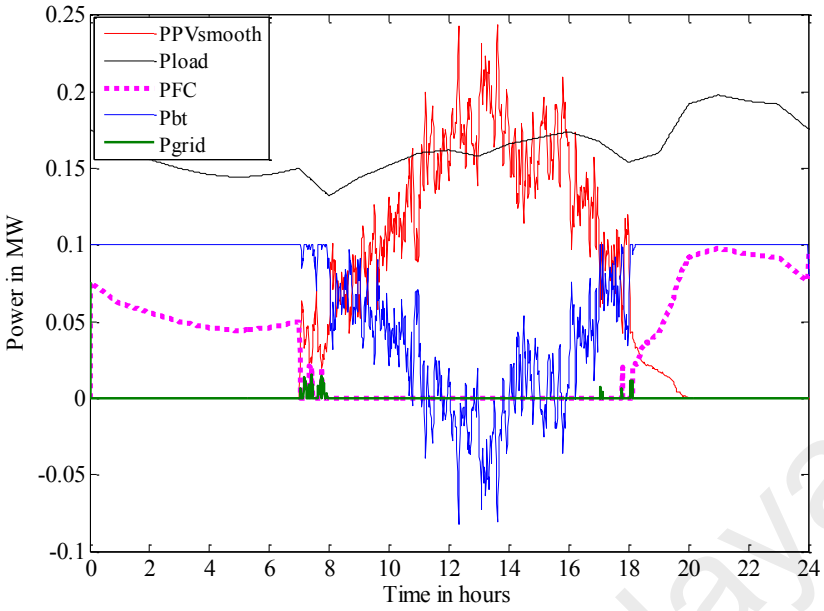

Figure 5.11: Microgrid operation using directive energy management system solved using RHED approach

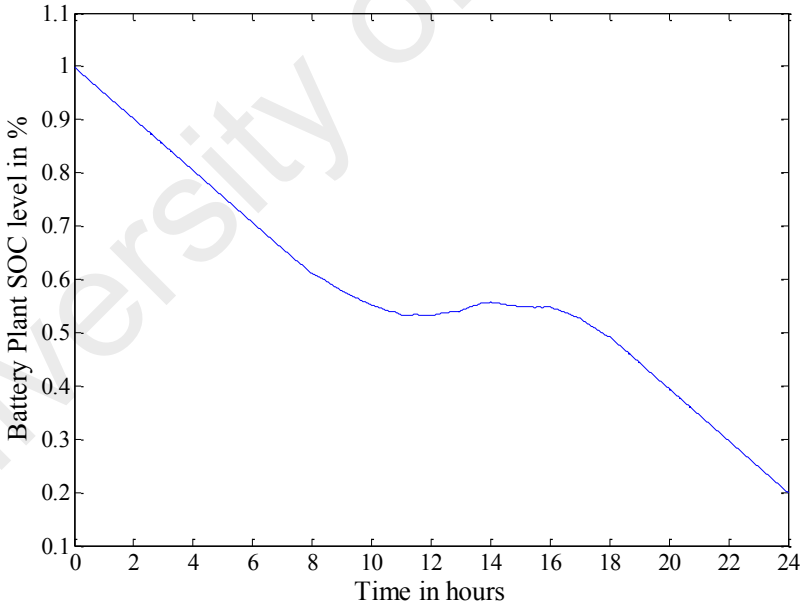

Figure 5.12: BESS SOC profile

During the daytime, rapid fluctuation in solar PV output power is found caused due to frequent movement of clouds. The solar PV plant is enhanced with the proposed ramp-rate control strategy where the ramp-rates for every minute are checked. The output power produced from the PV plant is the ramp-rate controlled output. During the

daytime the power required by the load is efficiently managed by solar and BESS. There are instances where the output power from the solar plant is greater than load demand for which the batteries in the plant are charged. There are also instances where the power is drawn from the utility grid, and fuel cell system can be found during the daytime. During the evening hours the power to the load is supplied by the BESS and fuel cell. It should be noticed that the power drawn from the utility grid during this time is almost zero because of higher grid pricing. During this entire time of operating hours the SOC of the BESS is also kept within the limit. Figure 5.12 shows SOC profile of BESS.

In this section, the performance of the proposed EMS solved using RHED approach is also compared with particle swarm optimization (PSO) and evolutionary programming (EP) optimization techniques. The comparison is based on the algorithm's ability to achieve lower operating cost with less run time. Therefore, for this purpose, the EMS is solved using PSO and EP optimization techniques. The comparison on the obtained operating cost with run time taken is presented in Tables 5.5. Viewing the operating costs in Table 5.5, EP proves to be less accurate in achieving the objective function. The solution obtained using PSO is very close to the solution obtained using RHED approach. The run time taken by PSO and EP optimization techniques in solving the EMS are longer than the run time taken by RHED approach.

Table 5.5: Comparison between operating cost obtained using RHED approach, PSO and EP

	RHED approach	PSO	EP
Overall cost, $	832.09	832.14	927.60
FC operating hours	13	12.95	6.16
Grid operating hours	0.6	0.65	7.51
Run time in sec	110.95	203.06	336.73

This shows that applying optimization techniques for the energy management problem for every minute requires significant computation time. On the other hand, RHED approach provides the optimal solution with lesser computation run time.

Here the implementation of simplex optimization method based dynamic PI controller for BESS and fuel cell plant's VSC power control is implemented. The simplex optimization based PI controller provides the *Kp* and *Ti* depending on the input reference values. The input reference values are provided by the EMS module. The controller's parameter (*Kp* and *Ti*) is dynamic in nature since the reference value are also dynamic. By implementing the proposed simplex optimization module for VSC's power control the ITAE is minimized therefore providing seamless over VSC. The ranges of optimal control parameters for PI controller obtained using simplex method is summarized in Table 5.6.

Table 5.6: Optimal K_P and T_i ranges found using simplex method for both BESS and fuel cell plants

Method	K_P	T_i	ITAE
Trail and error method	1.335	0.0005	133.38
Simplex based control	1 to 2	0.0003 to 0.001	91.15

The dynamic change in controller's parameter for simplex optimization method for different reference set points for BESS is shown in Figure 5.13 and Figure 5.14. Similarly the change in controller's parameter for different reference set points for fuel cell plant is shown in Figure 5.15 and Figure 5.16.

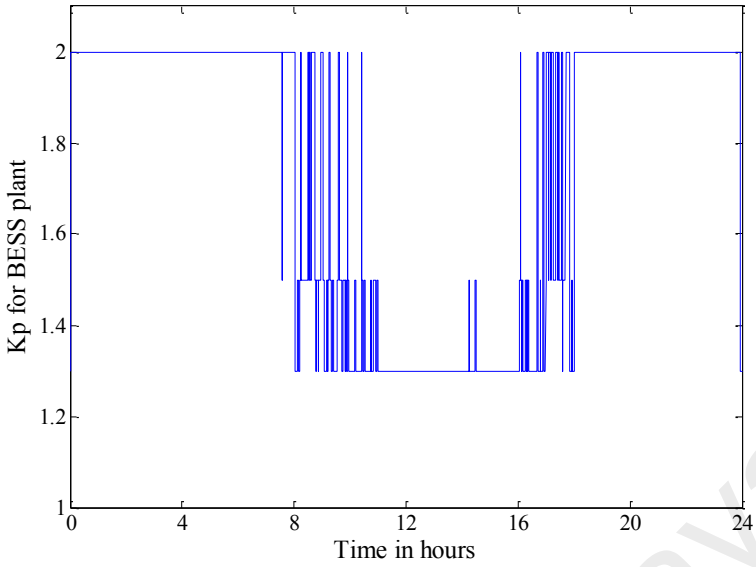

Figure 5.13: Variation of *Kp* for BESS plant

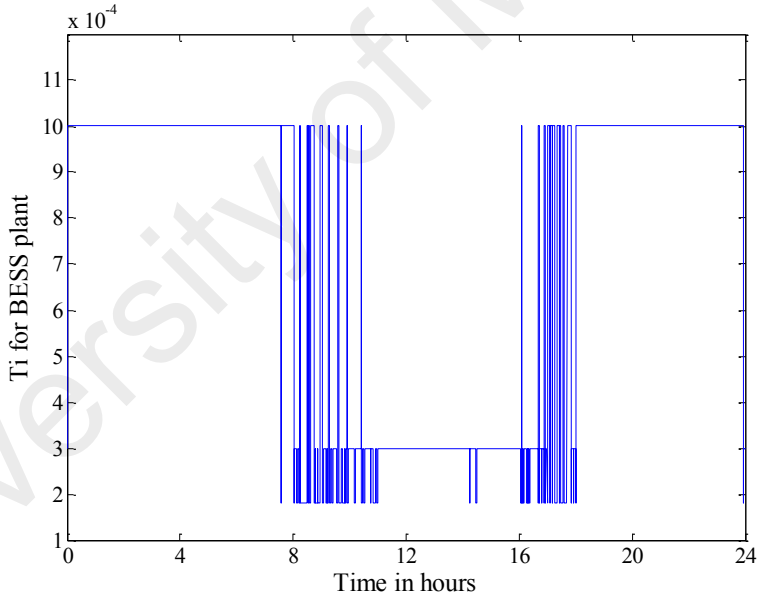

Figure 5.14: Variation of *Ti* for BESS plant

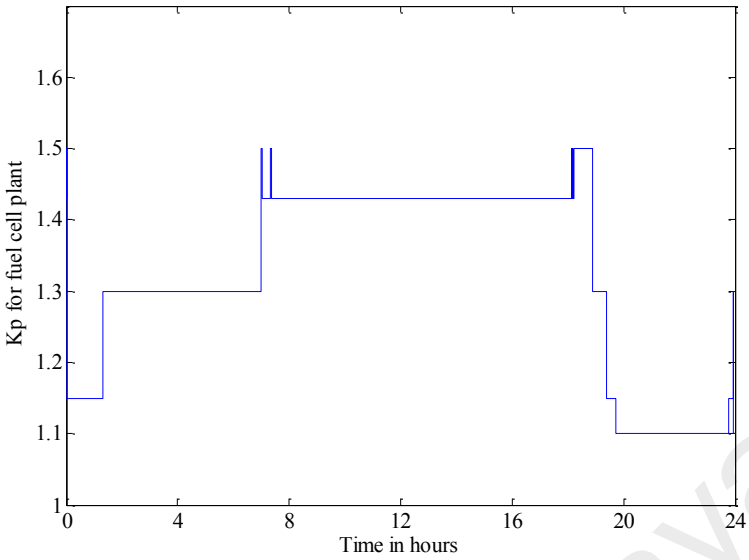

Figure 5.15: Variation of *Kp* for fuel cell plant

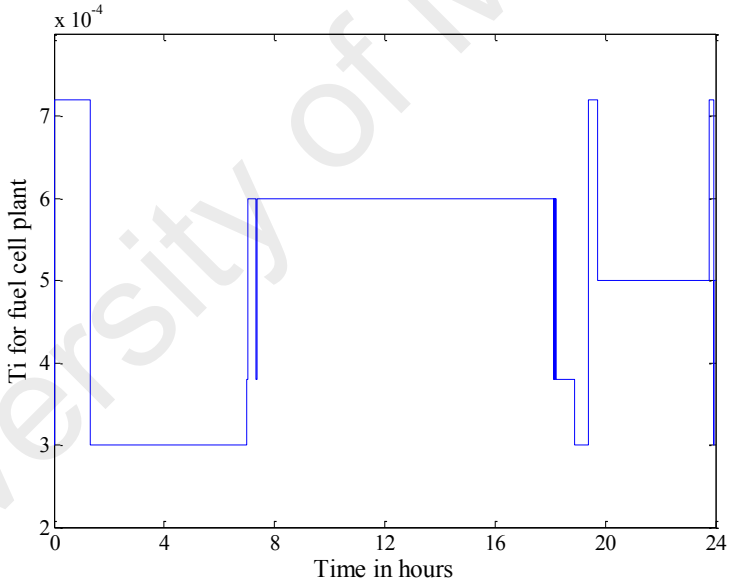

Figure 5.16: Variation of *Ti* for fuel cell plant

5.8 Energy Management System (EMS) with and without smoothing functionality

The main objective of the proposed EMS is to operate the microgrid with less operating cost. From the previous section it is evident that solving the EMS using RHED approach is faster and lowest operating cost when compared to other metaheurictic based approaches. The proposed EMS is enabled with PV ramp-rate control capability. It is our best interest to analyze the effect on microgrid's operating cost during the presence and absence of the proposed ramp-rate control strategy. Therefore in this section the variation in operating cost with and without smoothing functionality is presented.

The energy capacity of the BESS is sized to 2047kWh. Results of the EMS with smoothing functionality enabled can be obtained from section 5.7. The operating cost of the microgrid when the smoothing function is enables is calculated to be $832.09/day. Now the smoothing functionality is disabled, therefore the energy storage device installed in the solar PV power plant is switched off. The actual PV power produced by the PV array is the output power from solar PV. Results of the EMS where the smoothing function is disabled is presented in Figure 5.17. Figure 5.18 shows SOC profile of BESS when the smoothing function is disabled.

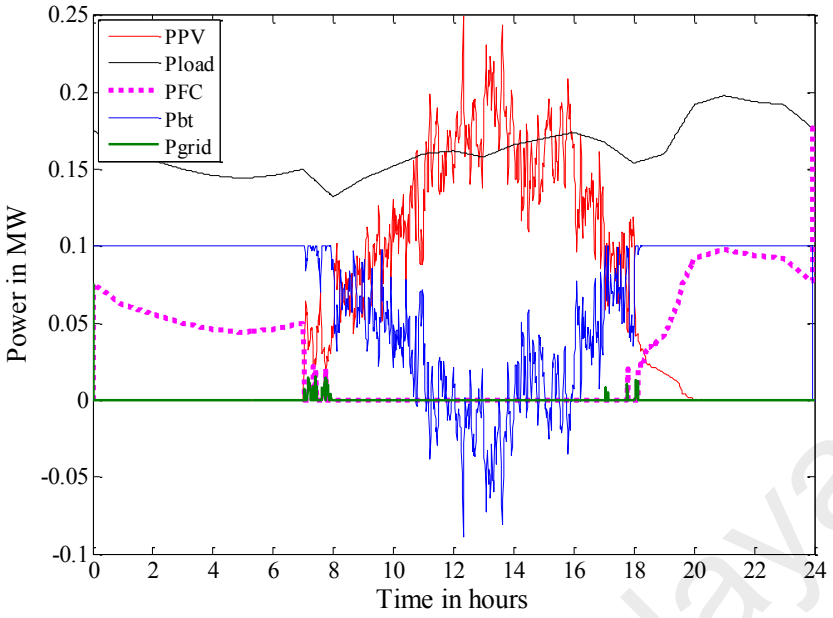

Figure 5.17: Microgrid operation using directive energy management system solved using RHED approach without smoothing function

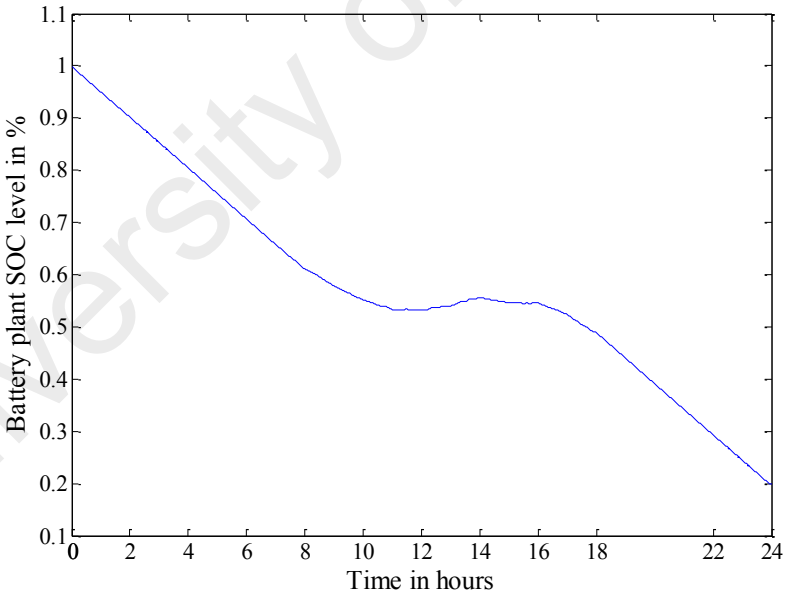

Figure 5.18: BESS SOC profile without smoothing function

Compared to the smoothing function enabled case, the operating cost of microgrid increases slightly when the smoothing function is disabled. The microgrid's operating cost for the smoothing function disabled case is calculated to be $838.48.

Since the smoothing function is disabled, larger energy capacity of BESS is required to reduce the microgrid's operating cost to its lowest value. Disabling of smoothing function is the reason for the decrease in BESS operating hours from 20.95hours to 20.86hours.

5.9 Summary

The BESS sizing problem is solved using GWO optimization methods and solving the sizing problem using GWO is highly accurate than other competitive optimization techniques. The proposed BESS sizing method is validated against the traditional trade-off method and is found to be highly accurate in calculating the energy capacity where the reduction in associated costs is found to be 0.7%.

In addition, in this chapter, the results of solving the EMS using RHED approach are presented. The EMS is enabled with ramp-rate control function. The EMS layer solves the economic dispatch problem for the mix-mode operating strategy as a RHED problem. From the table 5.5, it was found that RHED approach is about 45% faster in obtaining the optimal solution than metaheuristic methods. It is also evident that the RHED approach can minimize the operating cost by 0.1% and 10% than utilizing metaheuristic methods like PSO and EP respectively. Therefore, it can be concluded that RHED approach provides the optimal solution with lesser computation burden. A variation of microgrid's operating cost with and without smoothing function is also analyzed. It was found that larger capacity of BESS is necessary to reduce the microgrid's operating cost when PV smoothing function is disabled.

CHAPTER 6: CONCLUSION AND FUTURE WORKS

6.1 Conclusions

This work proposes an Energy Management System (EMS) which utilizes the microgrid sources efficiently. Microgrid consists of electronically interfaced generators like solar photovoltaic (PV) plant, BESS and fuel cell. Microgrid is subjected to operate in grid-connected mode.

The proposed EMS is enabled with PV ramp-rate control functionality in order to control the PV plant's ramp-rate within the prescribed limits. For this purpose, a ramp-rate control strategy which does not exhibit "memory effect" is proposed. The proposed ramp-rate control strategy is compared with Moving Average (MA) and Conventional Exponential Smoothing (CES) methods. It was found that MA and CES methods exhibit "memory effect", for which the energy storage used for smoothing purpose needs to operate all the time. On the other hand when the proposed ramp-rate control strategy is used it was found that the energy storage is switched ON only during ramp violation events and for rest of the time the energy storage remains switched OFF. Results show that the proposed ramp-rate control strategy will inject fewer harmonic in the phase voltages when compared to the other two methods. The proposed ramp-rate control strategy is included into the EMS module which generates the reference values to the energy storage present in the solar PV plant.

A method is also suggested to accurately evaluate the size of energy capacity in kWh of BESS considering the constraints. The BESS in the proposed system is used for the economic operation of the microgrid. The energy capacity is evaluated using GWO. A comparison of results with other optimization techniques like PSO, GA, ABC and GSA

is also conducted. From the obtained results, it was found that the application of GWO in solving the BESS sizing problem is more accurate. The obtained result was validated with traditional trade-off method and it was found that the proposed BESS sizing method is highly accurate in evaluating the energy capacity of BESS. In addition, an analysis on variation of microgrid's associated cost for a different level of BESS's initial SOC is carried out. In addition, variation of microgrid operating cost with different BESS's initial SOC level during the start of the day is carried out. From the above analysis, a recommendation on BESS's initial SOC level for an economical microgrid operation is also suggested.

In this research, a novel operating strategy namely "mix-mode" is proposed to operate the grid connected microgrid with lowest operating cost. The mix-mode operating strategy is solved for 24hours time period using three proposed strategies namely "continuous run mode", "power sharing mode" and "ON/OFF mode". While analyzing the operating cost, it was found that operating the microgrid under mix-mode operating strategy produces the lowest operating cost.

The EMS module integrates all the components into one system. The proposed EMS module consists of PV ramp-rate control strategy and mix-mode operating strategy. Based on the available input, the EMS generates appropriate dispatch values which is solved using RHED approach. In the energy management, the proposed ramp-rate control strategy is enabled with the solar PV plant and the output power from the PV plant is the smoothed one. The proposed BESS sizing method is applied to evaluate the size of BESS. The dispatches to the microgrid sources are generated using mix-mode operating strategy. From the obtained results it was found that solving the EMS using RHED approach is faster and produces better results than metaheurictic methods such as

PSO and EP. In addition an analysis of variation in microgrid's operating cost with and without the ramp-rate function is also carried out.

The overall operation of microgrid to limit ramp rates imposed on AC network and to operate the microgrid with lowest operating cost considering the size of BESS is found to be quite satisfactory.

6.2 Future Works

The topics that are proposed for a future work are presented in the next sections.

a) Extending EMS for Off-Grid Applications

The proposed EMS is subject to control the microgrid in grid-connected mode. However, during the period of disconnection from the grid (islanded mode) the microgrid needs a different operating strategy in order to sustain its stability. In islanded mode, voltage magnitude and system frequency drifts away from their nominal values and hence the stability of microgrid highly depends on the balance between generation and consumption. In this case, role of droop control mechanisms is very important to keep the frequency and voltage in microgrid at a certain level.

At the same time, there exists power fluctuations due to non-linearity of load and the stochastic behavior of solar PV plant. This matter exacerbates the situation and pushes the microgrid forward to become unstable. Therefore, a sophisticated energy management approach must be adopted to maintain the microgrid during the islanded operating mode.

b) Adding Load and Generation Forecasting Modules to EMS

In the proposed EMS, the solar PV generation and load demand are assumed to be forecasted one day ahead and the related data are used as inputs for the EMS. As a future work, load and generation forecasting modules can be added to the existing EMS

in this work. In this case, EMS is able to forecast the generation and load profiles by itself and hence it does not need any external source of data.

c) Considering Supplementary Factors in EMS

The issues such as demand response (DR) and demand side management (DSM) are not considered in the proposed EMS. Each concept can also be added as a function to the proposed EMS in this work.

REFERENCES

Abedi, S., Alimardani, A., Gharehpetian, G., Riahy, G., & Hosseinian, S. (2012). A comprehensive method for optimal power management and design of hybrid RES-based autonomous energy systems. *Renewable and Sustainable Energy Reviews, 16*(3), 1577-1587.

Aghamohammadi, M. R., & Abdolahinia, H. (2014). A new approach for optimal sizing of battery energy storage system for primary frequency control of islanded microgrid. *International Journal of Electrical Power & Energy Systems, 54*, 325-333.

Akatsuka, M., Hara, R., Kita, H., Ito, T., Ueda, Y., & Saito, Y. *Estimation of battery capacity for suppression of a PV power plant output fluctuation.* Paper presented at the 35th IEEE Photovoltaic Specialists Conference (PVSC), 2010

Akhil, A. A., Huff, G., Currier, A. B., Kaun, B. C., Rastler, D. M., Chen, S. B. (2013). *DOE/EPRI 2013 electricity storage handbook in collaboration with NRECA*: Sandia National Laboratories Albuquerque, NM, USA.

Al-Saedi, W., Lachowicz, S. W., Habibi, D., & Bass, O. (2012). Power quality enhancement in autonomous microgrid operation using particle swarm optimization. *International Journal of Electrical Power & Energy Systems, 42*(1), 139-149.

Alam, M., Muttaqi, K. M., & Sutanto, D. (2014). A novel approach for ramp-rate control of solar PV using energy storage to mitigate output fluctuations caused by cloud passing. *IEEE Transactions on Energy Conversion, 29*(2), 507-518.

Almada, J., Leão, R., Sampaio, R., & Barroso, G. (2016). A centralized and heuristic approach for energy management of an AC microgrid. *Renewable and Sustainable Energy Reviews, 60*, 1396-1404.

Amiri, M., Esfahanian, M., Hairi-Yazdi, M. R., & Esfahanian, V. (2009). Minimization of power losses in hybrid electric vehicles in view of the prolonging of battery life. *Journal of Power Sources, 190*(2), 372-379.

Anderson, P. (1985). The effect of photovoltaic power generator on utility operation. *IEEE transactions on power apparatus and systems, 104*(3), 524-530.

Arun, P., Banerjee, R., & Bandyopadhyay, S. (2008). Optimum sizing of battery-integrated diesel generator for remote electrification through design-space approach. *Energy, 33*(7), 1155-1168.

Bahmani-Firouzi, B., & Azizipanah-Abarghooee, R. (2014). Optimal sizing of battery energy storage for micro-grid operation management using a new improved bat algorithm. *International Journal of Electrical Power & Energy Systems, 56*, 42-54.

Bahramirad, S., Reder, W., & Khodaei, A. (2012). Reliability-constrained optimal sizing of energy storage system in a microgrid. *IEEE Transactions on Smart Grid, 3*(4), 2056-2062.

Barnes, F. S., & Levine, J. G. (2011). *Large energy storage systems handbook*: CRC Press.

Baziar, A., & Kavousi-Fard, A. (2013). Considering uncertainty in the optimal energy management of renewable micro-grids including storage devices. *Renewable Energy, 59*, 158-166.

Berrazouane, S., & Mohammedi, K. (2014). Parameter optimization via cuckoo optimization algorithm of fuzzy controller for energy management of a hybrid power system. *Energy Conversion and Management, 78*, 652-660.

Bhatnagar, P., & Nema, R. (2013). Maximum power point tracking control techniques: State-of-the-art in photovoltaic applications. *Renewable and Sustainable Energy Reviews, 23*, 224-241.

Blomen, L. J., & Mugerwa, M. N. (2013). *Fuel cell systems*: Springer Science & Business Media.

Borowy, B. S., & Salameh, Z. M. (1996). Methodology for optimally sizing the combination of a battery bank and PV array in a wind/PV hybrid system. *IEEE Transactions on Energy Conversion, 11*(2), 367-375.

Canever, D., Dudgeon, G., Massucco, S., McDonald, J., & Silvestro, F. *Model validation and coordinated operation of a photovoltaic array and a diesel power plant for distributed generation.* Paper presented at the IEEE Power Engineering Society Summer Meeting, 2001.

Carbone, R. (2011). *Energy storage in the emerging era of smart grids*: InTech.

Chang, Y., Mao, X., Zhao, Y., Feng, S., Chen, H., & Finlow, D. (2009). Lead-acid battery use in the development of renewable energy systems in China. *Journal of Power Sources, 191*(1), 176-183.

Chen, C., Duan, S., Cai, T., Liu, B., & Hu, G. (2011). Optimal allocation and economic analysis of energy storage system in microgrids. *IEEE Transactions on Power Electronics, 26*(10), 2762-2773.

Chen, C., Duan, S., Cai, T., Liu, B., & Hu, G. (2011). Smart energy management system for optimal microgrid economic operation. *IET Renewable Power Generation, 5*(3), 258-267.

Chen, S., Gooi, H. B., & Wang, M. (2012). Sizing of energy storage for microgrids. *IEEE Transactions on Smart Grid, 3*(1), 142-151.

Cheng, D., Mather, B. A., Seguin, R., Hambrick, J., & Broadwater, R. P. Photovoltaic (PV) Impact Assessment for Very High Penetration Levels.

Cheng, Y.-S., Chuang, M.-T., Liu, Y.-H., Wang, S.-C., & Yang, Z.-Z. (2016). A particle swarm optimization based power dispatch algorithm with roulette wheel re-distribution mechanism for equality constraint. *Renewable Energy, 88*, 58-72.

Chowdhury, S., & Crossley, P. (2009). *Microgrids and active distribution networks* (Vol. 6): IET.

Clark, N., & Doughty, D. (2005). Development and testing of 100kW/1min Li-ion battery systems for energy storage applications. *Journal of Power Sources, 146*(1), 798-803.

Cornforth, D. (2011). Role of microgrids in the smart grid. *Journal of Electronic Science and Technology, 9*(1), 9-16.

Dai, R., & Mesbahi, M. (2013). Optimal power generation and load management for off-grid hybrid power systems with renewable sources via mixed-integer programming. *Energy Conversion and Management, 73*, 234-244.

Datta, M., Senjyu, T., Yona, A., Funabashi, T., & Kim, C. H. (2009). A coordinated control method for leveling PV output power fluctuations of PV–diesel hybrid systems connected to isolated power utility. *IEEE Transactions on Energy Conversion, 24*(1), 153-162.

Daud, M. Z., Mohamed, A., & Hannan, M. (2013). An improved control method of battery energy storage system for hourly dispatch of photovoltaic power sources. *Energy Conversion and Management, 73*, 256-270.

Denholm, P., & Margolis, R. M. (2007). Evaluating the limits of solar photovoltaics (PV) in traditional electric power systems. *Energy policy, 35*(5), 2852-2861.

Ding, M., Xu, Z., Wang, W., Wang, X., Song, Y., & Chen, D. (2016). A review on China′ s large-scale PV integration: Progress, challenges and recommendations. *Renewable and Sustainable Energy Reviews, 53*, 639-652.

Divya, K., & Østergaard, J. (2009). Battery energy storage technology for power systems—An overview. *Electric Power Systems Research, 79*(4), 511-520.

Dougal, R. A., Liu, S., & White, R. E. (2002). Power and life extension of battery-ultracapacitor hybrids. *IEEE Transactions on Components and Packaging Technologies, 25*(1), 120-131.

Droste-Franke, B., Paal, B., Rehtanz, C., Sauer, D. U., Schneider, J.-P., Schreurs, M. (2012). *Balancing renewable electricity: energy storage, demand side management, and network extension from an interdisciplinary perspective* (Vol. 40): Springer Science & Business Media.

e Silva, G. d. O., & Hendrick, P. (2016). Lead–acid batteries coupled with photovoltaics for increased electricity self-sufficiency in households. *Applied energy, 178*, 856-867.

Elhadidy, M., & Shaahid, S. (1999). Optimal sizing of battery storage for hybrid (wind+ diesel) power systems. *Renewable Energy, 18*(1), 77-86.

Eltawil, M. A., & Zhao, Z. (2010). Grid-connected photovoltaic power systems: Technical and potential problems—A review. *Renewable and Sustainable Energy Reviews, 14*(1), 112-129.

Eltawil, M. A., & Zhao, Z. (2013). MPPT techniques for photovoltaic applications. *Renewable and Sustainable Energy Reviews, 25*, 793-813.

Feroldi, D., Degliuomini, L. N., & Basualdo, M. (2013). Energy management of a hybrid system based on wind–solar power sources and bioethanol. *Chemical Engineering Research and Design, 91*(8), 1440-1455.

Fossati, J. P., Galarza, A., Martín-Villate, A., & Fontán, L. (2015). A method for optimal sizing energy storage systems for microgrids. *Renewable Energy, 77*, 539-549.

García, P., Torreglosa, J. P., Fernández, L. M., & Jurado, F. (2013). Optimal energy management system for stand-alone wind turbine/photovoltaic/hydrogen/battery hybrid system with supervisory control based on fuzzy logic. *International Journal of Hydrogen Energy*, *38*(33), 14146-14158.

Gevorgian, V., & Booth, S. (2013). Review of Prepa Technical Requirements for Interconnecting Wind and Solar Generation. *National Renewable Energy Laboratory: Golden, CO, USA*.

Giraud, F., & Salameh, Z. M. (1999). Analysis of the effects of a passing cloud on a grid-interactive photovoltaic system with battery storage using neural networks. *IEEE Transactions on Energy Conversion, 14*(4), 1572-1577.

Glavin, M., Chan, P. K., Armstrong, S., & Hurley, W. (2008). *A stand-alone photovoltaic supercapacitor battery hybrid energy storage system.* Paper presented at the Power Electronics and Motion Control Conference, 2008. EPE-PEMC 2008. 13th.

Graham, V., & Hollands, K. (1990). A method to generate synthetic hourly solar radiation globally. *Solar Energy, 44*(6), 333-341.

Gu, W., Wu, Z., Bo, R., Liu, W., Zhou, G., Chen, W. (2014). Modeling, planning and optimal energy management of combined cooling, heating and power microgrid: A review. *International Journal of Electrical Power & Energy Systems, 54*, 26-37.

Guo, C., Bai, Y., Zheng, X., Zhan, J., & Wu, Q. (2012). Optimal generation dispatch with renewable energy embedded using multiple objectives. *International Journal of Electrical Power & Energy Systems, 42*(1), 440-447.

Guoju, Z., Xisheng, T., & Zhiping, Q. (2010). *Research on battery supercapacitor hybrid storage and its application in microgrid.* Paper presented at the Power and Energy Engineering Conference (APPEEC), 2010 Asia-Pacific.

Hall, D. J., & Colclaser, R. G. (1999). Transient modeling and simulation of a tubular solid oxide fuel cell. *IEEE Transactions on Energy Conversion, 14*(3), 749-753.

Hara, R., Kita, H., Tanabe, T., Sugihara, H., Kuwayama, A., & Miwa, S. (2009). Testing the technologies. *IEEE Power and Energy Magazine, 7*(3), 77-85.

Haruna, H., Itoh, S., Horiba, T., Seki, E., & Kohno, K. (2011). Large-format lithium-ion batteries for electric power storage. *Journal of Power Sources, 196*(16), 7002-7005.

Hasanuzzaman, M., Rahim, N., Hosenuzzaman, M., Saidur, R., Mahbubul, I., & Rashid, M. (2012). Energy savings in the combustion based process heating in industrial sector. *Renewable and Sustainable Energy Reviews, 16*(7), 4527-4536.

Hassmann, K. (2001). SOFC Power Plants, the Siemens-Westinghouse Approach. *Fuel Cells, 1*(1), 78-84.

Hatziadoniu, C., Lobo, A., Pourboghrat, F., & Daneshdoost, M. (2002). A simplified dynamic model of grid-connected fuel-cell generators. *IEEE Transactions on Power Delivery, 17*(2), 467-473.

Hawkes, A., & Leach, M. (2009). Modelling high level system design and unit commitment for a microgrid. *Applied energy, 86*(7), 1253-1265.

Hill, C. A., Such, M. C., Chen, D., Gonzalez, J., & Grady, W. M. (2012). Battery energy storage for enabling integration of distributed solar power generation. *IEEE Transactions on Smart Grid, 3*(2), 850-857.

. HIT Photovoltaic Module Power 210A. (2010). *In SANYO Energy (U.S.A.) Corp. (Ed.). the United States.*

Hooshmand, A., Asghari, B., & Sharma, R. K. (2014). Experimental demonstration of a tiered power management system for economic operation of grid-tied microgrids. *IEEE Transactions on Sustainable Energy, 5*(4), 1319-1327.

Hua, S., Zhou, Q., Kong, D., & Ma, J. (2006). Application of valve-regulated lead-acid batteries for storage of solar electricity in stand-alone photovoltaic systems in the northwest areas of China. *Journal of Power Sources, 158*(2), 1178-1185.

IEEE. (2000). *IEEE Recommended Practice for Utility Interface of Photovoltaic (PV) Systems*: IEEE.

Ina, N., Yanagawa, S., Kato, T., & Suzuoki, Y. (2004). Smoothing PV System's Output by Tuning MPPT Control. *IEEJ Transactions on Power and Energy, 124*, 455-461.

International Energy Agency, PVPS Trends in Photovoltaic Applications. (2014). Retrieved from Sweden:

Ishaque, K., & Salam, Z. (2013). A review of maximum power point tracking techniques of PV system for uniform insolation and partial shading condition. *Renewable and Sustainable Energy Reviews, 19*, 475-488.

Jewell, W., & Ramakumar, R. (1987). The effects of moving clouds on electric utilities with dispersed photovoltaic generation. *IEEE Transactions on Energy Conversion*(4), 570-576.

Jewell, W. T., & Unruh, T. D. (1990). Limits on cloud-induced fluctuation in photovoltaic generation. *IEEE Transactions on Energy Conversion, 5*(1), 8-14.

Jiang, Q., Xue, M., & Geng, G. (2013). Energy management of microgrid in grid-connected and stand-alone modes. *IEEE Transactions on Power Systems, 28*(3), 3380-3389.

Jung, H.-Y., Kim, A.-R., Kim, J.-H., Park, M., Yu, I.-K., Kim, S.-H. (2009). A study on the operating characteristics of SMES for the dispersed power generation system. *IEEE Transactions on Applied Superconductivity, 19*(3), 2028-2031.

Kakimoto, N., Satoh, H., Takayama, S., & Nakamura, K. (2009). Ramp-rate control of photovoltaic generator with electric double-layer capacitor. *IEEE Transactions on Energy Conversion, 24*(2), 465-473.

Kalantar, M. (2010). Dynamic behavior of a stand-alone hybrid power generation system of wind turbine, microturbine, solar array and battery storage. *Applied energy, 87*(10), 3051-3064.

Kan, S. Y., Verwaal, M., & Broekhuizen, H. (2006). The use of battery–capacitor combinations in photovoltaic powered products. *Journal of Power Sources, 162*(2), 971-974.

Karaboga, D., & Akay, B. (2009). A comparative study of artificial bee colony algorithm. *Applied mathematics and computation, 214*(1), 108-132.

Karimi, M., Mokhlis, H., Naidu, K., Uddin, S., & Bakar, A. (2016). Photovoltaic penetration issues and impacts in distribution network–A review. *Renewable and Sustainable Energy Reviews, 53*, 594-605.

Katiraei, F., Abbey, C., Tang, S., & Gauthier, M. (2008). *Planned islanding on rural feeders—utility perspective.* Paper presented at the IEEE Power and Energy Society General Meeting-Conversion and Delivery of Electrical Energy in the 21st Century, 2008.

Katiraei, F., & Agüero, J. R. (2011). Solar PV integration challenges. *IEEE Power and Energy Magazine, 9*(3), 62-71.

Katiraei, F., Iravani, R., Hatziargyriou, N., & Dimeas, A. (2008). Microgrids management. *IEEE Power and Energy Magazine, 6*(3), 54-65.

Kennedy, J. (2011). Particle swarm optimization. In *Encyclopedia of machine learning* (pp. 760-766): Springer.

Khalilpour, R., & Vassallo, A. (2016). Planning and operation scheduling of PV-battery systems: A novel methodology. *Renewable and Sustainable Energy Reviews, 53*, 194-208.

Koohi-Kamali, S., Rahim, N., & Mokhlis, H. (2014). Smart power management algorithm in microgrid consisting of photovoltaic, diesel, and battery storage plants considering variations in sunlight, temperature, and load. *Energy Conversion and Management, 84*, 562-582.

Kroposki, B., Lasseter, R., Ise, T., Morozumi, S., Papatlianassiou, S., & Hatziargyriou, N. (2008). Making microgrids work. *IEEE Power and Energy Magazine, 6*(3), 40-53.

Krumdieck, S., Page, S., & Round, S. (2004). Solid oxide fuel cell architecture and system design for secure power on an unstable grid. *Journal of Power Sources, 125*(2), 189-198.

Ku Ahmad, K. N. E., Selvaraj, J., & Rahim, N. A. (2013). A review of the islanding detection methods in grid-connected PV inverters. *Renewable and Sustainable Energy Reviews, 21,* 756-766.

Kwon, W. H., & Han, S. H. (2006). *Receding horizon control: model predictive control for state models*: Springer Science & Business Media.

Larminie, J., Dicks, A., & McDonald, M. S. (2003). *Fuel cell systems explained* (Vol. 2): Wiley New York.

Lasseter, R. H. (2002). *Microgrids.* Paper presented at the IEEE Power Engineering Society Winter Meeting, 2002.

Li, X., Song, Y.-J., & Han, S.-B. *Study on power quality control in multiple renewable energy hybrid microgrid system.* Paper presented at the IEEE Lausanne Power Tech, 2007

Li, X., Song, Y.-J., & Han, S.-B. (2008). Frequency control in micro-grid power system combined with electrolyzer system and fuzzy PI controller. *Journal of Power Sources, 180*(1), 468-475.

Li, Y., Rajakaruna, S., & Choi, S. (2007). Control of a solid oxide fuel cell power plant in a grid-connected system. *IEEE Transactions on Energy Conversion, 22*(2), 405-413.

Lidula, N., & Rajapakse, A. (2011). Microgrids research: A review of experimental microgrids and test systems. *Renewable and Sustainable Energy Reviews, 15*(1), 186-202.

Lim, Y. S., & Tang, J. H. (2014). Experimental study on flicker emissions by photovoltaic systems on highly cloudy region: A case study in Malaysia. *Renewable Energy, 64*, 61-70.

Liu, X., Cramer, A. M., & Liao, Y. (2015). Reactive power control methods for photovoltaic inverters to mitigate short-term voltage magnitude fluctuations. *Electric Power Systems Research, 127*, 213-220.

Liu, Y., Bebic, J., Kroposki, B., De Bedout, J., & Ren, W. *Distribution system voltage performance analysis for high-penetration PV.* Paper presented at the IEEE Energy Conference, 2008.

Lujano-Rojas, J. M., Dufo-López, R., Atencio-Guerra, J. L., Rodrigues, E. M., Bernal-Agustín, J. L., & Catalão, J. P. (2016). Operating conditions of lead-acid batteries in the optimization of hybrid energy systems and microgrids. *Applied energy, 179*, 590-600.

Maiti, D., Acharya, A., Chakraborty, M., Konar, A., & Janarthanan, R. (2008). *Tuning PID and PI/λ D δ controllers using the integral time absolute error criterion.* Paper presented at the 2008 4th International Conference on Information and Automation for Sustainability.

MalaysiaGasAssociation. (2015). *Malaysia: Natural Gas Industry Annual Review*. Retrieved from

Marcos, J., Marroyo, L., Lorenzo, E., Alvira, D., & Izco, E. (2011). Power output fluctuations in large scale PV plants: one year observations with one second resolution and a derived analytic model. *Progress in Photovoltaics: Research and Applications, 19*(2), 218-227.

Marzband, M., Ghadimi, M., Sumper, A., & Domínguez-García, J. L. (2014). Experimental validation of a real-time energy management system using multi-period gravitational search algorithm for microgrids in islanded mode. *Applied energy, 128*, 164-174.

Marzband, M., Sumper, A., Domínguez-García, J. L., & Gumara-Ferret, R. (2013). Experimental validation of a real time energy management system for microgrids in islanded mode using a local day-ahead electricity market and MINLP. *Energy Conversion and Management, 76*, 314-322.

McKenna, E., McManus, M., Cooper, S., & Thomson, M. (2013). Economic and environmental impact of lead-acid batteries in grid-connected domestic PV systems. *Applied energy, 104*, 239-249.

Mears, D., Gotschall, H., & Kamath, H. (2003). *EPRI-DOE handbook of energy storage for transmission and distribution applications*: EPRI.

Mills, A. (2012). Dark shadows. *IEEE Power & Energy Magazine, 9, 3, 33-41, May-June 2011*.

Mirjalili, S., Mirjalili, S. M., & Lewis, A. (2014). Grey wolf optimizer. *Advances in Engineering Software, 69*, 46-61.

Mohamed, F. A., & Koivo, H. N. (2010). System modelling and online optimal management of microgrid using mesh adaptive direct search. *International Journal of Electrical Power & Energy Systems, 32*(5), 398-407.

Mohamed, F. A., & Koivo, H. N. (2012). Multiobjective optimization using Mesh Adaptive Direct Search for power dispatch problem of microgrid. *International Journal of Electrical Power & Energy Systems, 42*(1), 728-735.

Mohammedi, A., Rekioua, D., Rekioua, T., & Bacha, S. (2016). Valve Regulated Lead Acid battery behavior in a renewable energy system under an ideal Mediterranean climate. *International Journal of Hydrogen Energy*.

Monai, T., Takano, I., Nishikawa, H., & Sawada, Y. (2004). A collaborative operation method between new energy-type dispersed power supply and EDLC. *IEEE Transactions on Energy Conversion, 19*(3), 590-598.

Moore, S., & Eshani, M. (1996). *An empirically based electrosource horizon lead-acid battery model*. Retrieved from

Mousavi G, S. (2012). An autonomous hybrid energy system of wind/tidal/microturbine/battery storage. *International Journal of Electrical Power and Energy Systems, 43*(1), 1144-1154.

Nair, N.-K. C., & Garimella, N. (2010). Battery energy storage systems: Assessment for small-scale renewable energy integration. *Energy and Buildings, 42*(11), 2124-2130.

Nasiri, A. (2008). *Integrating energy storage with renewable energy systems.* Paper presented at the 34th Annual IEEE Conference on Industrial Electronics (IECON) 2008.

Nazar, N., Abdullah, M., Hassan, M., & Hussin, F. (2012). *Time-based electricity pricing for Demand Response implementation in monopolized electricity market.* Paper presented at the IEEE Student Conference on Research and Development (SCOReD), 2012.

Nguyen, T. A., Crow, M. L., & Elmore, A. C. (2015). Optimal Sizing of a Vanadium Redox Battery System for Microgrid Systems. *IEEE Transactions on Sustainable Energy, 6*(3), 729-737.

Olivares, D. E., Cañizares, C. A., & Kazerani, M. (2014). A centralized energy management system for isolated microgrids. *IEEE Transactions on Smart Grid, 5*(4), 1864-1875.

Omran, W. A., Kazerani, M., & Salama, M. (2011a). Investigation of methods for reduction of power fluctuations generated from large grid-connected photovoltaic systems. *IEEE Transactions on Energy Conversion, 26*(1), 318-327.

Omran, W. A., Kazerani, M., & Salama, M. (2011b). Investigation of methods for reduction of power fluctuations generated from large grid-connected photovoltaic systems. *IEEE Transactions on Energy Conversion, 26*(1), 318-327.

Padulles, J., Ault, G., & McDonald, J. (2000). An integrated SOFC plant dynamic model for power systems simulation. *Journal of Power Sources, 86*(1), 495-500.

Park, J.-B., Lee, K.-S., & Shin, J.-R. (2005). A particle swarm optimization for economic dispatch with nonsmooth cost functions. *IEEE Transactions on Power Systems, 20*(1), 34-42.

Photovoltaics, D. G. (2009). IEEE Application Guide for IEEE Std 1547™, IEEE Standard for Interconnecting Distributed Resources with Electric Power Systems.

Poli, R., Kennedy, J., & Blackwell, T. (2007). Particle swarm optimization. *Swarm intelligence, 1*(1), 33-57.

PVPS, I. (2012). Trends in photovoltaic applications. Survey report of selected IEA countries between 1992 and 2011. *Report IEA-PVPS T1–21*.

Rajapakse, A. D., & Muthumuni, D. (2009). *Simulation tools for photovoltaic system grid integration studies.* Paper presented at the IEEE Electrical Power & Energy Conference (EPEC), 2009.

Rashedi, E., Nezamabadi-Pour, H., & Saryazdi, S. (2009). GSA: a gravitational search algorithm. *Information sciences, 179*(13), 2232-2248.

Rekioua, D., & Matagne, E. (2012). *Optimization of photovoltaic power systems: modelization, simulation and control*: Springer Science & Business Media.

RemcoLtd. (2012). REMCO Renewable Energy Manufacturing Company. *Hong Kong*.

Ren, H., & Gao, W. (2010). A MILP model for integrated plan and evaluation of distributed energy systems. *Applied energy, 87*(3), 1001-1014.

Renewable Energy Policy Network for 21st Century (REN21), Renewables Global Status Report (2015). Retrieved from Paris, France:

Ro, K., & Rahman, S. (1998). Two-loop controller for maximizing performance of a grid-connected photovoltaic-fuel cell hybrid power plant. *IEEE Transactions on Energy Conversion,13*(3), 276-281.

Salas, V., Olias, E., Barrado, A., & Lazaro, A. (2006). Review of the maximum power point tracking algorithms for stand-alone photovoltaic systems. *Solar Energy Materials and Solar Cells, 90*(11), 1555-1578.

Sedghisigarchi, K., & Feliachi, A. (2004a). Dynamic and transient analysis of power distribution systems with fuel Cells-part I: fuel-cell dynamic model. *IEEE Transactions on Energy Conversion, 19*(2), 423-428.

Sedghisigarchi, K., & Feliachi, A. (2004b). Dynamic and transient analysis of power distribution systems with fuel Cells-part II: control and stability enhancement. *IEEE Transactions on Energy Conversion, 19*(2), 429-434.

Senjyu, T., Datta, M., Yona, A., Sekine, H., & Funabashi, T. *A new method for smoothing output power fluctuations of PV system connected to small power utility*. Paper presented at the 7th IEEE Internatonal Conference on Power Electronics, 2007. .

Senjyu, T., Datta, M., Yona, A., Sekine, H., & Funabashi, T. (2007). *A coordinated control method for leveling output power fluctuations of multiple PV systems.* Paper presented at the IEEE Internatonal Conference on Power Electronics, .

Shah, R., Mithulananthan, N., Bansal, R., & Ramachandaramurthy, V. (2015). A review of key power system stability challenges for large-scale PV integration. *Renewable and Sustainable Energy Reviews, 41*, 1423-1436.

Sharafi, M., & ELMekkawy, T. Y. (2014). Multi-objective optimal design of hybrid renewable energy systems using PSO-simulation based approach. *Renewable Energy, 68*, 67-79.

Sharma, S., Bhattacharjee, S., & Bhattacharya, A. (2016). Grey wolf optimisation for optimal sizing of battery energy storage device to minimise operation cost of microgrid. *IET Generation, Transmission & Distribution*.

Sørensen, B., Breeze, P., Suppes, G. J., El Bassam, N., Silveira, S., Yang, S.-T. (2008). *Renewable Energy Focus e-Mega Handbook*: Academic Press.

Tam, K.-S., Kumar, P., & Foreman, M. (1989). Enhancing the utilization of photovoltaic power generation by superconductive magnetic energy storage. *IEEE Transactions on Energy Conversion, 4*(3), 314-321.

Tan, K., Peng, X., So, P., Chu, Y. C., & Chen, M. (2012). Centralized control for parallel operation of distributed generation inverters in microgrids. *IEEE Transactions on Smart Grid, 3*(4), 1977-1987.

Tan, K., So, P., Chu, Y., & Chen, M. Z. (2013). Coordinated control and energy management of distributed generation inverters in a microgrid. *IEEE Transactions on Power Delivery, 28*(2), 704-713.

Tan, X., Li, Q., & Wang, H. (2013). Advances and trends of energy storage technology in Microgrid. *International Journal of Electrical Power & Energy Systems, 44*(1), 179-191.

Teleke, S., Baran, M. E., Bhattacharya, S., & Huang, A. Q. (2010). Rule-based control of battery energy storage for dispatching intermittent renewable sources. *IEEE Transactions on Sustainable Energy, 1*(3), 117-124.

Tenfen, D., & Finardi, E. C. (2015). A mixed integer linear programming model for the energy management problem of microgrids. *Electric Power Systems Research, 122*, 19-28.

Tesfahunegn, S. G., Ulleberg, Ø., Vie, P. J., & Undeland, T. M. (2011). PV Fluctuation Balancing Using Hydrogen Storage–a Smoothing Method for Integration of PV Generation into the Utility Grid. *Energy Procedia, 12*, 1015-1022.

Tonkoski, R., Lopes, L., & Turcotte, D. *Active power curtailment of PV inverters in diesel hybrid mini-grids.* Paper presented at the IEEE Electrical Power & Energy Conference (EPEC), 2009

Tonkoski, R., Lopes, L. A., & El Fouly, T. H. (2011). Coordinated active power curtailment of grid connected PV inverters for overvoltage prevention. *IEEE Transactions on Sustainable Energy, 2*(2), 139-147.

Varaiya, P. P., Wu, F. F., & Bialek, J. W. (2011). Smart operation of smart grid: Risk-limiting dispatch. *Proceedings of the IEEE, 99*(1), 40-57.

Vazquez, S., Lukic, S. M., Galvan, E., Franquelo, L. G., & Carrasco, J. M. (2010). Energy storage systems for transport and grid applications. *IEEE Transactions on Industrial Electronics, 57*(12), 3881-3895.

Wang, C. (2006). Modeling and control of hybrid wind/photovoltaic/fuel cell distributed generation systems (Doctoral dissertation, Montana State University-Bozeman, College of Engineering).

Wang, X., Huang, B., & Chen, T. (2007). Data-driven predictive control for solid oxide fuel cells. *Journal of Process Control, 17*(2), 103-114.

Weckx, S., Gonzalez, C., & Driesen, J. (2014). Combined central and local active and reactive power control of PV inverters. *IEEE Transactions on Sustainable Energy, 5*(3), 776-784.

Whitaker, C., Newmiller, J., Ropp, M., & Norris, B. (2008). Distributed photovoltaic systems design and technology requirements. *Sandia/SAND2008-0946 P, Tech. Rep*.

Woyte, A., Van Thong, V., Belmans, R., & Nijs, J. (2006). Voltage fluctuations on distribution level introduced by photovoltaic systems. *IEEE Transactions on Energy Conversion, 21*(1), 202-209.

Yadav, A. K., & Chandel, S. (2014). Solar radiation prediction using Artificial Neural Network techniques: A review. *Renewable and Sustainable Energy Reviews, 33*, 772-781.

Yazdani, A., Di Fazio, A. R., Ghoddami, H., Russo, M., Kazerani, M., Jatskevich, J. (2011). Modeling guidelines and a benchmark for power system simulation studies of three-phase single-stage photovoltaic systems. *IEEE Transactions on Power Delivery, 26*(2), 1247-1264.

Zarina, P., Mishra, S., & Sekhar, P. (2014). Exploring frequency control capability of a PV system in a hybrid PV-rotating machine-without storage system. *International Journal of Electrical Power & Energy Systems, 60*, 258-267.

Zhou, H., Bhattacharya, T., Tran, D., Siew, T. S. T., & Khambadkone, A. M. (2011). Composite energy storage system involving battery and ultracapacitor with dynamic energy management in microgrid applications. *IEEE Transactions on Power Electronics, 26*(3), 923-930.

Zhu, Y., & Tomsovic, K. (2002). Development of models for analyzing the load-following performance of microturbines and fuel cells. *Electric Power Systems Research, 62*(1), 1-11.

LIST OF PUBLICATIONS AND PAPERS PRESENTED

This work has been reported through following publications:

Journal Papers

1. Shivashankar, S., et al., Mitigating methods of power fluctuation of photovoltaic (PV) sources–A review, Renewable and Sustainable Energy Reviews, 59, 2016, 1170-1184.

2. Shivashankar.S., et al., Mix-mode energy management strategy and battery sizing for economic operation of grid-tied microgrid, Energy, 2016.

3. Shivashankar.S., et al., Ramp-rate control approach based on dynamic smoothing parameter to mitigate solar PV output fluctuations, IEEE Transactions on Sustainable Energy, 2016. (under review).

4. Shivashankar.S., et al., Directive energy management system for optimal operation of grid connected microgid using receding horizon economic dispatch (RHED) approach, Energies, 2016. (under review).

5. Shivashankar.S., et al., A fuzzy based PI controller for power management of grid connected PV-SOFC hybrid system, Journal of Electrical Systems, 2016. (under review).

Conference Papers

1. Shivashankar.S., et al., Actice power control of SOFC for a grid tied PV-SOFC hybrid system considering variation in load, International Conference on Power, Energy, and Communication Systems, 2015.